QUANTITATIVE STUDIES IN T AND B CELL

EPITOPE MIMICRY

by

James Stephens Cavenaugh

A dissertation submitted to the faculty of
The University of Utah
in partial fulfillment of the requirements for the degree of

Doctor of Philosophy

Department of Pharmaceutics and Pharmaceutical Chemistry

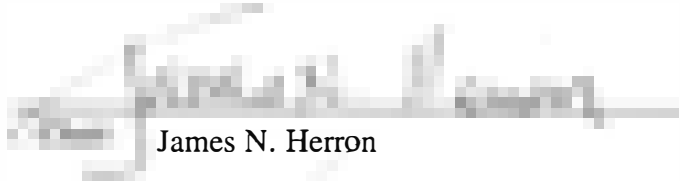The University of Utah

May 2003

THE UNIVERSITY OF UTAH GRADUATE SCHOOL
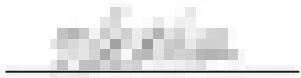
SUPERVISORY COMMITTEE APPROVAL

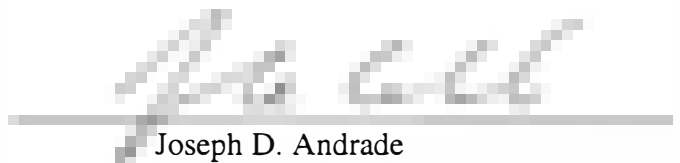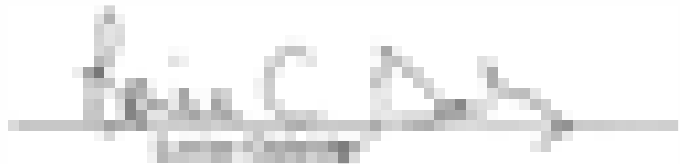of a dissertation submitted by

James Stephens Cavenaugh

This dissertation has been read by each member of the following supervisory committee and by majority vote has been found to be satisfactory.

James N. Herron

Arthur Broom

Joseph D. Andrade

ABSTRACT

For a peptide vaccine to be effective in generating an antibody response, it generally must incorporate both B cell epitopes, against which the antibody response is to be directed, and T cell epitopes, which are responsible for stimulating helper T cells. The first part of this work is concerned with the question, "How well can a T cell epitope replace the carrier protein from which it is derived?" To answer this question two studies were done: an initial, direct comparison between a protein (the Fab' fragment of murine monoclonal anti-fluorescein antibody 9-40) coupled to hen egg lysozyme (HEL) and the same protein coupled to the immunodominant T cell epitope from HEL for B10.A (H-2^a) mice, along with negative controls, and a second, dose response study with fluorescein (FL) as the B cell epitope attached to a multiple antigenic peptide (MAP) version of this T cell epitope, along with positive and negative controls (HEL and a MAP in which the epitope sequence was replaced by glycine residues, respectively). This study showed a half-sigmoidal curve for the FL-(T epitope) immunogen, no response to the negative control except at the highest dose used, and a fairly constant and high response for both the experimental MAP and the fluoresceinated HEL.

The initial study described above gave a very specific anti-idiotype response for the (9-40)Fab'-HEL construct. Another, follow-up study comparing a peptide mimic based on an important idiotope, the third complementarity determining region of the heavy chain (the CDR-H3 loop), to the intact idiotype was also conducted. In this study

the peptide mimic of the CDR-H3 loop was the B cell epitope; it was also coupled to HEL. The question being addressed was, "How well can an idiotope peptide mimic replace its parent idiotype?" B10.A mice were immunized with (B epitope)-HEL, (9-40)Fab'-HEL, (B epitope) + HEL mixed together, or just the B epitope. The essential issue was crossreactivity, and this was observed to increase with succeeding immunizations. Molecular dynamics simulations with generalized Born implicit solvation or particle mesh Ewald electrostatics were also used to provide insight into the structural basis of idiotopic phenomena.

Dedicated to my Creator,

and to my parents, who left behind a good example to follow

TABLE OF CONTENTS

LIST OF ACRONYMS AND ABBREVIATIONS

ANOVA, analysis of variance

Bep, intramolecular disulfide of GGGCTSYGYHGAYC

CG, conjugate gradients

CVFF, consistent valence force field

DCC, *N,N'*-dicyclohexylcarbodiimide

DMSO, dimethylsulfoxide

DSG, disuccinimidylglutarate

DTT, dithiothreitol

EDTA, ethylenediaminetetraacetic acid

ELISA, enzyme-linked immunosorbent assay

ESI-MS, electrospray ionization mass spectrometry

EtOEt, diethylether

FAB-MS, fast atom bombardment mass spectrometry

FL, fluorescein

HEL, chicken hen egg lysozyme

KLH, keyhole limpet hemocyanin

MALDI-MS, matrix-assisted laser desorption ionization mass spectrometry

MAP, multiple antigenic peptide

MHC, major histocompatibility complex

MPBH, 4-(4-N-maleimidophenyl)butyric acid hydrazide hydrochloride

PBS, phosphate buffered saline (100 mM NaCl, 50 mM NaPO$_4$, pH 7.4, 0.2% (w/v) NaN$_3$)

RMSD, root mean square deviation (from a reference structure)

SEC, size exclusion chromatography

SMCC, succinimidyl 4-*N*-maleimidomethyl-cyclohexane-1-carboxylate

SPDP, 3-(2-pyridyldithio)proprionic acid *N*-hydroxysuccinimide ester

THF, tetrahydrofuran

TLC, thin layer chromatography

CHAPTER 1

INTRODUCTION TO T AND B CELL EPITOPE MIMICRY:
TERMINOLOGY AND IMPORTANCE

The science of immunology has grown from a medical curiosity in the eighteenth century to one of the cornerstones of modern medicine, being intertwined with all infections, inflammation, cancer, aging, genetics, and even emotions - in short, with everything that determines whether a person is sick or healthy. From its beginnings as a separate field of study to the present day, vaccines have been a major aspect of immunology; indeed, the purpose of a vaccine is to stimulate the immune system to provide prophyllaxis or, more recently, therapy against a specific disease. Hence, a vaccine is really any immunogen that has been deliberately administered to elicit a prophylactic (or sometimes therapeutic) response without causing severe disease.

Types of vaccines

Classical vaccines are either live attenuated organisms (including viruses) or else are killed organisms and as such are poorly defined, chemically complex mixtures. With the rise of modern biochemistry it has become possible to identify the parts of the antigens that are recognized by the immune system. (As a matter of terminology, an antigen was initially defined as a substance that could evoke an immune response and was synonymous with *immunogen*. Usage has changed, however, so that nowadays an antigen is defined as a molecule that is capable of being recognized by the immune

system, whether or not it actually is, and an immunogen is a substance that can evoke an immune response.) These so-called antigenic determinants are also known as *epitopes* and are recognized by immunological biomolecules.[*]

Because they are poorly defined, chemically complex mixtures, classical vaccines can and do elicit immune responses against antigens that are not involved with protection. Worse, classical vaccines suffer from the fact that, for the most part, only organisms that can be grown in culture can be made into suitable vaccines. Identification of the protective epitopes allows subunit vaccines to be made with only the antigens involved in protective immunity or even with only just those epitopes; this can be especially useful with parasitic and cancer antigens. Such subunit vaccines can be prepared by genetic engineering methods or by chemical synthesis. Recombinant DNA technology can be used to prepare entire antigenic proteins. This is an advantage in cases in which the actual epitopes are unknown or vary from individual to individual within the population. A commercial example of this approach is a hepatitis B virus vaccine, which is produced in yeast cells (1, p. 110). However, purification of the antigen from the expression system can sometimes be difficult and there is the danger of immune reaction against residual host proteins (1). More recently, "naked" DNA vaccines have been used that code for the antigen in a plasmid construct (www.vical.com). These vaccines are effective and do not require purification of the antigen.

Another approach would be the minimalist approach of peptide vaccines, using just the epitopes that are actually involved in immunity. Synthetic peptides as vaccines

---

[*] Although not used in the remainder of this dissertation, other related terms are paratope (the portion of an antibody or TCR that contacts the epitope), mimotope (a peptide mimic

are attractive in that they would be expected to have excellent safety margins. They are especially promising for cancer vaccines, where the entire antigen already is encoded by the host genome but the cancer cells escape immune detection. For peptides to be used as vaccines it is essential that the epitopes be known. For a T cell dependent response, which is generally desirable since this type of response typically results in superior immunological memory, this requirement can be difficult due to the fact that the epitopes which a given antigen possesses will vary from individual to individual, depending on their MHC haplotypes (discussed more below). In contrast, type 2 T cell independent responses rely on B cell receptor (membrane bound Ig) crosslinking to directly stimulate the B cells. (Type 1 T cell independent responses involve direct B cell stimulation via endotoxin.)

MHC haplotypes

Genetic nomenclature can be confusing and this is especially so of immune system genes. Dozens of histocompatability loci have been genetically mapped to virtually every mouse chromosome (2 p. 180); those that correspond to rapid graft rejection were initially designated as the H-2 locus. The H-2 locus is actually a complex of genes rather than a single locus and was accordingly called the major histocompatibility complex (MHC) to distinguish it from the many other minor histocompatibility loci that were associated with slow graft rejection. Within the wider H-2 complex – the MHC – are two major subcomplexes: the classical H-2 complex[†] and

---

of a discontinuos epitope), and aggretope (the portion of an MHC-I or MHC-II protein that contacts the peptide).

[†] The MHC and the H-2 locus were originally synonymous, but how can the H-2 complex encompass the H-2 complex? For this reason I have referred to the larger complex as the

the Tla complex (2). Both of these consist of several regions; the H-2 complex consists of regions designated as K, I, S, and D (Figure 1). The MHC is also divided into three so-called classes, coding for the class I, class II, and class III gene products. The S region of the H-2 complex encompasses the class III genes, which encode some complement proteins, as well as some genes for proteins that are not especially immunological (3, p. 75). The class I gene products include those of the entire Tla complex as well as the transplantation surface antigens responsible for graft rejection, initially used to define the MHC. The former proteins are hematolymphoid differentiation antigens. Only the latter proteins are what immunologists typically refer to as MHC class I (or MHC-I) proteins; they are also termed serologically defined (SD) antigens and exhibit extreme polymorphism. Consequently, the Tla proteins and others like them are termed class IB (or class Ib) proteins and are encoded by "class I-like" or "nonclassical" or "class I-related" genes, in contrast to the class IA proteins, which are the conventional, polymorphic MHC-I polypeptides. Those are the transplantation antigens K, D, and L, which are encoded by genes in the K and D regions of the H-2 complex. (The L antigen is encoded in the D region.) Most class IB molecules are of unknown function. Both types of gene products associate noncovalently with another protein, β_2 microglobulin, which is encoded on another chromosome. Actually, when people speak of an MHC-I protein, they often mean the functional protein consisting of both the MHC class I gene product and β_2 microglobulin, rather than just the MHC-I

MHC. Furthermore, in humans the MHC is known as the HLA complex for historical reasons, and the class I and class II genes also bear different names. However, since it is essentially the same (albeit polymorphic) molecule as for other species, I will use "MHC" throughout this dissertation instead of "HLA", even when referring or potentially referring to humans.

```
      0 ─╫─□──□──□────□──□───(□─□──□─□)──(□─□)──────□────□──□──

marker loci   K    Ab Aa    Eb Ea     Slp Ss Bf C2    D  L     Qa-2,3  Tla Qa-1

class:        I    II II    II  II     III III III III  I  I     I        I   I

subregion:         A  B J     E        C

region:       K           I                        S          D      Qa-2,3   Tla  Qa-1

complex:              H-2                                          Tla
```
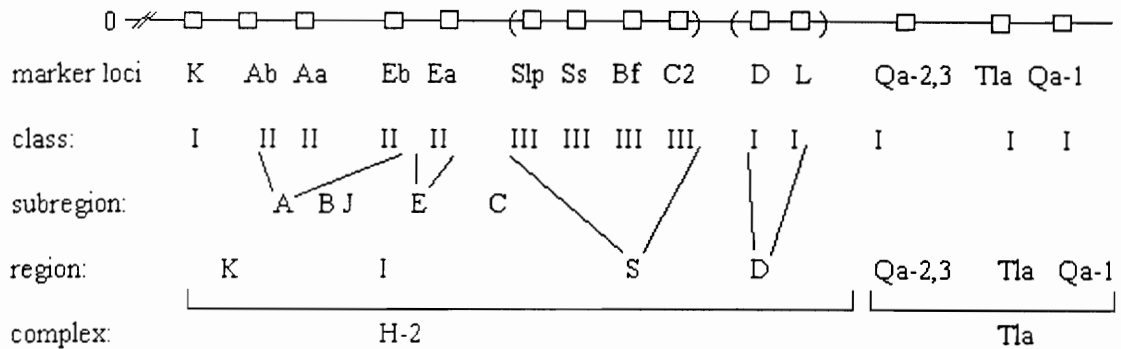
Figure 1. Schematic diagram of the MHC complex on mouse chromosome 17. *For the purpose of this dissertation, the most important point is that the I region encodes the class II genes.* Other class II genes encoding a proteasome complex, a peptide transporter, and other products are not shown for simplicity. Numerous other genes or pseudogenes are also present in the Tla, again not shown for simplicity. Adapted from (2) with corrections.

gene product. In this case the class I polypeptide is termed the heavy chain and the β_2 microglobulin the light chain. Furthermore, as if to add to the potential confusion, the K, D, and L antigens – the MHC-I polypeptides – are all essentially the same: they are all integral membrane glycoproteins ranging in molecular weight from 40 to 45 kDa, all have (in common with other class I proteins) three extracellular domains, a transmembrane domain, and a cytoplasmic domain, all share the same conserved interaction regions for CD8 molecules (unlike the class IB proteins), all exhibit extreme polymorphism but only in their peptide binding domains, and all have the same function: in conjunction with β_2 microglobulin, to present a peptide fragment to a T cell receptor (specifically one complexed with the CD8 molecule, typically found on cytotoxic T cells).

The immune response associated (alternatively designated as *Ia* (2) or *Ir* (3)) gene family is synonymous with the H-2 class II set of genes. These genes are located in the I

region of the H-2 complex of the MHC, which consists of subregions A and E (as well as B, J, and C, which are probably mapping artifacts). These code for the MHC class II molecules, which, like the MHC-IA molecules, exhibit extreme polymorphism in the peptide binding domains of their encoded proteins. The I-A subregion codes for the α and β chains of the I-A functional protein as well as the highly polymorphic β chain of the I-E MHC-II, whereas the I-E subregion codes only for the less polymorphic α chain of the I-E MHC-II. The general shape of MHC-I and MHC-II molecules is the same, except that MHC-II molecules do not use the β_2 microglobulin protein, and they are more open at the ends of the peptide binding groove, allowing greater heterogeneity of peptide lengths. Instead, both chains (α and β) are about the same size and are roughly symmetrical. Together they form a functional MHC-II protein, which presents a processed peptide to a T cell receptor (specifically one complexed with the CD4 molecule, typically found on helper T cells). Hence, an I-A gene is for a class II protein and should not be confused with an MHC-IA gene. Whether mixed haplotype heterodimers occur (e.g., H-2Aα^kEβ^k; see below) is controversial (3).

Inbred mice have been used to study the MHC. By inbreeding it is possible to establish a nearly uniform genetic background for a given inbred strain (e.g., B10), and by crossing such inbred strains with repeated backcrossing with a parental strain and selecting for recombinants of interest it is possible to establish congenic strains, such that they have the region of interest (e.g., the MHC) of one parental strain on a genetic background of the backcrossed parental strain. Such mice are designated as, e.g., B10.A, where B10 is the background strain and A is the donor strain (2). (Further appropriate breeding can give homozygous recombinant congenic strains, which differ from the

parental strains by just a few genes in the MHC.) A haplotype is the set of alleles found at two or more genetic loci on a single chromosome in a given individual (4). Because responsiveness to T cell epitopes is determined by the MHC haplotype of the animal, the proper choice of haplotype is critical to the success of a study involving T cell epitopes. H-2 haplotypes in inbred mice are arbitrarily designated by letter superscripts, so that an animal that has the k haplotype is designated as H-2^k. Except for my earliest pilot studies, all of the animal studies described in this dissertation use B10.A mice (H-2^a haplotype on a b background). These mice are a congenic strain derived from A/WySn as the H-2 donor and B10 as the background (2); the A strain (either A/WySn or A/J[‡]) was derived from (k x d) F1 mice, with recombination occurring between the E and S regions of the H-2 complex (3). Hence, B10.A mice are of the H-2^a haplotype, but this haplotype shares the same I-A and I-E alleles as other strains also derived from the H-2^k haplotype, namely I-A^k and I-E^k. Note that individual loci retain the designation of the founder strains, so that the full catalog description of the loci for the H-2^a haplotype is $K^k Ab^k Aa^k Eb^k Ea^k S^d D^d L^d Qa\text{-}2^a T18^a Qa\text{-}1^a$ (5). It is also potentially confusing that k refers to a commonly used haplotype, whereas the K region of the H-2 codes for MHC-I K antigens, so that I-A^k and I-E^k molecules are both MHC-II polypeptides (α and β chains) encoded by a mouse possessing k alleles at these loci.

Types of epitopes

For B cells the principal biomolecule is an antibody, which can exist in one of several antibody classes and can be membrane bound or secreted. Regardless of class, an

---

[‡] The /WySn or /J suffix simply means that this breed has been maintained for at least 20 generations at the particular breeding facility. Such mice are in principle the same but

antibody consists of a homodimer of heterodimers: there are two light chains and two heavy chains. (The class is determined by the heavy chain.) Both the light and the heavy chains have constant regions that are encoded by germline genes and also variable regions that are encoded by genes resulting from combinatorial shuffling of a set of germline genes with a specific recombinase. Within the variable region there are regions of lesser variability from one antibody molecule to another that are known as framework regions, and also other regions that show extreme variability, known as hypervariable regions. It is these hypervariable regions that impart antigenic specificity, and they are consequently also known as complementarity determining regions (CDRs). For T cells the principal biomolecule is the T cell receptor (TCR), and the T cell epitopes that it recognizes are linear peptide fragments displayed in the groove of an MHC-I or II molecule. TCRs are heterodimers of two roughly equally sized polypeptide chains, an α chain and a β chain, or else a γ chain and a δ chain. (γδ-TCRs are less common and much less understood than are αβ-TCRs.) As with antibodies, TCRs also possess CDRs, three on the α chain and three on the β chain. Most CDRs of antibodies and probably also of TCRs fall into certain classes or families; however the third CDR of the heavy chain (and the third CDR of the β chain) does not fall into a particular class, being the result of V-D-J gene rearrangements (6). Consequently the CDR-H3 exhibits the most variability of antibody CDRs and plays a key role in antigen binding (7).

As mentioned above, epitopes are the regions of antigens that are recognized by immune biomolecules. For antibodies these epitopes can be regions of an antigen that are spatially near each other and can be either contiguous or noncontiguous in the amino acid

---

could have evolved slight differences.

sequence of a protein antigen, for example. Hence, the B cell clonal population recognizes molecular shape and uses that to distinguish self antigens from foreign antigens.[§] T cells, in contrast, distinguish self from non-self by recognizing genetic information in the form of a peptide fragment that has generally been derived from either a self or a foreign protein. Such peptides are T cell epitopes. For most vaccines it is important to get a T cell dependent response, which requires the use of suitable T cell epitopes either as individual peptides or still incorporated into the parent protein.

T cell epitope mimicry

Although peptides have been used as immunogens for two decades, most of these studies have examined their use as B cell epitopes, i.e., can a polyclonal anti-peptide antibody response crossreact with the parent protein? Undoubtedly part of the reason for this is historical: antibodies were discovered many decades before TCRs and are easier to assay. Hence, the first studies involving peptides as epitopes used them as haptens coupled to a carrier protein. Later, in 1988 James Tam found that peptide epitopes could be joined together into a branched oligomer, known as a multiple antigenic peptide (MAP), and that one could dispense with carrier proteins using such a construct (10). Also in the late 1980s it became clear that T cell epitopes were different in their nature from B cell epitopes; they were always contiguous and were not affected by protein denaturation. Consequently in the early 1990s various investigators examined MAPs (reviewed in (11)) and compared them to the classical carrier protein approach and to monomeric peptides. For the most part MAPs were found to be superior to monomeric

---

[§] Self vs. nonself discrimination is a widely used terminology in the immunological literature but is not without some debate (8, 9). While I acknowledge the existence of this debate, I will not join it and will use this terminology as a convenience.

peptides and comparable to carrier proteins. These studies in which MAPs were compared against carrier proteins generally used keyhole limpet hemocyanin or some other foreign protein widely used in immunological studies, since that was what had been done in the past in generating anti-peptide antibodies and the authors of those studies were concerned with comparing the new technology against the traditional procedure. However, those comparisons were all somewhat unfair, "apples to oranges" comparisons since the T cell epitopes used in the MAPs were not from the same antigen as the carrier protein. Consequently we decided to investigate explicitly how well an immunodominant T cell epitope can replace its parent carrier protein in terms of generating a strong, T cell dependent antibody response. These studies comprise Chapters 3 and 4 of this dissertation.

B cell epitope mimicry

Although the immune system is designed for protecting against disease, it too can be pathological. Immune system pathologies include infections, cancers, insufficient immunity, and autoimmunity. In autoimmune diseases and in lymphocyte cancers it would obviously be advantageous to specifically target cytotoxicity to the clones responsible for the pathology. Such targeting requires that there be molecular differences that set the pathological clones apart from healthy cells.

Idiotopes are defined serologically as the epitopes on the variable regions of antibodies that are recognized by other, anti-idiotope antibodies (12). The complete set of idiotopes on a given antibody constitutes the idiotype (Id) for that antibody. Because they are unique to a given clone, idiotypes are ideal targets for those cases in which a particular clone is undesirable, such as in multiple myeloma, non-Hodgkin lymphomas,

leukemia, and certain autoimmune diseases. For a peptide vaccine to function as a B cell epitope mimic it is essential that there be crossreactivity with the parent protein, in this case the antibody that defines the pathological clone. Hence, our B cell epitope mimic was also an idiotope mimic.

The advantage of using idiotypes as targets is also their disadvantage: because they are unique, therapies need to be customized to each patient. Various groups have investigated the use of anti-idiotype antibodies in humans and in mice as a means for targeting a given clone for over two decades (13-17). These approaches can be divided into dichotomous categories: either one could generate anti-Id molecules (usually antibodies) from outside the patient and then treat the patient with such anti-Id molecules, or else one could vaccinate the patient using the patient's Id but in a form which will stimulate the immune system to mount a response against it. Both approaches seem to be effective, but because more is now known about immunology in general and because the latter, patient vaccine approach has the very significant advantage of not requiring antibody purification, the latter approach is now more popular. Within the patient vaccine approach, several approaches can be taken. Ideally one would like to simply use cDNA made from a tissue biopsy and not deal with protein purification at all. This is possible with peptide mimics of the major idiotopes (13, 18-24) and, more recently, with DNA vaccines (25-27).

The initial goal for the B cell mimicry aspects of this dissertation was to generate anti-idiotype antibodies against a murine model antibody. Specifically, we were interested in examining quantitatively the question of how well a cyclic peptide mimic of the heavy chain's CDR-H3 could replace the parent protein, i.e., how well an idiotope

mimic can replace an entire idiotype in terms of an anti-idiotype antibody response, thereby extending an earlier study in the literature (22).

Specific aims

As noted above, we hypothesized that the immunodominant T cell epitope from a commonly used carrier protein could effectively replace the use of the intact parent protein in terms of generating a T cell dependent response. We also hypothesized that a peptide mimic of a key idiotope, based on the third CDR of the heavy chain, would be a suitable antigen for generating crossreactive antisera. To test these hypotheses we set out to accomplish the following specific aims:

1. To use molecular graphics as an aid to picking the best sequence for use as a helper T cell epitope in B10.A mice. In particular, we wanted to know which residues from the p46-61 tryptic digest peptide played key roles in binding to the MHC-II ($I-E^k$) and to use this knowledge to extend or shorten the peptide as appropriate.

2. To use molecular graphics to design a peptide mimic of the CDR-H3 of a model antibody, BV04-01.

3. To use molecular modeling to evaluate the dynamics of an intact idiotype under two different solvation treatments: generalized Born implicit solvation and particle mesh Ewald explicit solvation.

4. To directly compare the potency of a peptide based on the immunodominant T cell epitope of a carrier protein with the intact carrier protein itself in terms of generating a strong T cell dependent response in vivo.

5. To use a peptide mimic based on the CDR-H3 of a model antibody, together with a carrier protein or a peptide based on the immunodominant T cell epitope of such a carrier protein, as an antigen against which crossreactive antibodies were to be generated, and to directly compare the crossreactivity of the antisera of mice immunized with the peptide mimic (the idiotope) with the antisera of mice immunized with the idiotype (similarly derivatized so as to make it foreign to the mouse immune system).

The first two specific aims are described in Chapter 2. As noted in Specific Aim 2, the antibody initially chosen for the purpose of evaluating idiotope mimicry was BV04-01, an IgG2b (κ light chain) derived from a murine model of systemic lupus erythematosus. This antibody proved to be difficult to work with, so later I changed the Id protein to be the Fab' fragment of 9-40, an anti-fluorescein murine IgG1. This is the focus of Specific Aim 5, and the results of that study are given in Chapter 5 of this dissertation.

Chapter 6 deals with Specific Aim 6 – how well one can model the structure of an Fv fragment, that is, the variable portion of a Fab fragment of an antibody. This builds upon similar work in Chapter 2. The scope of this modeling is strictly structural; it is to improve upon homology models by taking time averaged structures as a model for the solution structure of an antibody. I hope to publish this work along with ongoing and future work involving Ab-Ag binding free energies, but those studies are beyond the scope of this dissertation. Specific Aim 4 is the subject of Chapters 3-4.

Finally, Chapter 7 is a discussion of the conclusions of this dissertation as a whole and suggestions for future work. Because Chapters 3-4 have been submitted for

publication and Chapters 5-6 are intended to be submitted for publication, they are written as complete units with conclusions germane to those chapters. Consequently much of the future work mentioned in Chapter 7 pertains to further molecular modeling computational experiments.

CHAPTER 2

STUDIES WITH BV04-01 AS MODEL SYSTEM

This chapter discusses the original molecular modeling work on the CDR-H3 loop of anti-ssDNA antibody BV04-01, as well as the rationale and results for some of the wet lab work involving this antibody. Not all of the synthetic experiments are described since that would involve much discussion and details of a model system (BV04-01) which was eventually abandoned anyway. Nevertheless, the work with BV04-01 did provide the rationale for all the subsequent work, and there were some interesting experiments performed which I would like to describe.

Initial molecular modeling studies: MD and MM simulations

of a series of CDR-H3 peptide mimics

Abstract

Molecular dynamics (MD) simulations were performed on a series of cyclized peptide mimics of the third hypervariable region of the heavy chain (CDR-H3) of monoclonal Ab BV04-01, with the conformation of the peptide in the trajectory saved as molecular snapshots at 1 ps intervals. The initial conformations of these peptide mimics (CDQTGTAWFAC, CNQTGTAWFAC, and CQTGTAWC) were based on the liganded and the unliganded crystal structures of the Fab fragment of BV04-01. The simulations were performed on the peptides in the disulfide-bonded, cyclized state, conjugated to a

Lys via the crosslinker disuccinimidylglutarate, with the Lys atoms constrained and the crosslinker atoms restrained with a tethering function as an approximation to a carrier protein. All systems were hydrated and simulated using periodic boundary conditions. A 30 ps dynamics run was performed with snapshots taken at 1 ps intervals. These were minimized and compared against each other and against the native crystal structure of the CDR-H3. Modeling results indicate that within the time frame examined each set of conformers shows rms deviations from each other and from the initial starting structures that are within typical resolutions found by X-ray crystallography and roughly within a factor of 2 of the rms deviations of the liganded and unliganded structures in the first place. Hence, it appears that conformational variabililty of these peptides is low enough for them to serve as acceptable mimics for use in vaccines, although a longer simulation time would have been better.

Background and purpose

Central to the antigenicity of a peptide is the shape that it presents to the immune system. As discussed in Chapter 1 and later in Chapter 5, the best idiotope for a peptide mimic is the CDR-H3. Some early studies using a linear peptide mimic of this region were unsuccessful, however (Prof. David M. Kranz, University of Illinois at Urbana-Champaign, personal communication). One possibility for this result is that the peptide exhibited too much conformational flexibility, so that the immune system did not encounter a single antigenic hapten. We hypothesized that a cyclic version of such a peptide might instead be a better mimic, and desired to study the conformational mobility of the peptide to see how it relates to the conformation in the parent antibody. The goal of this initial study was to get some measure of how well such peptides should mimic the

original BV04-01 CDR-H3. The expectation was that a disulfide bridge would limit the set of conformers that would be presented to the immune system when using these peptide mimics as B cell epitopes in vaccines.

The antibody chosen for this purpose was BV04-01, an autoantibody (against ssdT) derived from a murine model of systemic lupus erythematosus. Besides being an autoantibody, for which we hoped that it could serve as a proof of principle for anti-idiotype targeting in the context of an autoimmune disease, BV04-01 has another important advantage: the crystal structures of both the liganded (with dT_3) and the unliganded Fab fragments are available (28). Our initial goals in molecular modeling were (1) to use molecular graphics as an aid to picking the most appropriate peptide mimics, and (2) to use molecular dynamics as an aid to understanding the similarity of the peptide mimic to the actual CDR-H3 loop.

The CDR-H3 of BV04-01 is a hairpin loop. This loop is mostly solvent exposed; however, the C-terminal residue in this region (Tyr H110 by strict numbering or Tyr H102 by the Kabat numbering scheme (29)) is not well exposed. This residue was replaced by Cys in our peptide mimic. An N-terminal Cys was also added in order to allow cyclization through disulfide formation. Thus, this constituted one of our peptide mimics (CDQTGTAWFAC).

The molecular graphics provided insight into two other reasonable peptide mimics. In the crystal structure the D in the CDR-H3 (Asp H95, Kabat numbering) makes a salt bridge with Arg H50, which would partially neutralize the charge density around H95. This suggests that a $D \rightarrow N$ mutation might work as well or better as the original sequence, and also has the significant synthetic advantage that there is only one

carboxylic acid group through which attachment of the peptide mimic via standard carbodiimide chemistry could occur. In that case there is no possibility of coupling through the Asp side chain. Since we ultimately desired to synthesize these mimics and incorporate them as actual immunogens, we considered this sequence as well. Finally, based on the computer graphics display we could see that cyclization through a shorter peptide could still encompass the most accessible residues of the CDR-H3, so we designed a third peptide mimic, CQTGTAWC.

Methodology

We used a Silicon Graphics Iris Indigo XS24 4000 to run the molecular graphics program *InsightII* (formerly BIOSYM Software, now Accelrys) Version 2.3.5 as an aid to chosing which amino acids to include. MD is sensitive to the starting conditions, and the most reasonable starting conditions are the liganded and unliganded crystal structures (1CBV and 1NBV respectively in the Protein Data Bank) for each of the three sequences, giving six simulations. The nonrelevant residues were deleted. The flanking residues (e.g., 100H and 110H) were changed to cysteines and then disulfide bonded. The resulting cystine was minimized to a 0.001 maximum rms derivative using conjugate gradients and the default consistent valence force field (CVFF) while keeping the other atoms fixed to preserve the native structure of the peptide using the software *Discover* Version 94.0 (Biosym/Accelrys). Then a minimized homobifunctional crosslinker, disuccinimidyl glutarate (DSG), was attached to the N terminus, and a Lys was attached to the other carbonyl of the DSG. This was again minimized, again keeping the peptide fixed (except for the Cys residues). Then the molecule was hydrated and put in a box with space group 3 symmetry. Minimum image periodic boundary conditions were

applied. Each box had at least 3 Å on each side of the molecule to allow sufficient hydration. Because the molecules folded up into different conformations in vacuum (and also one of the peptides is smaller than the others), the boxes for the six simulations were not all the same size and shape. Since the waters add most of the computational burden, this sharply cut down the computer time required for simulating the smaller and more compact molecules.

The hydrated molecule was then relaxed to a 0.05 maximum rms derivative, this time allowing the peptide and part of the DSG to freely relax while the Lys was fixed. This was done because the peptides had been synthesized and crosslinked with a large carrier protein (keyhole limpet hemocyanin, KLH) by means of disuccinimidylglutarate (DSG), which forms amide bonds between the N terminus of the peptide and Lys side chains of the carrier protein. Since it was computationally impractical to try to include the structure of KLH in the simulations, the fixed Lys was intended as a simplistic approximation. The DSG carbonyl closest to the Lys had a force constant of 100 kcal/Å, the methylene group after this had a force constant of 50 kcal/Å, and the one after this had a force constant of 25 kcal/Å. Finally, a dynamics run was initialized and performed for 30 ps simulation time at a temperature of 310.15 K using the default constant volume, constant density ensemble, with snapshots of the system taken at 1 ps intervals. These were minimized (again using CG and CVFF but to a 0.05 rms derivative) and compared against each other and against the starting liganded and unliganded CDR-H3s.

Results

All of the peptides show a jagged appearance in graphs of total energy vs. frame (i.e., minimized conformer). Also, the cluster graphs show approximate families of

conformers, which tend to correspond with the energy vs. frame graphs. Cluster graphs show the rms deviation of a given frame versus every other frame in that simulation (i.e., versus every minimized snapshot) by assigning ranges of rms deviations to different colors. (They are actually three dimensional plots with the z axis perpendicular to the viewer.) Frames of low rms deviation may or may not be separated by clusters of higher rms deviation. Some of the total energy vs. frame plots show a general decrease in time (i.e., frame), indicative of a presently relaxing system. This implies that the starting condition was still exerting an artifactual effect, so that 30 ps was insufficient for achieving good sampling of the low-energy conformers. Maximum rms deviations of conformers (i.e., the highest color-coded cluster in the cluster graphs) is shown in Table 1. A typical energy and cluster graph pair (for the first entry in Table 1.) is shown in Figure 2. For comparison, a 1.169994 Å rms difference is found between the initial apo and holo forms of the peptide CDQTGTAWFAC (i.e., the unliganded and liganded CDR-H3 loops but with flanking cysteines).

Conclusions

The energy vs. frame plots show qualitative agreement between total energy and conformers with little rms difference from each other. The rms differences between the minimized conformers are within typical values for resolutions found by X-ray crystallography and roughly within a factor of two of the rms differences between the initial, native apo and holo structures. (The 1CBV structure was solved to 2.66 Å and the 1NBV structure to 2.00 Å.) The present results show the extent to which a typical, small, disulfide-linked peptide can vary in its conformations. The limit for which good antigenicity can be attained has not been determined in the present study. Other than the

Table 1. Early MD results.

Peptide and initial conformer	Rms deviation, Å	Comments
CDQTGTAWFAC apo	1.80	possibly insufficient time, 1st frame is second highest in energy
CDQTGTAWFAC holo	2.57	ibid.
CNQTGTAWFAC apo	2.40	likely sufficient time, 1st frame is highest in energy
CNQTGTAWFAC holo	2.57	possibly sufficient time, 1st frame is highest in energy
CQTGTAWC apo	2.14	likely insufficient time, 1st frame is highest in energy
CQTGTAWC holo	2.14	possibly sufficient time, 1st frame is highest in energy
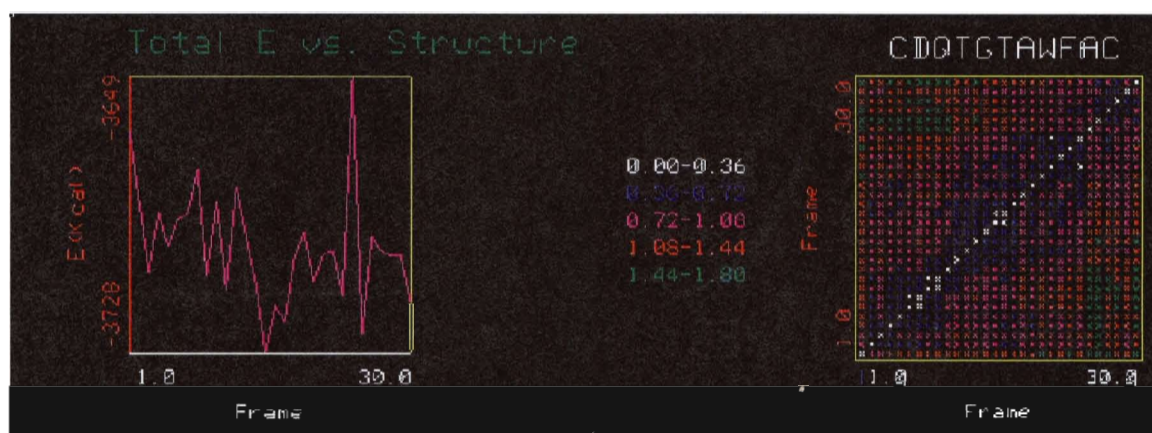
Figure 2 Sample energy versus time and cluster graph for one of the six simulations listed in Table 1.

native holo and apo crystal structures, which were used as starting structures, none of the other, computed conformers are of special interest in themselves.

It is apparent that the simulation time was insufficient to adequately sample a representative number of low energy solvated conformers, with maybe one exception. Hence, somewhat more time, perhaps 100 ps, would have probably been demonstrative of an absence of a strong initial conformer effect. A complete study of the conformations which the present peptides could attain would require far more computer time than that used in this study.

Pilot studies with peptides coupled to KLH

Synthesis and immunization methodology

Each of the above three peptides were synthesized at the University of Utah's Peptide Facility (now the Peptide/DNA Facility) by standard Fmoc solid phase peptide synthesis, purified by HPLC, cyclized by air oxidation of the disulfides, and analyzed by MALDI-MS. Each was then coupled to the commonly used carrier protein keyhole limpet hemocyanin (KLH) via the homobifunctional crosslinker disuccinimidylglutarate (DSG; Pierce Chemical Co.) after the manner of the DSG instructions provided with the product. Female BALB/c mice were immunized intraperitoneally or subcutaneously with these immunogens in Hunter's adjuvant (1st, 2nd, and 3rd injections) or Freund's incomplete adjuvant (subsequent immunizations). Bleedings were performed approximately 2 weeks later.

ELISA results

Titers were measured by a sandwich ELISA with the coating antigen being either BV04-01 Fab or one of the peptides coupled to another protein (bovine serum albumin,

BSA). Many of the ELISAs exhibited an edge effect in which the outside edges were more strongly positive than they would be expected to be. This phenomenon necessitated considerable optimization and control reactions. Hence, the assay was sensitive but imprecise. Titer was defined as the maximum dilution at which a positive response could be distinguished from the background or negative control for an arbitrary confidence level by a many-one t test such as the Bonferroni t test or Dunnett's test. Mice were ranked based on both their absolute response to BV04-01 Fab and their preferential response to BV04-01 Fab relative to 9-40 Fab. Hence, the product of these two quantities was used to rank the mice (Figure 3).

Conclusions

From Figure 3 it can be seen that of 9 surviving mice (out of 15 originally) only one (mouse 1-0) showed a good anti-idiotype response. Two showed a mediocre response, and the others showed no specific anti-(BV04-01 Fab) response. Monoclonal antibody production was attempted but these attempts were unsuccessful for various
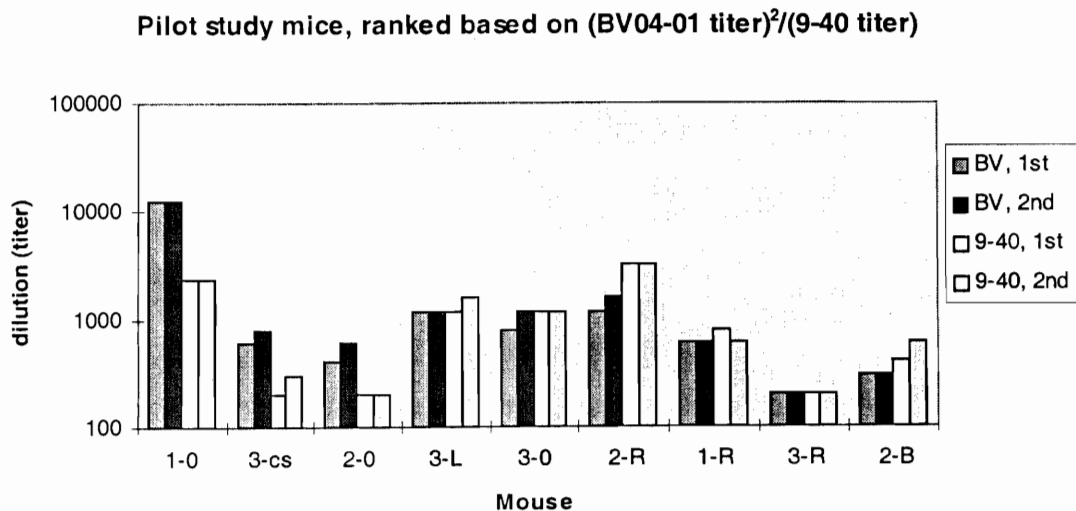
Figure 3. ELISA ranking of initial pilot study mice.

reasons. Although these studies had originally been intended as the stepping stone for a discovery-oriented dissertation project that made pharmaceutical use of anti-idiotype antibodies (as opposed to a more hypothesis-driven project), they had to be regarded as pilot studies only. However, they did offer data that could be used for power calculations.

Why was the response so low? Because KLH is a huge protein (ca. 100 kDa in its monomeric form, and it oligomerizes), it was very difficult to see how much peptide actually got conjugated. Light scattering was attempted but not useful. Since all the mice eventually died with no monoclonal antibodies, and since KLH has the analytical difficulties that it does, I decided to start over with another protein, chicken hen egg lysozyme (HEL). HEL is a model protein that has been extensively studied both chemically and immunologically, as well as being small, inexpensive, possessing 6 lysine residues through which coupling could occur, and possessing an immunodominant T cell epitope that lacks Lys or Cys (important so that the T cell epitope would not be disrupted by coupling to it B cell epitopes, i.e., peptide mimics of the CDR-H3 loop), and that is immunodominant in several mouse strains, including B10.A (and likely related strains with the same I-E and I-A alleles).

Qualitative modeling with H-2^k I-E molecule

The crystal structure of the I-E^k molecule was solved by Daved Fremont and others (30). Dr. Fremont kindly supplied me the coordinates prior to releasing the final copy to the Protein Data Bank. They were used in conjunction with *InsightII* and the reference article to determine that the most important residues in the peptide NTDGSTD**Y**GI**L**Q**I**NS**R** (p46-61, the immunodominant T cell epitope of HEL in B10.A

mice and likely other strains also possessing I-A^k and I-E^k molecules) were the ones shown above underlined in bold font. The C terminal R fits into the narrow hydrophobic pocket at P9, making a salt bridge with I-E^k's Glu$^{\beta 9}$. Among the peptides that are known to bind to murine I-E^k, this pocket has a strong preference for R or K (30). The pockets P6 and P4 are fairly accommodating to many residues and can accommodate the I and the L respectively. P1 is a medium sized hydrophobic pocket that can accommodate the Y. This simple modeling gave a better feeling for which residues would be indispensable in picking the exact sequence for the T cell epitope peptide.

Use of BV04-01 as model idiotype

Rationale and design considerations in synthesizing
idiotype-HEL conjugates

In order to compare the T cell epitope with HEL itself, we desired to have both the construct (Bep-Tep)$_4$-MAP, compared with the Bep-HEL, as well as the idiotype (Id) protein Id-HEL, compared with Id-(Tep), where the Id can be either the entire antibody or a fragment thereof that still retains at least the Fv portion. Because the Id and HEL are both proteins with primary amine groups present, it would be possible to use amine reactive crosslinkers to couple them to each other. That approach has the disadvantages of (1) difficult or potentially intractable work-up due to HEL-HEL coupling, Id-Id coupling, and higher order crosslinkings if done at high protein concentrations, (2) long reaction times and low yields due to crosslinker hydrolysis if done at low protein concentrations, and (3) diminished antigen binding activity due to HEL coupling near the antigen binding site and providing steric hindrance. Using a Fab' fragment would be the optimal choice because (1) it would allow amine and sulfhydryl heterobifunctional

crosslinkers to be used in a two-step synthesis, resulting in higher yields and no Id-Id nor HEL-HEL crosslinking, (2) it would couple the HEL away from the antigen binding site, and (3) it would be relatively easy to analyze by PAGE or MALDI-MS due to the molecular weights involved. The difficulty with that approach is that BV04-01 is an IgG2b, which, unlike other antibody classes, does not readily yield F(ab')$_2$ fragments with pepsin digestion. A third approach is possible because IgG has carbohydrate moieties that can be converted to aldehydes, allowing heterobifunctional crosslinking of the HEL with the carbohydrate (31). That approach has the additional advantage of coupling HEL away from the antigen binding site but the minor disadvantage of most likely generating anti-Fc antibodies. It also turned out to be difficult to analyze.

Overview of synthetic attempts

Each of the above strategies was pursued, but the first gave mixtures that were difficult to analyze with our available equipment. The second strategy, namely using Fab' fragments instead of intact antibody, was attempted with lysyl endopeptidase, which has been shown to achieve satisfactory yield with IgG2a antibodies (32). Some Fab' product was made with the IgG2b antibody BV04-01, but the yield was low and this was deemed not likely to be cost effective. Consequently the most attention was put on the third strategy, i.e., coupling through the carbohydrate moieties.

The initial approach was to use the amine and sulfhydryl reactive heterobifunctional crosslinker SPDP (Figure 4) to prepare SPDP-HEL, i.e., with HEL with the Lys side chains extended and ending with maleimides. The pyrridyl disulfide group of the SPDP was then removed with DTT to generate 2-pyrridylthione and HS-HEL. The Ig was oxidized with NaIO$_4$ to convert the terminal carbohydrate moieties to aldehydes, and
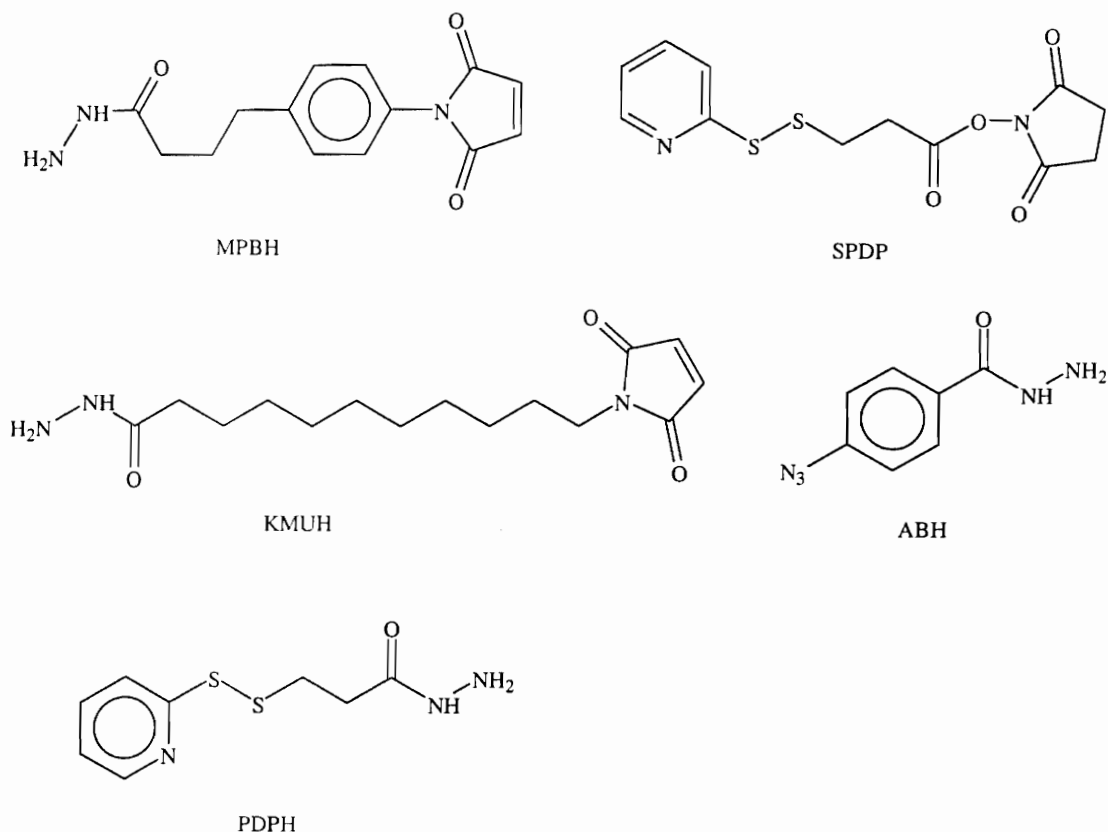
Figure 4. Structures of SPDP and some hydrazide containing crosslinkers mentioned in this dissertation (available from Pierce Biotechnology, Inc., Rockford, IL).

then reacted with MPBH to have maleimides attached to the Fc region. Finally, the HS-HEL was mixed with the MPBH-IgG. This reaction failed, however, and thus began dozens of diagnostic and alternative conjugation experiments.

The first step with the antibody, oxidation with $NaIO_4$, proceeded well. This is shown most clearly in the kinetics of this reaction (see Appendix A). The resulting hydrazone bond is unstable (again, see Appendix A for details). Other crosslinkers were also tried: KMUH, PDPH, ABH (Figure 4), as well as a couple that were not available commercially (described in Appendix A), as well as simply letting the HEL in high concentration form an imine linkage with the Ig^{ox}. Such linkages were tried both with

and without reduction of the imine with $NaCNBH_4$. Some couplings proceeded with at least partial success (e.g., with ABH), but it was difficult then to quantify the stoichiometry of the conjugate. Both Western blotting and ELISA can be quantitative with appropriate standards, which were lacking, but also which apparently suffered from a surprising crossreactivity between our polyclonal goat anti-(mouse IgG), HRP conjugate and HEL itself. Mass spectrometry should show such conjugation easily in principle, but in fact MALDI itself seemed to break the linkage between the Ig and the HEL.

Conclusion of BV04-01 as idiotype of interest

Although the IgG-HEL conjugate was made in some yield by various techniques, it was very difficult to quantify the yield. Since the B epitope hypothesis (idiotope vs. idiotype mimicry) could be tested by a Fab'-HEL coupling, without requiring MAPs (so that the use of zero-length crosslinkers to maintain similarity of coupling between the B epitope and the MAP as with the B epitope and the carrier protein is not an issue), and since the T cell epitope hypothesis could be tested without requiring Id-HEL coupling (or MAPs), we felt that it was better to switch to the Id of another antibody which could be made readily into Fab' fragments. For this purpose we chose 9-40, an IgG1 for which the optimization of Fab' fragment preparation had already been worked out in our laboratory. The disadvantages of switching were (1) that 9-40 is not an autoantibody, unlike BV04-01, so the immediate relevance to lupus and other autoimmune diseases is lost, and (2) my modeling work had been done with the CDR-H3 of BV04-01. However, the first disadvantage is trivial because this is only a model system to test specific hypotheses and no clinical relevance in lupus-prone mice to BV04-01 itself has been shown, nor was that

in the scope of my project. The second disadvantage was likewise very weak since it would be desirable to do longer, more extensive computational experiments that were also hypothesis driven. Those studies constitute the succeeding chapters of this dissertation.

CHAPTER 3

HOW WELL CAN A T CELL EPITOPE REPLACE ITS PARENT

CARRIER PROTEIN? PART 1: AN ANOVA STUDY

Abstract

Purpose

Peptide vaccines require T cell stimulating epitopes in order to generate an effective T cell dependent response. The goal of this study was to see how well an immunodominant T cell epitope can replace its parent protein in terms of generating an antibody response.

Methods

The immunodominant T cell epitope (modified by replacing Cys-64 with Ser, thus: GSTDYGILQINSRWWSND) for B10.A mice (H-2^a) from chicken hen egg lysozyme (HEL) was synthesized and conjugated to the Fab' fragment of anti-fluorescein monoclonal antibody 9-40 using SMCC as a heterobifunctional linker. Similarly, the 9-40 Fab' fragment was coupled to the intact HEL molecule. Both sets of constructs were injected subcutaneously into B10.A mice. Control mice were immunized with 9-40 or with a noncovalently attached mixture of 9-40 and HEL on a roughly equimolar basis. ELISA was used to measure titers of specific anti-idiotype antibodies directed towards the 9-40 idiotype.

Results

Anti-idiotype antibodies were raised against 9-40 using the (9-40)Fab-HEL conjugate, but not for the control cohorts nor for the (9-40)Fab-(T epitope) conjugate ($p =$ 4.89 x 10^{-13}). These antibodies were crossreactive with idiotypically related clone 4-4-20 but not with ELISA controls BV04-01 nor BDC1.

Conclusions

A monomeric immunodominant T cell epitope conjugated to an immunologically silent protein is unlikely to provide an effective T cell dependent response. This result poses a challenge for the development of efficacious peptide vaccines and is explored more fully in Part 2 of this study (Chapter 4), dealing with the dose response functions of this epitope.

Introduction

Next to sanitation, vaccines are the most cost-effective means to improving public health. Early vaccines used live attenuated or heat-killed organisms for their success, but this approach is not suitable for widespread use for cases in which the organism cannot be easily grown in culture (e.g., malarial and schistosomal parasites). In these cases subunit vaccines are especially promising. Cancer vaccines are also particularly amenable to the subunit approach, since simply formulating killed cancer cells as a vaccine could potentially elicit immune responses against antigens that are not cancer specific. Subunit vaccines could be based on either entire proteins through molecular biology techniques, or simpler peptides that incorporate the epitopes recognized by T cells and by B cells, depending on the desired type of response (cytotoxic or humoral, for

example). Peptide vaccines in particular offer the advantage of not including those regions of a protein or virus not involved in immunity. The main difficulty with peptide vaccines is the need to overcome genetic restriction by extremely diverse HLA (MHC) haplotypes. Immunological understanding in the 1970s and '80s held that peptides and other haptens are not immunogenic unless coupled to a foreign carrier protein and that the size of the carrier protein somehow imparts immunogenicity. This idea still finds its way into the introductions of research articles and the technical support pieces of product vendor literature, but it is not size as such that imparts immunogenicity. Rather, foreign proteins possess within their primary sequence regions that are processed and then displayed in the binding groove of an MHC molecule, thereby alerting T cells that they have been derived from a foreign source (33). These T cell epitopes are linear peptides enzymatically derived from a protein and play an important role in the activation, tolerization, or ignorance of the immune system, and consequently much work has been done to elucidate the T cell epitopes for a number of proteins associated with various pathogens as well as in autoimmune diseases.

Once such T cell epitopes are identified, they can then be used as part of a vaccine formulation to activate cytotoxic T cells or to provide T cell help in the response against a separate B cell epitope. This has been done repeatedly in the case of multiple antigenic peptides (reviewed in (11, 34)), in liposomes (35-38), as tandem oligomeric repeats or linear peptides (39, 40), and as pendant groups from a polymeric backbone (41). Most such studies involve rodents with well-defined MHC haplotypes, but as noted above, individual T cell epitopes pose problems for consideration as vaccines in outbred populations such as humans. This difficulty is complicated by the fact that there are

dominant, subdominant, and cryptic T cell epitopes within a typical protein (reviewed in (42)). Fortunately there exist so-called promiscuous T cell epitopes which are recognized by a wide variety of MHC haplotypes (43). In any case, the question then arises as to how well an immunodominant T cell epitope can substitute for its parent carrier protein when used as part of a peptide vaccine formulation. To the best of our knowledge, no one has specifically investigated this issue.

We chose chicken hen egg lysozyme (HEL) to answer this question, as this protein is small (14.3 kDa), inexpensive, easily soluble, and very well characterized chemically and immunologically (44). Because the synthesis of the immunodominant T cell epitope would be more convenient if one did not need to bother with disulfide formation or side reactions involving crosslinker derivatization of Lys side chains, we decided to use the immunodominant T cell epitope in B10.A mice along with its flanking residues (but modified by replacing Cys-64 with Ser, thus: GSTDYGILQINSRWWSND) (45).

The simplest approach to evaluating how well a T cell epitope can replace its parent carrier protein would be to conjugate a hapten or an immunologically silent protein to either the epitope or the carrier protein and then to compare cohorts of mice for the immune response. Because we were also interested in preparing anti-idiotype antibodies in a model system with the ultimate goal of targeting pathological B lymphocytes for the patient-specific treatment of numerous diseases (such as hairy cell leukemia, various non-Hodgkin's lymphomas, multiple myeloma, systemic lupus erythematosus, Hashimoto's thyroiditis, insulin-dependent diabetes mellitus, Graves' disease, and Addison's disease), we decided to use the Fab' fragment of the murine anti-

fluorescein antibody 9-40 as the immunologically silent protein. 9-40 is a very well characterized murine monoclonal anti-fluorescein IgG1 (46, 47) available in our laboratory, for which preparation of Fab' fragments has been optimized. It is a good choice for anti-idiotype studies because its idiotype has been well studied (48); it is a member of a family of idiotypically crossreactive antibodies (49-51), including high-affinity antibody 4-4-20, for which the crystal structure of the liganded Fab fragment has been solved (52). A potential difficulty with 9-40 would be that it is derived from a different strain of mice than B10.A (specifically, BALB/c), so that there is the potential for an anti-allotype response that could be difficult to distinguish from an anti-idiotype response. However, because we used only the Fab' fragments in our immunogens instead of derivatizing the intact antibody with HEL (for example, through the carbohydrate moieties (31)), the epitopes responsible for an anti-allotype response are largely missing, and so this potential concern should not be too problematic. Our results fully support this supposition.

Materials and methods

Synthesis of (9-40)Fab'

The (9-40)F(ab')$_2$ was prepared by the method of Grey and Kunkel (53). In brief, the 9-40 IgG was digested by pepsin at 37 °C for 18 h using 0.1 M acetate buffer (pH 4.2) with an enzyme:Ab mass ratio of 1:33 (= 1/7.56 molar ratio). The reaction was quenched by addition of a few drops of 1.0 M Tris base to pH 8.0. The reaction mixture was then concentrated after SEC (PD-10, Amersham) to ~1 mg/mL; 1 mL was then used for subsequent modification. The resulting (9-40)F(ab')$_2$ was then cleaved in the same reaction vessel with DTT to generate (9-40)Fab'. Specifically, 220 μL of Tris buffer was

added to 1.0 mL of ~1 g/L (9-40)F(ab')$_2$ solution, vortexed, then 22 μL of 0.2 M EDTA

solution (in the same Tris buffer) was added and vortexed. Then 22 μL of the DTT stock

solution (0.1 M, freshly prepared in 1 M Tris buffer, pH 7.37) was added, vortexed, and

then put in the dark at room temperature for 1 h. Meanwhile, a PD-10 SEC column was

equilibrated with 0.1 M NaPO$_4$, pH 6.0, 5 mM EDTA. The protein was then eluted with

this buffer and appeared after ca. 1.5 - 4.0 mL. The purified (9-40)Fab' was then

measured by UV spectrophotometry and immediately reacted with the desired

electrophilic partner. For the (9-40)Fab' negative control this was iodoacetamide.

Synthesis and analysis of (9-40)Fab'-HEL

HEL was dissolved in pH 8.0 PBS and then derivatized with a large (~100-fold)

excess of SMCC (Pierce) for several hours at room temperature. Excess SMCC was

removed by SEC and the derivatized HEL was set aside until the (9-40)Fab' was made, at

which point it was immediately added to the (9-40)Fab' and allowed to react overnight.

Specifically, 1.2 mL of the freshly prepared (9-40)Fab' solution, 9.22 μM (ε = 47,600 M⁻

^{1}cm^{-1}), was added to 0.1 mL of 35 μM SMCC-HEL in pH 7.4 PBS and allowed to react

overnight at 4 °C. The reaction product was analyzed by several different techniques

including SEC, ELISA, SDS-PAGE, and MALDI-MS. SEC chromatogram fractions

were assayed for both 9-40 Fab' and HEL by ELISA. Fractions testing positive for both

were pooled, concentrated, and then characterized by SDS-PAGE. These techniques

indicated that although the conjugation reaction had been successful, the yield was

relatively low (20%, or less). The conjugate was not purified further because the 65 kDa

conjugate could not be resolved from the 50 kDa 9-40 Fab' using SEC. This was not

deemed a problem, however, because the underivatized antibody fragment was not

expected to be immunogenic (a postulate that was later confirmed by our control experiments). Subsequent preparations of the (9-40)Fab'-HEL were made using the same procedures and further validated by MALDI-MS.

Synthesis and analysis of (9-40)Fab'-(T epitope)

The T cell epitope GSTDYGILQINSRWWSND was made by batch Fmoc solid phase synthesis at a professional peptide synthesis service located on the University of Utah campus (the DNA/Peptide Facility) and was analyzed by RP-HPLC. This material was then derivatized with SMCC and again analyzed by HPLC (Figure 5). The putative product peak was confirmed by MALDI-MS (Figure 6) and then evaporated (Speedvac) to a solid. It was later redissolved in DMF and reacted with freshly prepared (9-40)Fab' at pH 6.0 at 4 °C. Later this material formed a precipitate. This precipitate was re-dissolved in TFA prior to MALDI-MS confirmation. It was diluted 1:10 with pH 10.0 Na_2HPO_4 buffer with a final pH of 7.5 - 8.0 (measured by ColorpHast strips, EM Science) prior to making an emulsion with Freund's adjuvant.

Immunization protocol - pilot study

Ten female B10.A mice (Jackson Laboratories, cat. # 000469) at 9 1/2 months were immunized with about 14 µg total protein of the (9-40)Fab'-SMCC-HEL preparation (based on a calculated extinction coefficient of 1.9719 $(g/L)^{-1}cm^{-1}$ for the 1:1 conjugate; see Appendix B), and five female B10.A mice were injected with half of this amount. The mice received about 60-70 µg total protein for the secondary immunization (with the second batch, assayed by ELISA). Freund's complete adjuvant was used for the first immunization and incomplete for the second. Bleedings were three weeks after the
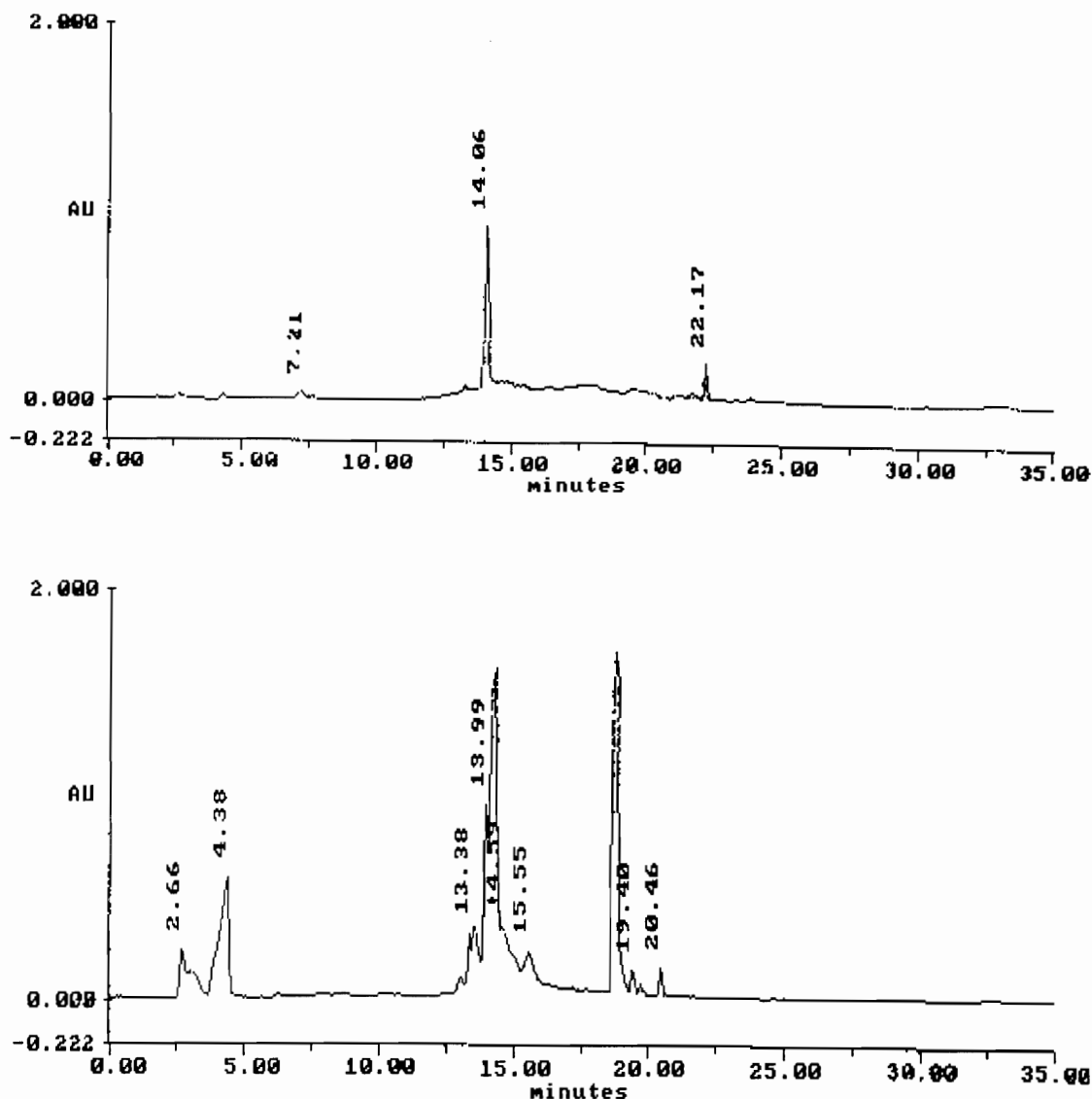
Figure 5. The top HPLC chromatogram is of the T epitope by itself; the bottom is of the T epitope + SMCC reaction mixture, the product at 18.72 min being the desired peak. This peak was confirmed by MALDI-MS. The T epitope mass was 2112.02; the measured mass for the product was 2334.93 (expected: 2333.28) as well as various (0-8) Na^+ peaks. Solvent A: water, solvent B: acetonitrile; 100 Å phenyl (Rainin) with C18 guard (Phenomenex). Gradient: 0-5 min, 5% B; 5-20 min, 5-100% B; 20-25 min, 100% B; 25-30 min, 100-5% B; 30-35 min, 5% B (wash). Diode array detection was used, but 280 nm detection is shown.
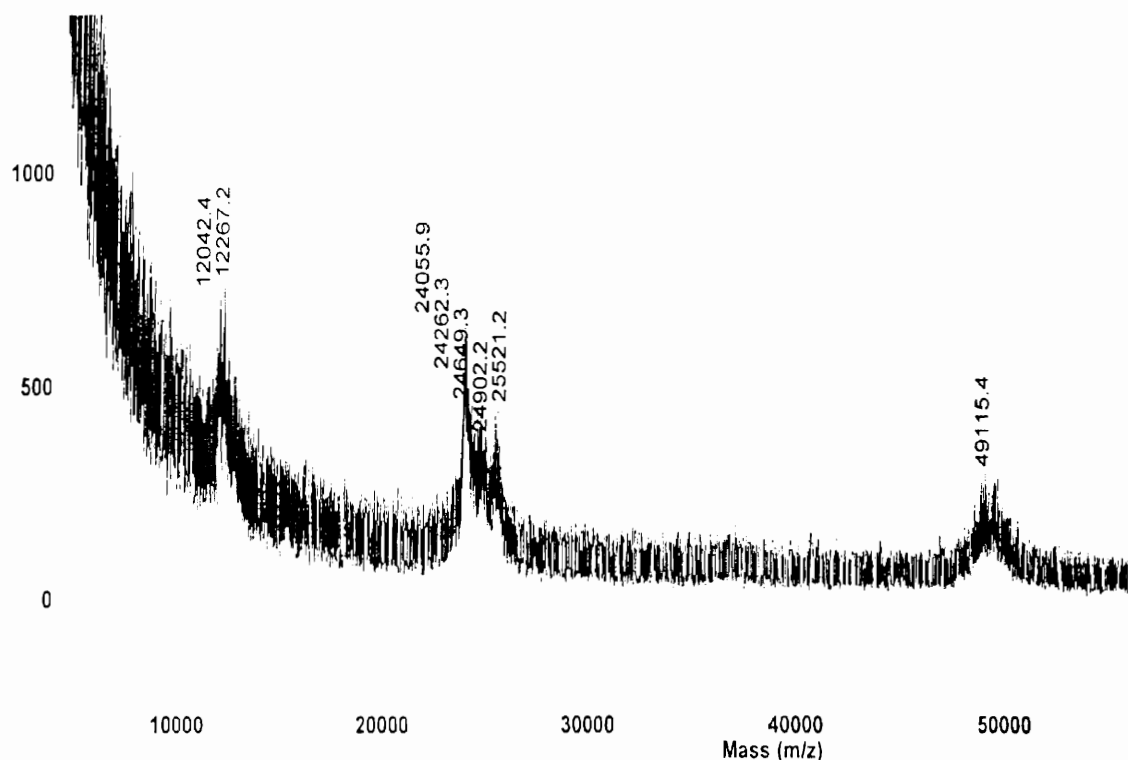
Figure 6. MALDI-MS of (9-40)Fab'-Ac (i.e., acetylated to prevent sulfhydryl re-oxidation) and of (9-40)Fab'-(T epitope), top and bottom respectively. The numbers are approximate due to the noise and peak width but are sufficiently accurate to determine that the synthesis succeeded.

primary immunization and 15 days after the secondary. As with the ANOVA study below, the research adhered to the "Principles of Laboratory Animal Care" (NIH publication #85-23, revised 1985).

Immunization protocol - ANOVA study

For each group ten female B10.A mice were injected subcutaneously with the above-mentioned antigens in a 1:1 (v/v) emulsion with Freund's adjuvant. Freund's complete adjuvant was used for the primary immunizations and incomplete adjuvant for the secondary immunizations. The mice were 11-13 weeks old for the Fab', Fab'-HEL, and Fab' + HEL cohorts and were 15-17 weeks old for the Fab'-(T epitope) cohort upon

their $1°$ immunizations. Assuming $\varepsilon = 1.9719$ $(g/L)^{-1}cm^{-1}$ for the (9-40)Fab'-SMCC-HEL preparation, 6.7 µg of total protein (estimated 1.3 µg of actual conjugate based on the yield cited above) were injected for the primary immunizations, and 17.23 µg total protein (estimated 3.4 µg of conjugate) for the secondary, with the same nominal molar amount being used for the negative control cohorts (9-40)Fab' and (9-40)Fab' + HEL. The animals were bled 14 days after the primary immunization. The secondary immunization was 6 weeks, 3 days after the primary, and the $2°$ bleeding occurred 14 days after the $2°$ immunization. The secondary immunization for the Fab'-(T epitope) cohort was 6 weeks, 6 days after the primary, with the bleeding 2 weeks after that.

Determination of antibody response by ELISA

A sandwich ELISA was used to measure the antibody response to the various vaccines. The capture molecules were Fab fragments (prepared by papain digestion as described in (54)) of 9-40, 4-4-20, BV04-01, or BDC1. Digestion times were based on our experience in preparing Fab fragments for each individual antibody. Specifically, digestion times of 15 min, 60 min, 30 min, and 30 min were used for 4-4-20, 9-40, BDC1, and BV04-01, respectively. These were adsorbed onto polystyrene 96-well microtiter plates (Nunc MaxiSorp™) for approximately 1 h, then washed with ELISA wash buffer (150 mM NaCl, 10 mM Tris, 1 mM EDTA, 0.01-0.05% Tween 20), then the serum was applied and incubated at room temperature for 1 h, then washed away, then the tracer antibody (goat anti-(mouse Fab) AP conjugate [Biodesign International]) was added and incubated for 1 h, then extensively washed away, and finally substrate (Blue Phos, KPL) was added and the absorbance read at 630 nm after 30 min.

Results

Pilot study response

The purpose of the pilot study was to verify that we could make anti-idiotype antibodies with a Fab'-carrier protein construct such as described above. In order to establish that the response seen was truly anti-idiotypic, we used as controls the Fab fragments of three other murine antibodies (4-4-20, BV04-01, and BDC1) as coating antigens in the ELISAs. 4-4-20 is another anti-fluorescein antibody and is known to be idiotypically crossreactive with 9-40 (47, 49). BV04-01 is an anti-(ssdT) autoantibody derived from a murine model of lupus and shares the same framework regions on the heavy chain and almost the same light chain as 9-40 and 4-4-20 (28, 47). BDC1 is also an anti-fluorescein antibody (IgG2a, κ) that was developed in our laboratory but is not idiotypically crossreactive with 9-40 or 4-4-20. We performed full titrations and observed a very distinct "serum effect" in which the maximal response was not at the lowest dilution (Figure 7, Panel A). It was also clear from these pilot studies that the mice were generally giving a good anti-(9-40) response, although the interanimal variability was high. Furthermore, the response was anti-idiotypic as evidenced by the low anti-(BV04-01 Fab) and anti-(BDC1 Fab) responses (Figure 7, Panels B and C respectively). In fact, while 4-4-20 is known to be idiotypically crossreactive with 9-40 and the response is as one might expect (Figure 7), one mouse did show a weak anti-(9-40 Fab) response but no anti-(4-4-20) response, thus clearly demonstrating the fine specificity achievable using this conjugate.
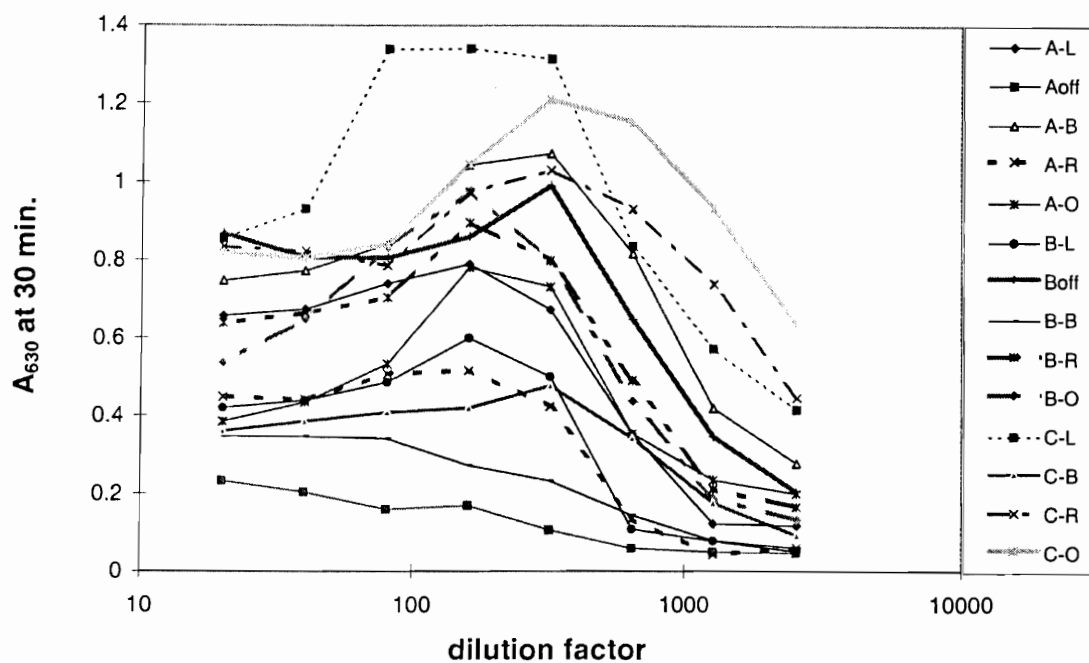
Panel A
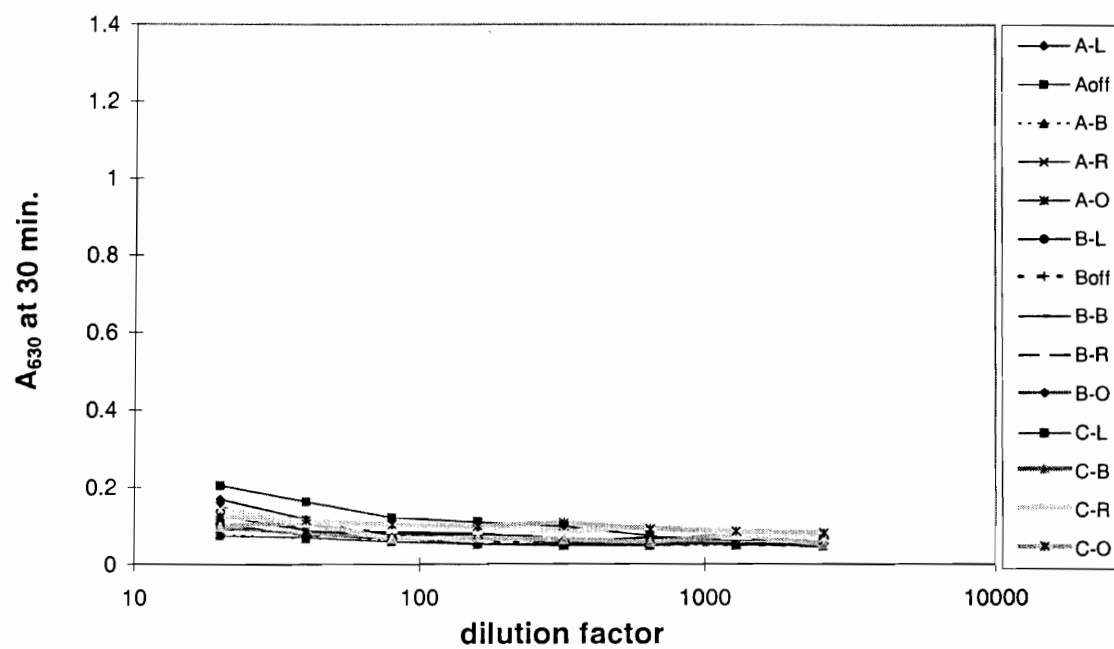
Panel B

Figure 7. Full titers for 2° anti-idiotype responses for all mice in pilot study (1st cohort after 2nd immunization.) The Fab coating antigens were 9-40 (Panel A), BV04-01 (Panel B), BDC1 (Panel C), and 4-4-20 (Panel D).
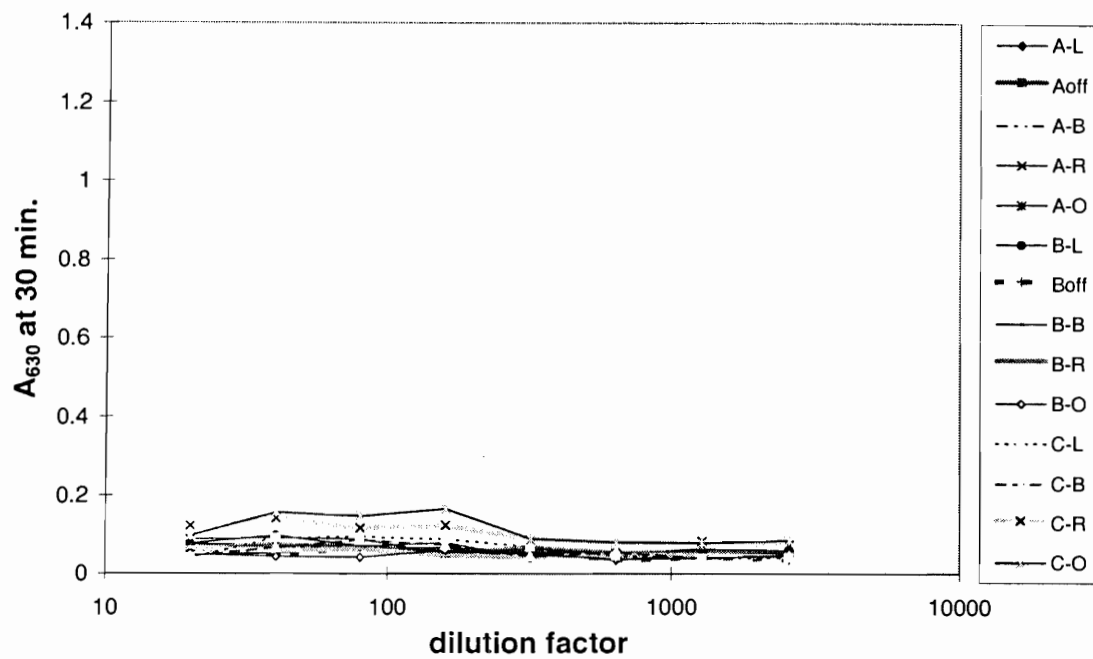
Panel C
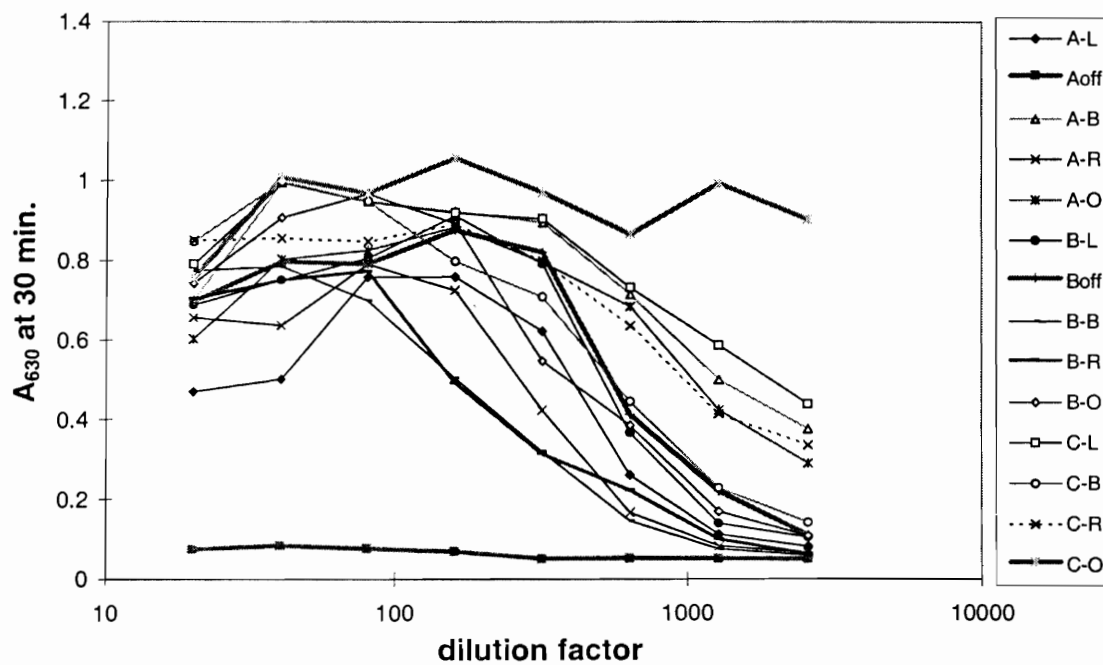
Panel D

Figure 7, continued.

Lack of efficacy for T epitope (ANOVA study)

Having established in the pilot study that the Fab'-HEL conjugate elicited an anti-idiotype response in the mice, the immunological determinants of this response were explored in greater depth by comparison of Fab'-HEL to a Fab'-(T epitope) conjugate in which the carrier protein was replaced by a synthetic peptide. A mixture of Fab' and HEL (without crosslinking) and the Fab' itself were also included as negative controls. Analysis of variance was used to provide statistical weight to our conclusions (Table 2). The anti-(9-40) ELISA data for the secondary responses for the Fab-HEL, Fab, Fab + HEL, and Fab-(T epitope) cohorts is shown in Figure 8 Panels A-D respectively. The data for the primary immunizations were similar (data not shown). The pronounced serum effect seen in the pilot study is absent in these mice; it is not clear why this is the case. It is obvious that the anti-(9-40) response for the Fab-HEL cohort was significantly different from the response of the other cohorts ($p = 4.89 \times 10^{-13}$ by single factor ANOVA on the lowest dilution of the ELISA data (Table 2)), and it is equally clear from the results that the anti-(9-40) response was negligible for the cohort immunized with the (9-40)Fab'-SMCC-(T epitope) preparation.

Proof of anti-idiotype response for the ANOVA study

Figure 9 shows a summary of titrations similar to those shown for the individual mice in Figure 8, except that only the Fab-HEL cohort is shown in Figure 9. The other curves shown are for the response to the various coating antigens used in the ELISA: 9-40 Fab, 4-4-20 Fab, BV04-01 Fab, and BDC1 Fab. The anti-(9-40) and anti-(4-4-20) responses were the highest. Although the mice were not immunized with 4-4-20 antigen, 4-4-20 is idiotypically crossreactive with 9-40 and so would be expected to also give a

Table 2: Statistical summary of cohorts. Single factor analysis of variance (ANOVA) was used to evaluate whether the immune responses observed from the different cohorts of mice were statistically different. (The single factor was the dose used.) These results are for the ELISA readings at the lowest dilution of the secondary response for cohorts of 10 mice immunized with the denoted antigens. The low P-value clearly shows that the cohorts are not all the same.

Table 2: Single Factor ANOVA[1]

Summary of ELISA variance:

Groups	Count	Sum	Average	Variance
Group 1: Fab'-HEL	10	5.064	0.5064	0.0318
Group 2: Fab'	10	0.837	0.0837	0.000167
Group 3: Fab' + HEL	10	0.764	0.0764	0.000571
Group 4: Fab'-(T ep.)	10	1.137	0.1137	0.00153

Analysis of ELISA variance:

Source of Variation	SS	df	MS	F	P-value	F crit
Between Groups	1.3003	3	0.4334	50.95	4.89×10^{-13}	2.866
Within Groups	0.3063	36	0.008507			
Total	1.607	39				

[*] Notation used in Table 2: SS, sum of squares; df, degrees of freedom; MS, mean square; F, ratio of between-group variance to within-group variance; P-value, the probability of being wrong in asserting that a difference exists between the groups; F crit, the critical value of F in determining the P-value.

positive response. It is remarkable, though, that the anti-(4-4-20) response is actually greater than the anti-(9-40) response ($p = 0.03$ by t-test). The anti-(BV04-01) response is present but mild, and the anti-BDC1 response is truly small, probably due to an anti-framework antibody present in one of the mice, as this mouse also gave the highest anti-(BV04-01) response. Taken together, these results give a good indication of the specificity of the response.
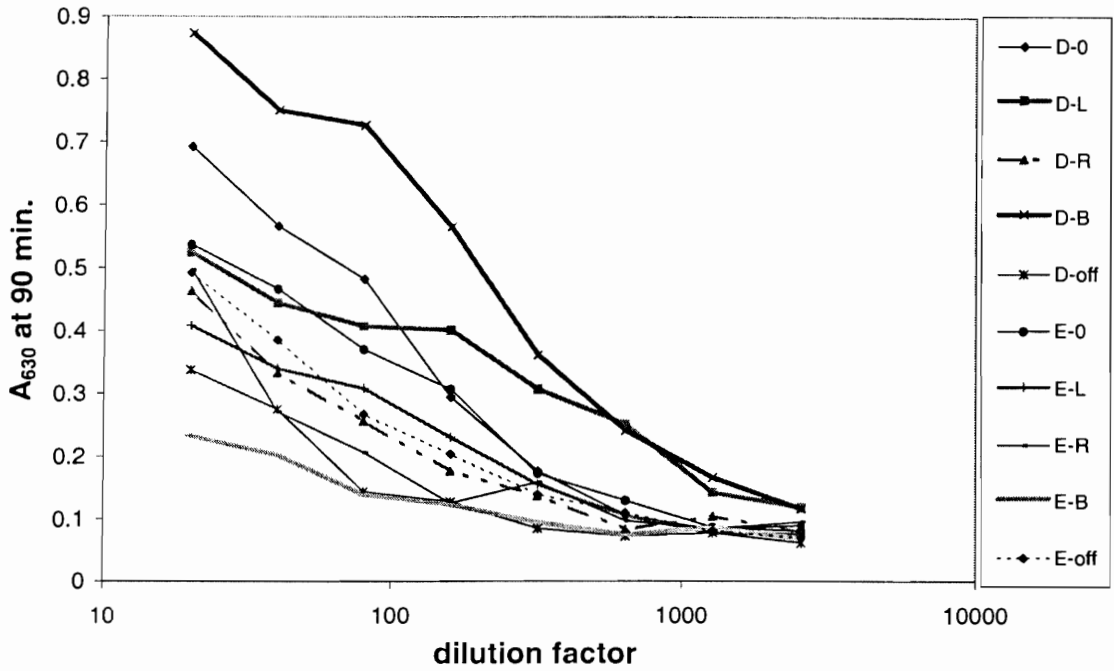
Panel A
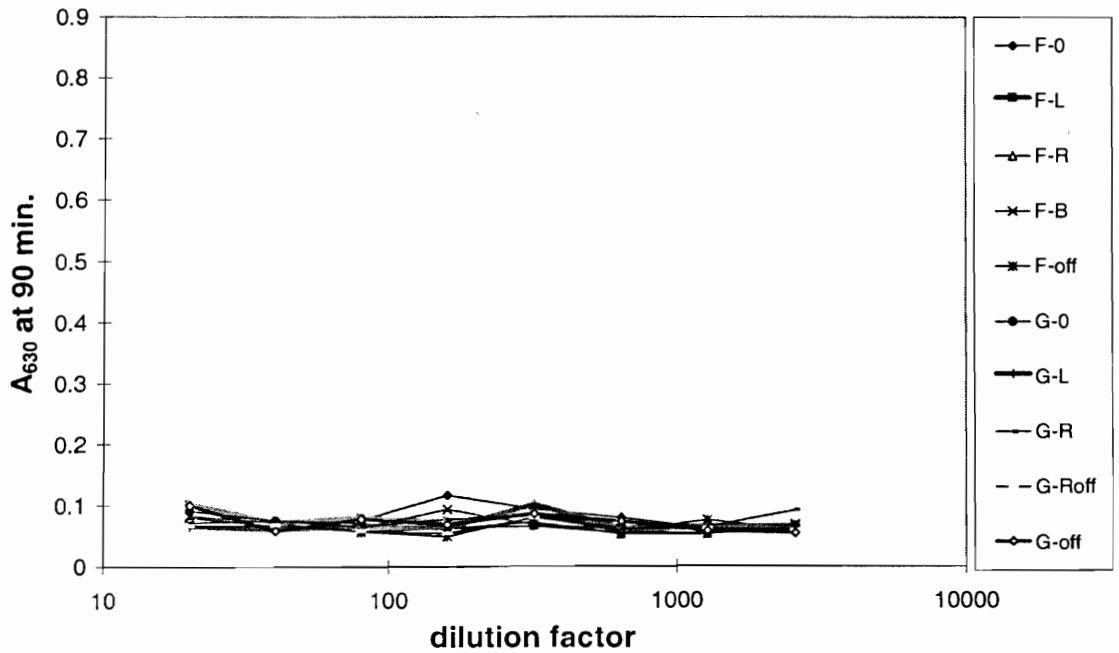
Panel B

Figure 8. Secondary anti-(9-40 Fab) response for mice immunized with the following immunogens: Panel A, (9-40)Fab'-SMCC-HEL conjugate; Panel B, (9-40)Fab' + HEL (noncovalently attached, just mixed together); Panel C, (9-40)Fab'; Panel D, (9-40)Fab'-SMCC-(T epitope).
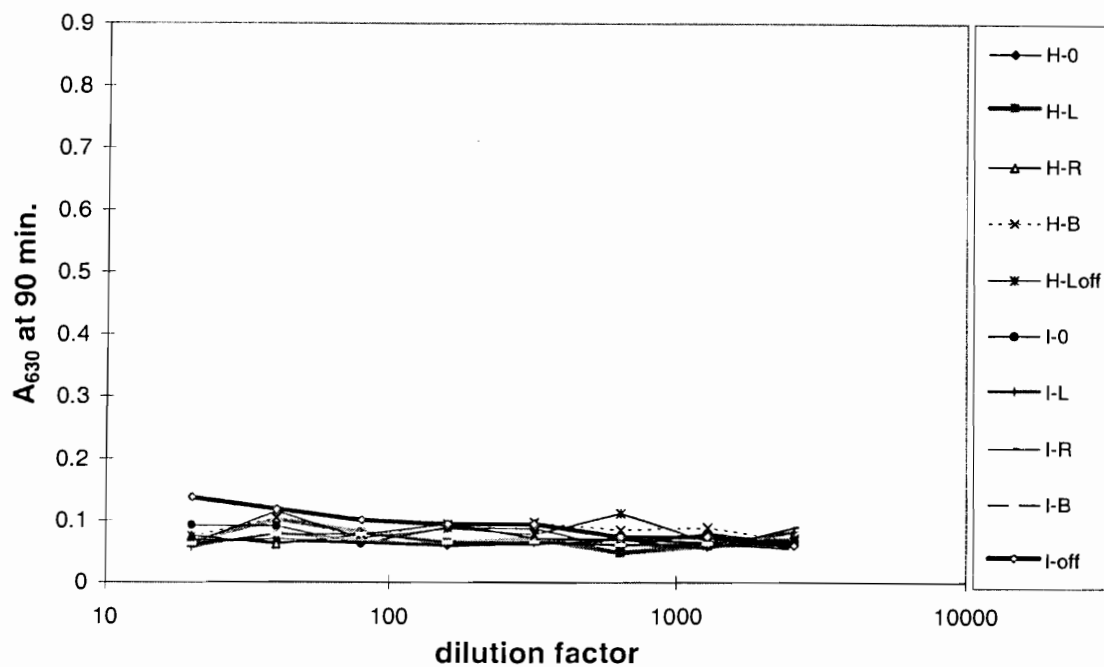
Panel C
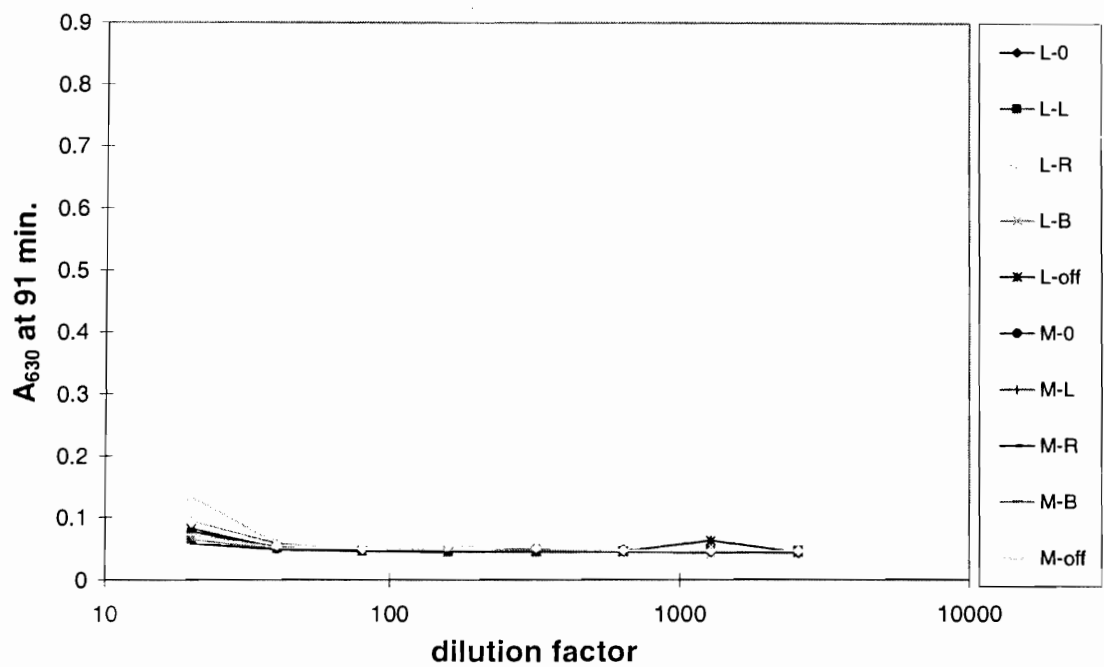
Panel D

Figure 8, continued.
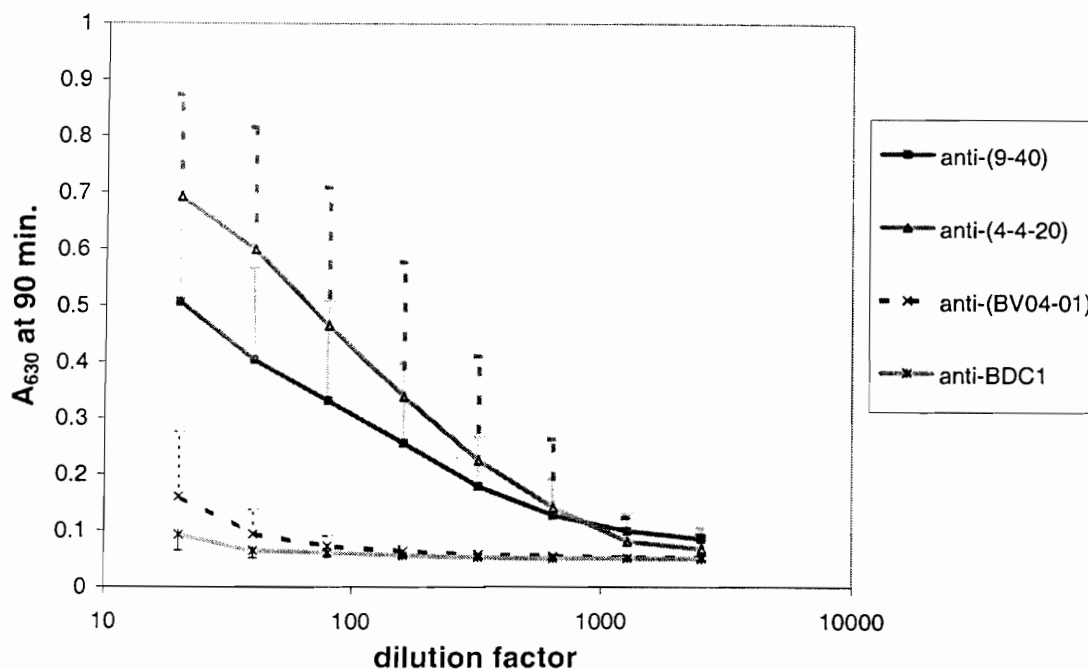
Figure 9. Averaged ELISA responses for various coating Ag after secondary immunization with (9-40)Fab'-SMCC-HEL. Summary of full ELISA titrations for different coating antigens for the experimental B10.A mice (i.e., immunized with (9-40)Fab'-SMCC-HEL).

Discussion

In both the initial pilot study and in the controlled study used for the ANOVA, anti-idiotype antibodies were generated in mice immunized with a Fab'-carrier protein construct ((9-40)Fab'-SMCC-HEL). The anti-idiotype response has conclusively been shown for the mice in the experimental group, and not for mice in either of the control groups. As expected from the literature (48), 4-4-20 is crossreactive with anti-(9-40) antibodies and vice versa. There was a low level of anti-framework regions seen in the primary immunization (data not shown) but this seems to have decayed away with the

secondary immunization. Because BDC1 was derived from BALB/c mice and therefore shares the same allotypic determinants as do 4-4-20 and 9-40, it is an excellent negative control for idiotype specificity. Had there been a significant response to BDC1, it would indicate either an anti-idiotype response (i.e., cross-reactivity with either 4-4-20 or 9-40) or an anti-allotype response. No significant anti-BDC1 response was seen in either the pilot study or in the full ANOVA study.

Contrary to our expectations, the Fab'-(T epitope) conjugate did not give an anti-idiotype response. Possible reasons are poor processing or presentation of antigen, damage of the Fab' portion of the conjugate by the TFA needed to redissolve the material, or too low a dose (~277 pmol or less for the secondary, < 1/2 of this for the primary). (It is very unlikely that the dose was too high, given the typical recommendations for antibody generation (55).) This issue is resolved in the next chapter, in which a dose response study was undertaken using the same T cell epitope but with a simpler, more easily quantitated antigen (the hapten fluorescein) instead of the 9-40 Fab' as the B cell epitope. The results strongly support the conclusion that the dose of (9-40)Fab'-(T epitope) was too low.

Assuming then that it is only a quantitative matter of dose, it is still unclear why the immunodominant T cell epitope should fail as a carrier protein replacement. To put it another way, why is a lower dose sufficient when other residues which contain subdominant or cryptic epitopes are also present? This would suggest that the outward phenomenological parameter of dosage is a surrogate for the more immunologically relevant, internal phenomena of antigen processing and presentation. Would a single chain Fv that incorporated the T cell epitope as part of its sequence have also failed to

elicit an immune response in B10.A mice? This is an intriguing possibility given the report in the literature (18) of a peptide that was derived from the hypervariable region of an anti-idiotype antibody, in which the peptide was both a B cell epitope and a T cell epitope. Although these authors did not incorporate this peptide as a carrier protein substitute as such (i.e., they did not try to make an autologous protein immunogenic), this peptide by itself failed to generate a strong antibody response but did do so as part of a multiple antigenic peptide (MAP) construct. So while we thought that the old immunological paradigm of "a carrier protein is necessary to make a hapten or peptide immunogenic due to its large size" was incorrect, perhaps size does matter after all for secondary processing effects. The dose response work spans a 300-fold range encompassing the T cell epitope doses used herein. The results of that study are consistent with the results presented here as well as in (18) and other reports in the literature.

Finally, it is worth noting that another anti-idiotype vaccine based on a patient-specific, naked DNA vaccine that codes for a single chain Fv (Vical's Vaxid product) is in clinical trials (long term studies) for non-Hodgkin's lymphoma, with positive initial results reported slightly over a year ago (www.vical.com). That construct relies on murine framework regions to provide T cell epitopes for human responses, which would support the supposition that the T cell epitope in the present study could possibly work in a 1:1 valency with the idiotype protein (9-40 in this case) had they been fused together as part of a single polypeptide chain rather than attached somewhat extraneously through a crosslinker. Clearly that would have profound implications for peptide vaccines in general. As with increasing the valency (MAPs), such a result would be an effect of the

superior antigen processing or presentation relative to the present case of an attached epitope.

CHAPTER 4

HOW WELL CAN A T CELL EPITOPE REPLACE ITS PARENT CARRIER PROTEIN? PART 2: A DOSE RESPONSE STUDY

Abstract

Purpose

To more fully explore the relationship between an immunodominant T cell epitope and the carrier protein from which it is derived, this work examines the dosages required for synthetic peptide vaccines containing a T cell stimulating epitope.

Methods

The hapten fluorescein (FL) was conjugated to chicken hen egg lysozyme (HEL) and to the following three synthetic immunogens: (1) the immunodominant T cell epitope of HEL in B10.A mice, (2) a multiple antigenic peptide (MAP) form of this same T cell epitope, and (3) a negative control MAP in which the only non-core amino acid was glycine. Cohorts of B10.A mice were immunized subcutaneously with equimolar quantities of FL-(T epitope) or negative control MAP at varying dosages spanning a 300-fold range. The dose was not changed for the secondary immunization but was reduced 100-fold for every cohort for the tertiary.

Results

For the primary immune response, the control $(FL-Gly_{18})_4$-MAP gave no antibody response except at the highest dosage. The FL-(T epitope) immunogen showed a half-sigmoidal dose response curve, linearly increasing above a threshold, although with moderately high variability in the responding animals. Increasing the valency of the immunogen to $(FL-(T \ epitope))_n$-MAP (n = 2-4, due to variabilities in the degree of branching in a nominally 4-branched MAP core resin supplied by different vendors) resulted in dramatically increased immunogenicity at the lowest doses, but there was little change over the concentration range examined. The FL-HEL positive control showed a decreasing antibody response with increasing dose, although with fairly high variation among animals. The lowest dose with the FL-HEL was equivalent in antibody titer to the highest dose of the FL-(T epitope) peptide. For the secondary response, there was little evidence of affinity maturation, except that in the peptide FL-(T epitope) at low doses a strong all-or-none response was seen. Neither the $(FL-(T \ epitope))_n$-MAP nor the FL-HEL positive control showed a strong dose dependency, but now the FL-HEL was slightly more immunogenic than the MAP. Surprisingly, the tertiary response at 14 days was practically indistinguishable from the secondary response at 56 days.

Conclusions

The monomeric T cell epitope was at least 300-fold less potent than its parent carrier protein. Incorporation of the epitope into a dendrimer such as a MAP increased its potency so that it was practically indistinguishable from the parent protein. This fully explained our earlier results in which the T cell epitope failed to replace the parent carrier protein. Furthermore, the negative control MAP worked as a probable TI-2 immunogen.

This control effectively removed antigen valency as a confounding variable. As to the use of MAPs as peptide vaccines, this work demonstrates that a vendor's quality assurance is sometimes insufficient and it is worthwhile to make small, easily analyzed test peptides using the same resins as those for which the desired MAPs are to be made.

Introduction

Peptides have been investigated as immunogens in vaccines since the 1980s, but initially only as haptens conjugated to a carrier protein. However, peptide haptens conjugated to carrier proteins can be difficult to characterize due to variable degrees of labeling and variable batch consistency. Also, there is the possibility of eliciting an immune response to extraneous epitopes particular to the carrier protein, with the potential for allergies or other immunological side effects. Consequently it is advantageous to dispense completely with carrier proteins for human and livestock animal vaccines and to use instead well-defined, immunologically relevant peptides. In order to be effective (involving a T cell dependent response), a true peptide vaccine formulation must include one or more T cell epitopes that match the MHC haplotypes encountered in the population. With this in mind, several different pharmaceutical approaches (liposomes (35-37), iscoms (56, 57), microspheres (58), numerous adjuvants (59)) have appeared in the literature with the goal of improving the efficacy of peptide (and other) vaccines.

In 1988 Tam introduced the multiple antigenic peptide (MAP) consisting of a branched oligolysine core to which are attached the peptide epitopes of interest (10). This gives an advantage over the carrier protein approach in that it is a chemically well-defined immunogen, as well as having other possible synthetic and safety issues. There

have now been over 150 papers involving MAPs, some using peptides as simultaneous T cell and B cell epitopes (60, 61), some using a more cassette approach with distinct T and B cell epitopes (62-64), and some comparing MAPs with the traditional carrier protein approach (65, 66). Nevertheless, to the best of our knowledge, there have been no studies aimed specifically at addressing how well a T cell epitope can replace the carrier protein from which it is derived, from the pragmatic point of view of an in vivo immune response.

The simplest way to address this question would be to do a t-test on animal cohorts immunized with a hapten (or equivalently, with a non-immunogenic protein against which an antibody response is desired) coupled either to a carrier protein or to a T cell epitope derived from such a carrier protein. Considerable effort has gone into mapping many of these epitopes for a variety of proteins; one model protein used for immunological studies is chicken hen egg lysozyme (HEL) (44). Consequently, we initially compared a murine Fab' fragment conjugated to HEL with the same fragment conjugated to the immunodominant T cell epitope from HEL in an inbred strain of mouse, B10.A (H-2^a haplotype). Single-factor ANOVA on the lowest dilution of the ELISA results of the various cohorts showed clearly that the T cell epitope completely failed to render the murine antibody fragment immunogenic, whereas the carrier protein worked well in this regard ($p = 4.89 \times 10^{-13}$) (Chapter 3). This was contrary to our expectations, so we decided to do a more thorough investigation of how well an immunodominant T cell epitope compares to its parent carrier protein. The most quantitative way to do this was as a dose response study using well-defined and easily measured haptens for the B cell epitope. Fluorescein (FL) was chosen for this purpose

due to its ease of detection and to its widespread successful use as a hapten (67). Because peptides are generally believed to be non-immunogenic unless coupled to a carrier protein or incorporated into a MAP (or other special delivery system), we also included in our comparison a MAP version of the peptide, as well as a negative control MAP consisting of the same number of amino acids as in the experimental MAP, but with the T epitope sequence replaced by glycine residues.

Four immunogens were prepared: FL-HEL, FL-(T epitope), (FL-(T epitope))$_n$-MAP (n = 2-4, see Methods), and (FL-(Gly)$_{18}$)$_4$-MAP, where (T epitope) is the immunodominant T cell epitope from chicken hen egg lysozyme (HEL) for B10.A mice along with its flanking residues (modified by replacing Cys-64 with Ser, thus: GSTDYGILQINSRWWSND) (45). Because the FL-HEL species is not a chemically well-defined species, there was some variability in the degree of labeling of the HEL with the FL (about 2-4 FL per HEL).

We examined the primary, secondary, and tertiary responses over what we thought initially would be a wide enough concentration range to see the interesting region of the dose response function. This range was chosen based on the typical recommendations for protein immunogens, about 25 to 100 μg per mouse (55). Consequently, in the present study we spanned 1 to 300 μg per mouse for the FL-HEL case, as a positive control. This was converted to a molar basis and then the same epitope molar concentrations were used for the other immunogens. Because the primary and secondary immunization results showed that this range did not extend far enough into the low concentration region of the dose response curves for the FL-HEL and for the (FL-(T epitope)$_n$)-MAP, the doses for all cohorts were reduced 100-fold for the tertiary

immunization. The assay for measuring total antibody as a function of dose was a sandwich ELISA.

Materials and methods

Preparation of FL-HEL

HEL was purchased from Sigma, dialyzed against water, lyophilized, and stored frozen until use. Then it was dissolved in formamide and reacted with fluorescein NHS ester, dialyzed, and lyophilized. There was still some undialyzed FL remaining, which was removed by dissolving the FL-HEL in formamide, diluting it with dimethylformamide, and then precipitating this out with diethyl ether. TLC showed that the removal of free FL was quantitative. Degree of labeling was assessed by MS and UV/VIS and found to be approximately 3.

Preparation of fluoresceinated peptide immunogens

A professional peptide synthesis facility located at the University of Utah synthesized the sequence GSTDYGILQINSRWWSND by batch method solid phase peptide synthesis using standard Fmoc chemistry both as the linear peptide and as a MAP construct using the tetrameric MAP resin supplied by Advanced ChemTech. This facility also prepared a control tetrameric MAP consisting of the same number of residues but with every residue replaced by glycine. The control MAP was synthesized using the tetrameric MAP resin commercially available from Novabiochem; different suppliers were used for the two MAP constructs simply due to availability at the time. All of these synthetic peptides were fluoresceinated with 5- (and 6-) carboxyfluorescein using DCC as coupling reagent while still attached to the resin.

Purity and structure assessment of fluoresceinated

peptide immunogens

Purity was assayed by HPLC and MS. The latter worked very well for the linear peptide and produced a mass within 1.0 dalton of the expected value. However, it had been the experience of the peptide synthesis facility, and also reported in the literature (68), that MAPs sometimes failed to give clean mass spectra. Nevertheless, both the experimental and control MAPs were analyzed by MS. MALDI-, ESI-, and FAB-MS failed to give interpretable and self-consistent spectra for the $(FL-Gly_{18})_4$-MAP and MALDI-MS for the experimental MAP formulation showed mostly dimeric MAP. Although this latter result was unexpected, its validity was questionable for the reasons mentioned above. Thus, we turned to amino acid sequencing to validate the experimental MAP and amino acid analysis to validate the control MAP (amino acid sequencing was not thought to be productive for the control MAP because of its branched Gly_{18} sequence).

Amino acid sequencing of a small portion of experimental MAP that was left un-fluoresceinated was found to be in agreement with the expected sequence. Comparison of the ratios of Gly: FL, Lys: FL, and Gly: Lys from amino acid analysis and UV spectrophotometry was done for the control MAP. (Note that although the MAP resins from both vendors were sold as a β-Ala plus three Lys, so that taking Lys: β-Ala would seem to be the most accurate measure, this turned out to be problematic because the different vendors - especially Novabiochem - used an excess of β-Ala but capped it, resulting in an excess of β-Ala, which rendered this ratio non-informative.) The expected ratio of Gly: Lys was 24:1 and the experimental value by amino acid analysis performed

at the University of Utah's Amino Acid Analysis Facility was in agreement with the expected, within experimental uncertainty. Furthermore, the ratio of Gly:FL (expected, 18:1) was also acceptable within experimental error. Based on these results, the purity of the fluoresceinated peptide immunogens was deemed adequate for immunization.

Immunization protocol

Male B10.A mice (Jackson Laboratories, ME) from 4-6 weeks of age were immunized subcutaneously in two injections of 100 µL each, with the dose comprised of a 1:1 emulsion of the desired dilution of the appropriate immunogen and Freund's complete adjuvant for the primary immunization or Freund's incomplete adjuvant for the secondary immunization. The animals were bled 2 weeks after they immunized for both injections by tail vein or artery bleeding. The blood was allowed to clot in Eppendorf tubes, centrifuged and stored frozen. The primary, secondary, and tertiary immunizations were eight weeks apart. The research adhered to the "Principles of Laboratory Animal Care" (NIH publication #85-23, revised 1985).

ELISA protocol

ELISA test strips were purchased from Nunc and coated with a preparation of FL-KLH (i.e., fluoresceinated keyhole limpet hemocyanin) made in our laboratory, diluted with a high-salt coating buffer (1.2 M NaCl, 50 mM NaPO$_4$, pH 7.5). All steps were done at room temperature. After coating the wells for 60-90 min, the plates were washed by tap de-ionized water and tap dried (turned upside down on paper towels sharply), then post-coated (blocked) with casein in ELISA wash buffer (150 mM NaCl, 10 mM Tris, 1 mM EDTA, 0.01-0.05% Tween 20) adjusted to pH 11 with NaOH. After post-coating for ~30 minutes the plates were washed again, then samples were applied and serially

diluted. The plates were then washed and goat anti-(mouse Fab) (Sigma) was used in a 1:10,000 dilution in ELISA wash buffer, then the plates were washed again. Substrate (Blue-Phos, KPL) was used but diluted 1:1 with water, and the absorbances were read in a Titertech plate reader 63 min after applying the substrate.

Further analysis of the MAP resins using test peptides

Our structure assessment of the experimental and control MAPs did not yield any information about the distribution of the number of branches per MAP, so we decided to have a test peptide synthesized at the same peptide facility using the same resins as were used for the control and experimental MAPs. The sequence FLRG was made into a MAP using both the Novabiochem resin used for the $(FL\text{-}Gly_{18})_4$-MAP and the Advanced ChemTech resin used for the $(FL\text{-}(T\ epitope))_4$-MAP, and then analyzed by MALDI-MS. The MAP with the former resin was >95% tetramer whereas the latter resin gave mostly dimer with only one lysine as being the core; both are supposed to have a β-Ala residue that is used for anchoring the growing peptide to the resin during synthesis. These results with the test peptide would strongly support the conclusion that the control MAP was predominantly tetrameric, whereas the experimental MAP was predominantly dimeric. For this reason we have chosen to designate the experimental MAP as "$(FL\text{-}(T\ epitope))_n$-MAP".

<div align="center">

Results

</div>

Primary response

Twenty-one cohorts of five mice each (less one that died) utilizing the above-mentioned four immunogens at five different concentrations were immunized subcutaneously with their respective immunogen and complete Freund's adjuvant in a 1:1 (v/v)

emulsion. The vaccine dose range spanned from 65.0 pmol to 19.5 nmol (equivalent to 1 - 300 μg for the FL-HEL case). The dose was administered in two 100 μL injections. Concentrations were based on the fluorescein absorption with the assumption that for every mole of fluorescein there was a mole of T cell epitope, except in the case of FL-HEL, in which the assumption was that for every 3 moles of fluorescein there was one mole of HEL, based on the degree of labeling seen in the MALDI-MS. The mice were bled 2 weeks after immunization, and anti-fluorescein antibody responses were measured by ELISA. For the ELISAs each mouse had a full titration done on its serum to be sure that there were no "serum effects," in which a maximum is seen in the response at a concentration that is not the most concentrated, as we have occasionally observed in the past with other ELISA systems (69). This sort of effect was not seen in the sera of the mice analyzed (with one minor exception, excluding background variations), and in fact the precision of the assay was excellent. Figure 10 shows the titration curves for 4 replicates of the same sample, showing a low intra-assay variability (CV = 6.5%). Figure 11 shows the response at the 1.95 nmol dose for the FL-HEL, in order to more clearly show the differences in titrations from animal to animal. These results show clearly that the assay variability is much less than the mouse-to-mouse variability. The other samples in the ELISA were done with only one titration per mouse.

The results from Figure 11 and other similar titrations from the primary immunization are summarized in Figure 12. Because there were almost no odd serum effects, the titrations generally decreased in response with increasing dilution, and so the best signal was with the highest concentration. The average of this highest-concentration signal is shown in Figure 12, with the vertical error bars (shown either down or up for the
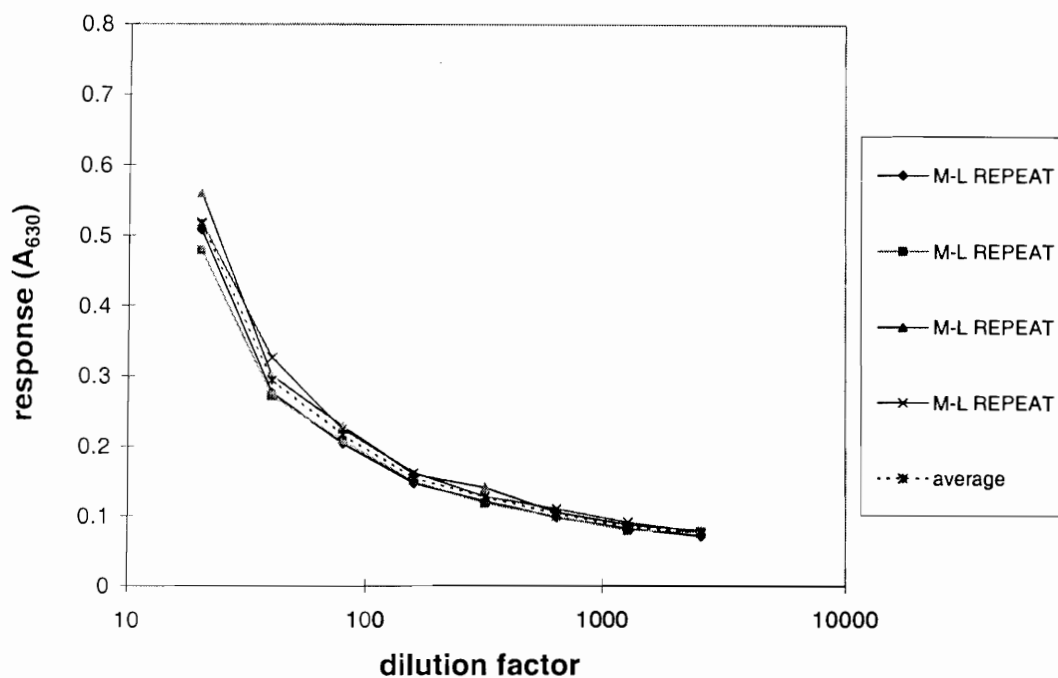
Figure 10 Intra-assay variability. Repeat titrations for mouse M-L in cohort M. These curves were for four polystyrene ELISA strips coated with fluorescein-KLH and blocked with casein to which the samples were applied and then subjected to two-fold serial dilutions. Goat anti-(mouse Fc) was used as the tracer antibody, washed, and then substrate was added and the color read after 63 min from the time at which the substrate was added. An intra-assay coefficient of variation (CV) of 6.5% was determined from these data.

sake of clarity) being the standard deviations for the different mice in each cohort. For the primary immune response, the negative control $(FL-Gly_{18})_4$-MAP gave no antibody response except at the highest dosage. We surmise that this branched vaccine is acting as a type 2 T cell independent (TI-2) immunogen (33, p.210). The FL-(T epitope) immunogen showed a half-sigmoidal dose response curve, linearly increasing above a threshold, although with moderately high variability in the responding animals. Increasing the valency of the immunogen, i.e., switching to the experimental (FL-(T epi-
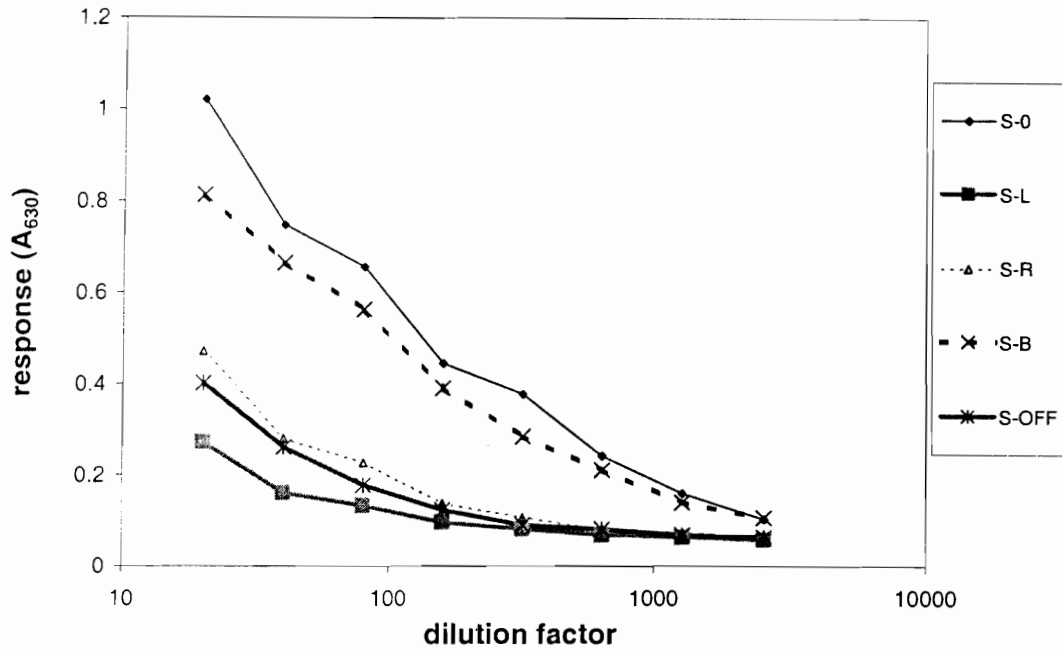
Figure 11. Primary response for 19.5 μM FL-HEL cohort. The five curves are titrations for the five mice in this cohort (designated as S). ELISA conditions are as in Figure 10.

tope))$_n$-MAP, resulted in dramatically increased immunogenicity at the lowest doses, but there was little change over the concentration range examined. Hence, it seems that increasing the valency of the peptide vaccine resulted in a strong shift in the dose-response curve to the left. The experimental MAP gave the strongest overall primary antibody response among the four immunogens. Finally, the FL-HEL positive control actually showed a decreasing antibody response with increasing dose, although with fairly wide variation among animals. This would suggest that tolerization is beginning to occur in some of the mice, even though Freund's complete adjuvant was used. The lowest dose with the FL-HEL was equivalent to the highest dose of the FL-(T epitope) peptide in terms of antibody response.

Figure 12. Primary dose-response functions for control and experimental immunogens in B10.A mice measured by ELISA with FL-KLH as coating Ag. This summarizes the primary immune response for all cohorts except for the adjuvant-only (infinite Ag dilution) cohort, due to the log scale. The adjuvant-only cohort was indistinguishable in response relative to the cohorts for the lowest concentration of (FL-Gly_{18})$_4$-MAP or of FL-(T epitope). Every datum shown represents the average of five mice per cohort, except for the second to lowest dose for the (FL-Gly_{18})$_4$-MAP negative control, which had four mice (one died). The error bars are the sample standard deviations, shown either up or down for clarity. The arrow denotes the approximate dose used in Part 1 of this study, and therefore explains those results.

Secondary response

Freund's incomplete adjuvant was used for the secondary and tertiary immunizations. The dose was not changed for the secondary immunization for any of the mice. For the secondary response, there was some evidence of affinity maturation in the FL-(T epitope) immunogen and, surprisingly, in the (FL-Gly_{18})$_4$-MAP immunogen, but not in the other two. (It is important to note, however, that because titers were being measured

rather than affinities, the increase in titer could be due to an increase in the number of cells in the responding clones rather than to affinity maturation.) FL-(T epitope) at low doses exhibited a strong all-or-none response, as shown in Figure 13. Similarly, the negative control MAP showed one responder at a lower dose than previously. The newly responding mouse in the intermediate dosage cohort was of the IgM isotype, whereas the other responding mice were primarily of the IgG isotypes. At the highest dose the response for $(FL-Gly_{18})_4$-MAP was amplified in the secondary immunization over that in the primary, as shown in Figure 14. Because thymus independent antigens are believed to show little if any memory, one might conclude that this negative control vaccine is in fact
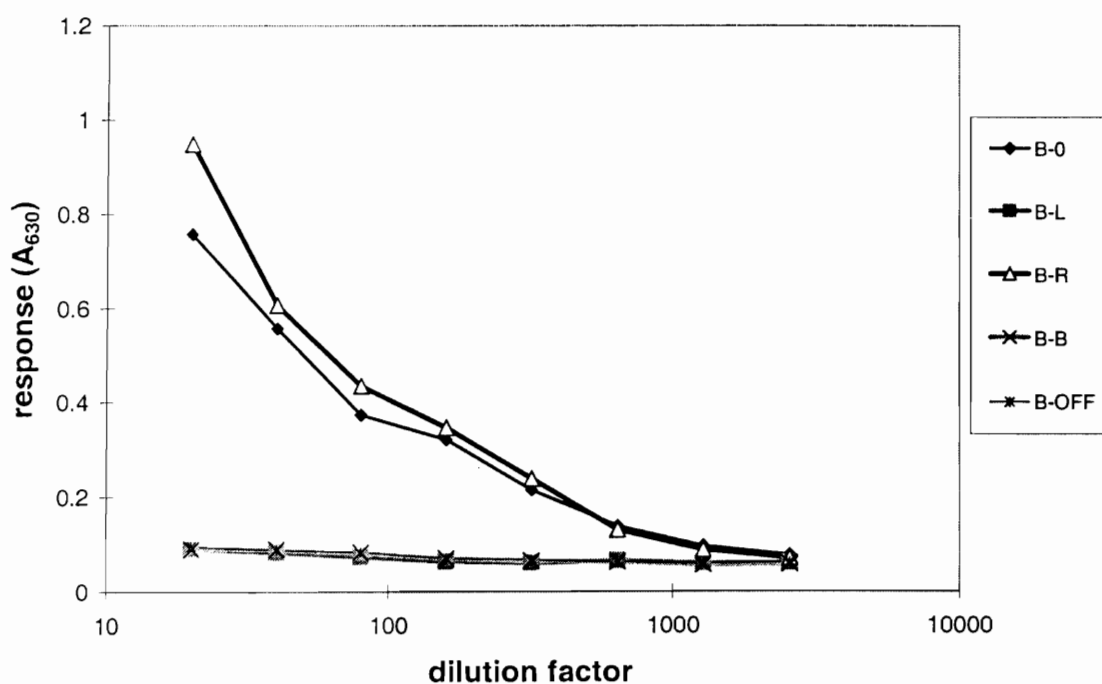
Figure 13: Secondary response for 0.65 μM FL-(T epitope) cohort. Two mice showed strong secondary responses but three showed no response in this low dosage cohort. The next higher dosage was similar. The ELISA conditions were as in Figure 10 and Figure 11.
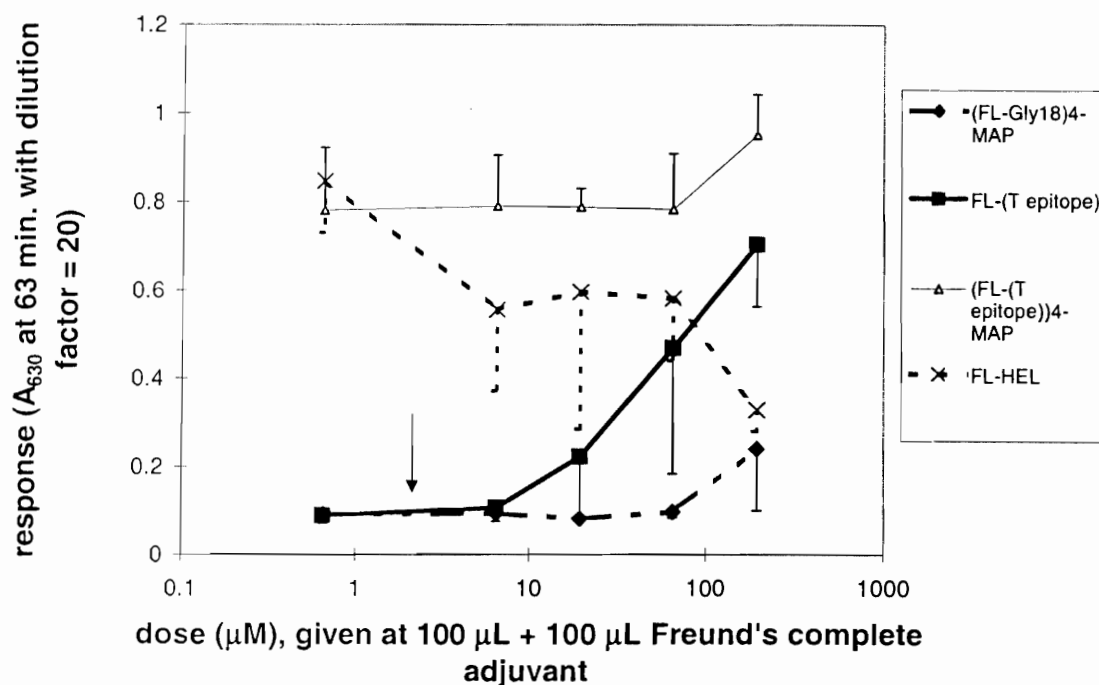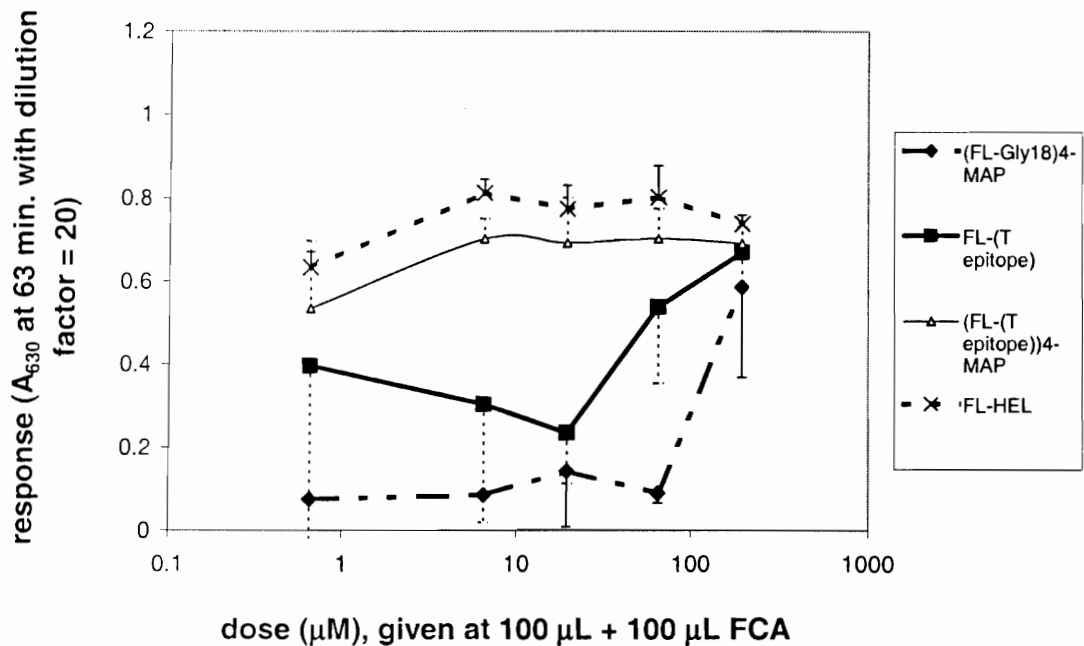
Figure 14: Secondary dose-response functions for control and experimental immunogens in B10.A mice using ELISA with FL-KLH as coating Ag. This is analogous to Figure 12, and again the infinite dilution (adjuvant only) cohort is not shown but gave no response. The very wide error bars in the FL-(T epitope) case is due to the strong all-or-none response shown in detail in Figure 13.

acting in a T cell dependent fashion. This is certainly possible but would be difficult to reconcile with current understanding of how peptides are presented in the MHC and recognized by the T cell receptor. We believe that it is more likely that this negative control immunogen is in fact a T cell independent immunogen, but that class switching and possible affinity maturation are nevertheless being seen.

Affinity maturation was not observed for either the FL-HEL or the (FL-(T epitope))$_n$-MAP immunogens. The doses of these immunogens were already in the saturation region of the dose response curve, so there is little, if any competition for

antigen and hence very limited selective pressure on high affinity clones in the germinal centers (70). Neither the (FL-(T epitope))$_n$-MAP nor the FL-HEL positive control showed a strong dose dependency in the concentration range examined. Also, the FL-HEL was now slightly more immunogenic than the MAP at every concentration used. These results are summarized in Figure 14.

Tertiary response

Prior to immunizing the animals the third time, the mice were bled so that carryover from the secondary immunization could be estimated. Those results are shown in Figure 15 and the results of the tertiary immunization in Figure 16. As can be seen, there is still considerable carryover from the secondary immunization even after 56 days. This makes it difficult to say how much of the response from the tertiary is due to the tertiary immunization and how much is just carryover from the secondary immunization. As can be seen from Figure 15 and Figure 16, there is little difference between the two. Comparing Figure 14 and Figure 15 shows that for the middle dose of the (FL-Gly$_{18}$)$_4$-MAP in Figure 14 there is a small (1 mouse out of 5) response, but that this is gone in Figure 15. The reason is simply that this mouse died in the interim. The most striking observation is that the response for the FL-(T epitope) immunogen is higher at 56 days than at 14 days, and the others are still about as high. Probably this is due to the sustained release of the vaccine, adjuvant mixture.
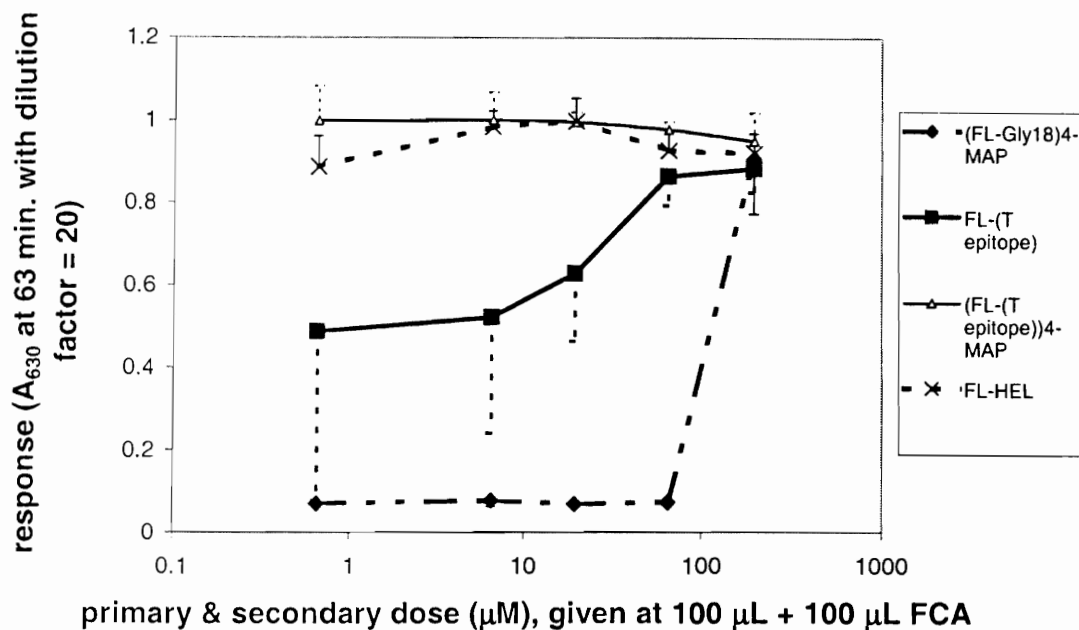
Figure 15: Secondary dose-response functions 56 days postimmunization for control and experimental immunogens in B10.A mice using ELISA with FL-KLH as coating Ag. This shows the carryover from 2° immunization, 56 days post-immunization. This is analogous to Figure 12 and Figure 14, but now more mice had died. The middle dose for the FL-(T epitope) cohort, the middle and second-highest control MAP dose cohorts, and the second-highest and highest doses of the (FL-(T epitope))₄-MAP all had four mice.
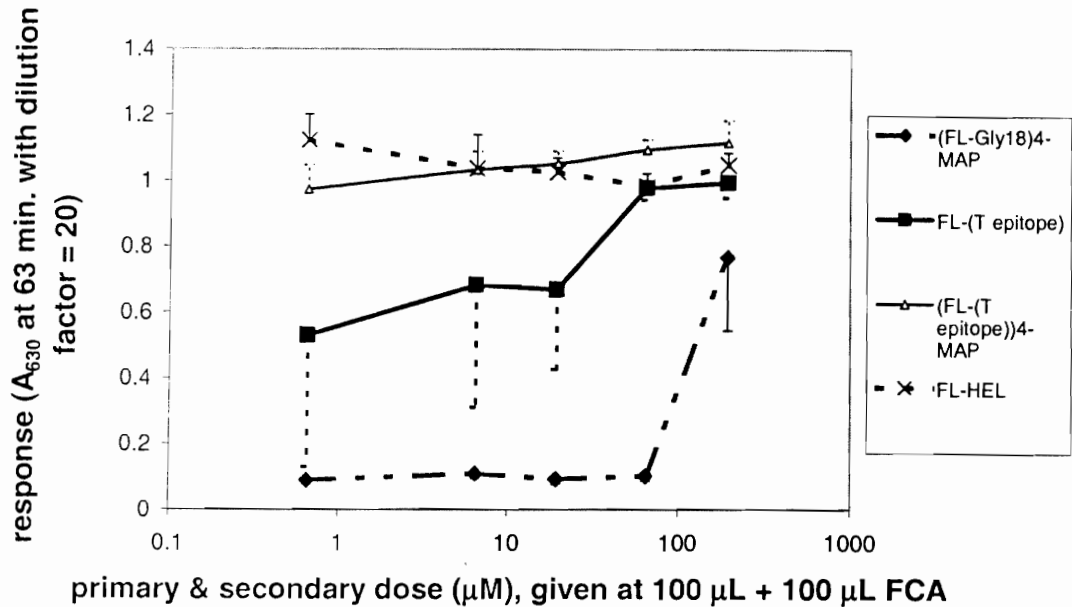
Figure 16: **Tertiary dose-response functions for control and experimental immunogens in B10.A mice using ELISA with FL-KLH as coating Ag.** Results of $3°$ immunization. No further mice had died from those in Figure 15.

Discussion

Four different immunogens (vaccines) were prepared and characterized, and then injected into mice known to be responsive to the T cell stimulating epitope used in two of these immunogens (the monomeric and the tetrameric FL-(T epitope) species). These vaccines were (1) the FL-HEL used as a positive control; (2) the FL-(T epitope), where the "T epitope" is the immunodominant T cell stimulating epitope from HEL in B10.A mice; (3) the dendrimeric multiple antigenic peptide version of the fluoresceinated T epitope, designated (FL-(T epitope))$_n$-MAP; and (4) a control MAP wherein the eighteen residues in the T epitope were replaced by glycine. The anti-FL titers were compared for each of these vaccines in the primary, secondary, and tertiary responses. Of the six

possible pairwise comparisons between the four immunogens at a given point in time, the three most meaningful are (1) between the monomeric and multimeric versions of the fluoresceinated peptide; (2) between the monomeric fluoresceinated peptide and the intact HEL; and (3) between the experimental MAP (i.e., the (FL-(T epitope))$_n$-MAP) and FL-HEL. The latter two comparisons address the question originally posed, i.e., how well a T cell epitope can substitute for its parent carrier protein in terms of generating an antibody response. The negative control MAP is useful in accounting for the effect of multivalency of the FL in the FL-HEL and in the (FL-(T epitope))$_n$-MAP, which would otherwise be a confounding variable.

Comparing the monomeric vs. the multimeric MAP versions of the fluoresceinated peptide clearly shows a dramatic increase in the effectiveness of the T epitope upon incorporation as part of a MAP.[**] This is consistent with earlier studies comparing the valency of different monomeric or multiple antigenic peptides (62), but also extends these results across a much wider concentration range. However, the multimeric MAP was not nearly as easy to prepare in good purity as was the monomeric peptide of the same sequence. In fact, although initially we believed that there was a problem with the mass spectra for the (FL-(T epitope)$_4$)-MAP and so decided to proceed with the immunizations based on the satisfactory amino acid sequencing results, we later

---

[**] One possible objection to this statement would be the possibility that the increased titers seen in the MAP cohorts were due to increased background (decreased specificity) rather than increased potency of the T cell epitope. This could be tested directly by performing a series of ELISAs on related haptens similar to fluorescein, although this was not done. This alternative explanation also seems unlikely given the fact that not only have MAPs been observed to increase the potency (or decrease the specificity) in a very wide range of B cell epitopes, they have also been shown to be effective in increasing the potency of cytotoxic T cell epitopes as well (71-73), which would suggest

learned that the actual $(FL-(T \text{ epitope})_4)$-MAP was a minor species, perhaps 15-20% of the total, based on PAGE and on the results of a small test peptide made on the same MAP resin. (The vast majority of this MAP formulation was a dimeric MAP based on only a single Lys for the core; see Materials and Methods for details.) While this does compromise the results of the dose response study in terms of pharmacodynamic parameters which one might derive particular to the individual immunogens (fitted perhaps to a sigmoid maximum effect model), it actually strengthens the central conclusion, namely that T cell epitopes incorporated into MAPs are far more potent than linear peptides on an epitope molar basis except at extremely high (mid-nmol) doses, where they become equivalent. It is impossible to say how much of the $(FL-(T \text{ epitope}))_n$-MAP cohorts' antibody responses were due to true $(FL-(T \text{ epitope}))_4$-MAP and how much were due to dimeric species based only on the present evidence. Since the $(FL-(T \text{ epitope}))_n$-MAP cohorts exhibit a plateau as it is, it is unlikely that highly purified $(FL-(T \text{ epitope}))_4$-MAP would show a dose response curve markedly different from what was observed. However, had lower concentrations been used, then this difference likely would become apparent. (It is also possible that had highly purified $(FL-(T \text{ epitope}))_4$-MAP been used, that tolerization similar to that seen with the FL-HEL might have occurred and been mistakenly interpreted as evidence that MAPs are only marginally more effective than are monomeric peptides.) In such a case it would be very interesting to see whether the steepness of the curve (related to the exponent in a sigmoidal maximum effect model) correlates with the number of branches.

---

that their mechanism of action does increase potency at the T cell epitope level rather than decrease the specificity of the humoral response.

The biological reason for why oligomerization shifts the dose response curve strongly to the left is not well understood but possibly has more to do with antigen uptake by antigen presenting cells rather than with antigen processing. (One might expect that the monomeric peptide would require less processing than would the tetrameric MAP, and possibly that dendritic cells would more easily recognize a larger, multivalent species than a smaller peptide.) Because of the high analytical sensitivity of the fluorescein hapten, it may be possible to test this hypothesis in the future with these constructs.

As for the original question of how well a T cell epitope can replace the carrier protein from which it is derived, a comparison between the monomeric peptide and the carrier protein shows that the immunodominant peptide from HEL for B10.A mice is at least 300 times less potent at stimulating a T cell dependent response than is the intact carrier protein. It is worth noting that FL-HEL is also monomeric in terms of the immunodominant T cell epitope but is roughly trimeric in terms of the hapten fluorescein. However, when the T cell epitope is incorporated into a MAP, there is little difference between the MAP and the carrier protein, with the MAP possibly being slightly more potent for the primary response and the carrier protein slightly more potent for the secondary response, although there is considerable variability within cohorts. The present data could also explain why there was no effect seen in Part 1 of this study: the dose of the Fab'-(T epitope) conjugate was in the nonresponding, flat portion of the T epitope curve, whereas at this same dose the carrier protein HEL is fully potent.

B cells can differentiate into antibody secreting plasma cells by one of three known mechanisms: (1) direct stimulation by a T helper cell specific for the same antigen (albeit different epitopes) as is the B cell, (2) activation by a type 1 T cell independent

(TI-1) response (which actually does have some T cell dependency), or (3) activation by a type 2 T cell independent (TI-2) response (which is truly T cell independent) (33). TI-1 responses involve polyclonal B cell activators, but TI-2 responses rely on receptor crosslinking and therefore require that the antigen be polymeric or at least multimeric with respect to the epitope recognized by the reactive B cell clone. In the present case this would mean that the valency of the FL-HEL with respect to FL, and likewise of the (FL-(T epitope))$_n$-MAP, is, strictly speaking, a confounding variable; the response seen could be due to the B cell receptor crosslinking or it could be due to specific assistance by helper T cells. However, the negative control (FL-Gly$_{18}$)$_4$-MAP does effectively control for B cell receptor crosslinking. (It was made with a different manufacturer's resin and the same test peptide made with this resin gave >95% tetrameric MAP; again, see Materials and Methods for details.) Hence, the response seen in the case of the FL-HEL was due to the immunodominant and subdominant epitopes present in HEL, and not due to direct crosslinking of the B cell receptors, at least at the lower concentrations used. Likewise, the response due to the (FL-(T epitope))$_n$-MAP preparation is not simply due to B cell receptor crosslinking but rather involves T cell help. Also, because crosslinking is concentration dependent, it is reasonable to assume that the anti-FL response seen in the control MAP at the highest concentration is due to B cell receptor crosslinking of FL-specific clones, and that this response should not exist at lower concentrations. Nevertheless, it is noteworthy that one mouse did show a primary response at a lower (intermediate) concentration after the second immunization.

It is also interesting that while this was originally intended as a dose response study over a fairly broad concentration range, the optimal concentrations were not known

a priori and it can be seen from Figure 12 that the concentration range used shows a significant dynamic range only for the FL-(T epitope) species. The (FL-(T epitope))$_n$-MAP function has reached a plateau in its dose response curve, which is presumably sigmoidal in appearance. However, unlike most other saturation phenomena in biology, T cell stimulation with respect to increasing antigen dose does not simply reach a stable plateau but rather exhibits a maximum. It is well known that at "high" antigen doses T cell anergy or deletion become operative (33, Ch. 10), and this is beginning to be seen in Figure 12. It is somewhat surprising that this tolerization is seen over a concentration range typically used for protein antigens, but it should be remembered that HEL is a low molecular weight protein and so a typical dose of 50 to 100 μg of HEL corresponds to a greater number of molecules than 50 to 100 μg of a higher molecular weight protein.

Presumably if the concentration range used had been over a much wider scale, then the (FL-(T epitope))$_n$-MAP would also show a decrease in response at very high doses and a sigmoidal response at lower doses. Instead the response is essentially flat over the 300-fold concentration range used. Likewise, the control MAP should continue to show a higher level of stimulation at higher concentrations, but because T cell stimulation and anergy are not issues for T cell independent means of B cell stimulation, it is unclear if a decrease would be seen at extremely high levels of antigen (tens to hundreds of nanomoles). At such high levels one also runs into the difficulty of solubility; the (FL-Gly$_{18}$)$_4$-MAP is not as soluble as one might expect based on its structure. Furthermore, at such extremely high doses it is possible that secondary effects, such as unexpected toxicity, may become important.

No affinity maturation was seen for the FL-HEL or for the $(FL-(T\ epitope))_n$-MAP, probably due to the fact that antigen competition is not limiting in the case of saturating responses. However, affinity maturation is seen in the negative control MAP, which is surprising, and in the FL-(T epitope) immunogen at the lowest doses but only in some mice. Class switching does seem to be occurring based on the fact that the newly stimulated mouse in the intermediate concentration of control MAP is of the IgM isotype whereas the other secondary response data for responding mice are of IgG isotypes (data not shown).

The data show a trade-off between intensity of response and number of responders in the secondary immunization for low concentrations of FL-(T epitope). One might expect this to also be seen with the other antigens as well in their lower portions of their respective curves. Sampling lower concentrations was done in the tertiary immunization but the results are practically indistinguishable from the carryover of the secondary even after 56 days. Measuring carryover after the primary immunization was not performed since the literature would indicate that the B cell activation is at a maximum after nearly 2 weeks (74), and since we expected to see an increase in titer due to the 2° immunization. In hindsight, this should have been done, especially given the presentation in the literature (albeit for guinea pigs) that the ELISA titer to MAPs is highest at about 28 days and barely drops thereafter even to 56 days (66).

Finally, it should be noted that commercially available, off-the-shelf MAP resins do not always yield the products that they are supposed to, and it is advisable to first synthesize a small test peptide that one can use to verify the quality of the resin for a longer run, or else to double-check the quality control of the vendor's lot used. The

MAPs used in this paper were synthesized using the same level of care as are ordinary peptides routinely synthesized at the University of Utah's Peptide Facility, but one vendor's resin gave mostly the expected four-branched MAP whereas another's gave mostly two-branched MAP.

CHAPTER 5

AN INVESTIGATION INTO HOW WELL AN IDIOTOPE PEPTIDE MIMIC CAN REPLACE ITS PARENT IDIOTYPE

Abstract

Purpose

This study's motivation was to evaluate how well an idiotope peptide mimic of the third complementarity determining region of the heavy chain (CDR-H3) of an antibody could substitute for the entire idiotype of an antibody, with the ultimate goal of using such a peptide mimic in a vaccine formulation for targeting pathological B lymphocytes.

Methods

The protein chicken egg lysozyme (HEL) was used as a carrier protein, to which was attached via SMCC either the Fab' fragment of mAb 9-40, or else the B epitope peptide mimic ("Bep"). Cohorts of B10.A mice were immunized subcutaneously with Freund's complete (1° immunization) and then incomplete (2° and 3° immunizations) adjuvant. Bep and Bep + HEL negative control cohorts were also used. Serum was assayed by ELISA for anti-peptide and anti-(9-40 Fab') activity.

Results

As expected, antibodies against the B epitope were generated with the B-HEL conjugate, and antibodies against the intact idiotype were generated with the (9-40)Fab'-HEL conjugate. No crossreactivity was seen for these two responses for the primary immunization. After boosting with the secondary dose, crossreactivity was seen in 3/10 of the mice immunized with the B-HEL conjugate. A strong serum effect, in which there was a maximum response for an intermediate dilution, was seen in the ELISAs for the crossreacting mice. Little or no crossreactivity for the peptide was seen in mice immunized with the (9-40)Fab'-HEL conjugate. In all cases the negative control mice cohorts showed negligible response. The fraction of crossreacting mice increased with continuing immunizations, from 0 to 3/10 to 5/8 (two died).

Conclusions

A fair crossreactivity was demonstrated for an idiotope peptide mimic in relation to the intact idiotype. In accord with other reports this paper demonstrates the potential for this methodology as a therapeutic vaccine, but it is probably insufficient by itself to supplant intact idiotype, carrier protein fusion proteins (or conjugates) by means of idiotope peptide mimics. However, the increase in crossreactivity seen with increasing immunizations suggests that an assortment of idiotope mimics based on two or more CDRs, or perhaps co-immunization with the idiotype, would be a suitable area for further studies. This work is the most direct comparison to date of idiotope and idiotype immunogens.

Introduction

Cancer vaccines rely on antigens expressed uniquely or at least predominantly on cancer cells in order for them to achieve specificity. Ideally, the cancer antigen should be unique to the cancer cell, and this is the case in most lymphomas and leukemias. Typically only one or a few clones is involved in the pathology[††] (4, 75), and the cancerous lymphocytes express on their surfaces either T cell receptors (TCRs) (as in the majority of lymphomas) or B cell receptors (BCRs). Because of the gene rearrangement involved in the ontogeny of these cell lines, the particular BCR or TCR is unique to the clone that encodes it and thus serves as an operational definition of that clone. Hence, the idiotype - the unique portion of a TCR or a BCR - presents an ideal target for immunotherapy for lymphocyte cancers. This ideal specificity nevertheless comes at a cost: it becomes necessary to personalize the immunotherapy to each patient's pathological clone(s).

In the early years following the introduction of monoclonal antibody technology this sort of specific immunotherapy was attempted by raising murine monoclonal antibodies and then using these as an experimental treatment for lymphoma patients. This sort of approach has been undertaken by several groups, notably Ronald Levy's at Stanford University (15, 25, 75-94) and Freda K. Stevenson's of Southampton University Hospitals, UK (14, 26, 27, 95-98), and has the disadvantages that specific monoclonal antibodies need to be prepared for each patient, which takes precious time and is

---

[††] From an immunological perspective, with a clone operationally (serologically) defined by its idiotype, this is a true statement. However, one should bear in mind that other genotypic alterations (mutations, chromosomal rearrangements, aneuploidy) may exist that do not result in an idiotypic difference but which nevertheless result in a

expensive, and that the antibodies used were mouse antibodies and could engender a human anti-mouse antibody response (12), although the toxicity was reported to be low (75). The initial idea was to use such monoclonal antibodies as molecular homing devices for another therapeutic agent such as a conjugated toxin or radioactivity (75), but in fact the BCR target is such that if it is crosslinked by antigen or anti-idiotype antibodies without a second, activating signal, apoptosis ensues and so the antibodies alone also proved surprisingly effective. Furthermore, it can be difficult to obtain sufficient quantities of purified patient-specific antigen, so other less ideal molecular targets have also been pursued, e.g., CD20 (75) but not surprisingly these also target some healthy cells.

The historical method of producing anti-idiotype antibodies has been to immunize another species with the idiotype antibody and then to absorb out the anti-allotype and anti-isotype antibodies (12). For an anti-idiotype antibody therapy to work it should ideally be possible to generate such anti-idiotypes with minimal material. There are two ways that such immunotherapy could be accomplished, and both have been tried: either one could generate anti-idiotype antibodies and use these alone or in combination with other therapy for the treatment of active disease, or else one could make a therapeutic vaccine to educate the patient's own immune system to recognize the pathological clones as being foreign and hence to mount an immune response against them. According to Ronald Levy's perspective, the former approach is more suitable for patients in relapse while the latter approach is more suitable for patients in remission (75). It would be preferable if one could simply use the cDNA from a biopsy to determine the idiotype of

polyclonality that could be detected by subtractive hybridization or other biochemical or

the pathological clone and then to generate anti-idiotype antibodies based on this information (99). One possibility to achieve this would be to use a single-chain variable fragment (scFv), carrier protein fusion construct based on the idiotype as a therapeutic vaccine. Vical, Inc. announced positive phase I/II clinical trial results of personalized DNA vaccines encoding an scFv (with murine constant region domains to make it foreign) under the brand name Vaxid (www.vical.com, March 27, 2001 press release). Another approach has been to use tobacco viruses encoding the idiotype as an insert (90). Both approaches have shown positive results in animal models.

Yet another possibility would be to make a peptide mimic based on one or more of the idiotopes that comprises the idiotype, and then to use the idiotope mimic as a vaccine to generate anti-idiotope antibodies in the hope that they will also crossreact with the parent idiotype. This approach was undertaken in the 1980s in animal models by groups using linear peptides corresponding to the either the first (20), second (20, 21, 23), or third CDR of the heavy chain (20, 22, 100, 101). One study involved an idiotope peptide mimic of the second CDR of the light chain of a human autoantibody (24). The third hypervariable region of the heavy chain – the CDR-H3 loop – has been shown to be superior to the other loops with respect to making crossreactive antisera (20). In general, these approaches found that the anti-peptide anti-sera produced in another species were crossreactive with the parent idiotype antibody. However, only a few (22, 23) of these studies actually compared the crossreactivity between the idiotype and the idiotope mimic directly in terms of immunizations, and those comparisons were flawed to a degree because the foreign T cell epitopes used were not the same. (They used the mouse

---

genetic techniques.

antibody itself but in another species to make it foreign, whereas the peptides were coupled to KLH instead.) This is the focus of the present study – to compare directly an idiotope-carrier protein immunogen versus an idiotype-carrier protein immunogen.

The particular antibody chosen as the idiotype for this study is 9-40, a murine anti-fluorescein antibody of medium affinity (46) belonging to a family of clonotypically related anti-fluorescein antibodies whose idiotypes have been well characterized (47-51). Because we intended to study a peptide mimic of the idiotype as a vaccine, it was necessary to derivatize the idiotype antibody in order to make it foreign to the mouse immune system. Consequently we chose to use chicken hen egg lysozyme (HEL) as a carrier protein due to the fact that this protein has been well studied chemically and immunologically (44), and is small (14.3 kDa), cheap, and easily dissolved. Because it is easier to ascertain whether coupling between the carrier protein and the idiotype has been successful when the relative change in molecular weights is large, we used the Fab' fragment of 9-40 as the idiotype rather than the intact antibody. Hence, the 9-40 Fab' fragment acts as a giant hapten. We also used the CDR-H3 as the idiotope peptide mimic (hereafter designated the B epitope) likewise coupled to HEL. An important consideration is whether or not a linear peptide or a cyclic peptide should be used. Although the earliest studies of idiotope peptide mimicry reported good crossreactivity with just a linear peptide (22-24, 100, 101), other studies found no crossreactivity with a linear peptide (Prof. David M. Kranz, University of Illinois at Urbana-Champaign, personal communication), and we felt that a cyclic peptide would be superior, so our peptide mimic was cyclized. Negative controls were with the B epitope and the HEL simply mixed together rather than covalently coupled, and with the B epitope by itself.

Materials and methods

Preparation of the (9-40)Fab'-HEL

The (9-40)Fab'-HEL conjugate was prepared as described in Chapter 3 and elsewhere (69). Briefly, HEL was dissolved in pH 7.99 PBS and then derivatized with a large (~100-fold) excess of SMCC (Pierce) for several hours at room temperature. Excess SMCC was removed by SEC (PD-10 column [Amersham Pharmacia], eluted with PBS). This was set aside until the (9-40)Fab' had been prepared and purified by SEC (as described in Chapter 3). The purified (9-40)Fab' in its elution buffer (0.1 M $NaPO_4$, pH 6.0, 5 mM EDTA) was then immediately added to the derivatized lysozyme and allowed to react overnight at 4 °C. The product was purified by size exclusion chromatography and the fractions were assayed for both murine (i.e., 9-40) Fab' and for HEL by ELISA; both tested positive.

Preparation of the B-HEL

The 9-40 CDR-H3 idiotope peptide mimic (disulfide of GGGCTSYGYHGAYC, designated as the B cell epitope or Bep for short – it includes an N terminal triglycyl spacer), was prepared by standard Fmoc solid phase peptide synthesis by the University of Utah's DNA/Peptide Facility. It was characterized by MALDI-MS and found to be in agreement with the expected mass (1395.5 expected vs. 1393.47 measured). 2.0 mg of HEL were dissolved in 70 μL of formamide, then diluted with 20 μL of PBS. 1.0 mg of Bep was dissolved in 70 μL of DMSO, then diluted with 20 μL of PBS. 2.0 mg of DSG were dissolved in 40 μL of DMSO and then transferred to the Bep solution for 5 min. Excess DSG was removed by precipitating the reaction mixture with THF (~2 mL) and then EtOEt, then centrifuging. The DSG-Bep conjugate was then redissolved in 40 μL of

DMSO and then added to the HEL solution and allowed to react overnight. Characterization was by MALDI-MS (Figure 17) and then reconfirmed after a period of storage by SDS-PAGE (Figure 18). As can be seen clearly in Figure 17, not all of the six Lys residues on HEL were derivatized; there are peaks corresponding to 0, 1, 2, and 3 Bep per HEL. This is to be expected based on steric considerations of the Bep as well as the reported unequal reactivity of HEL's six Lys (102). (In that study, Lys 33 was the most reactive, followed by Lys 97 and Lys 116, whereas Lys 1 [and the N terminus itself], Lys 13, and Lys 96 were unreactive.)

Immunization protocol

Cohorts of female B10.A mice (H-2^a haplotype; Jackson Laboratories, cat. # 000469) 3-5 weeks old were injected with 65 pmol of either the B-HEL conjugate, the (9-40)Fab'-HEL conjugate, B + HEL mixture, or B by itself. The concentrations of the Fab'-HEL and the Bep-HEL were estimated based on scanned electropherograms or mass spectrometry integrated peak heights using the software Un-Scan-It (Silk Scientific, Provo, Utah) and adjusted molar extinction coefficients calculated from Trp, Tyr, and Phe residues (103) (see Appendix B). Thus, 65 pmol of Bep-HEL is the total amount of (Bep)-HEL + (Bep)$_2$-HEL + (Bep)$_3$-HEL, for example. Mice were bled by tail vein or artery 2 weeks later (primary and secondary; 16 days for tertiary). They were also bled prior to the boosts as described in the Results. All immunogen preparations were mixed 1:1 (v/v) with Freund's complete adjuvant for the primary immunization and with Freund's incomplete adjuvant for the secondary and tertiary immunizations. Each immunization consisted of two subcutaneous injections of 50 µL. The research adhered to the "Principles of Laboratory Animal Care" (NIH publication #85-23, revised 1985).

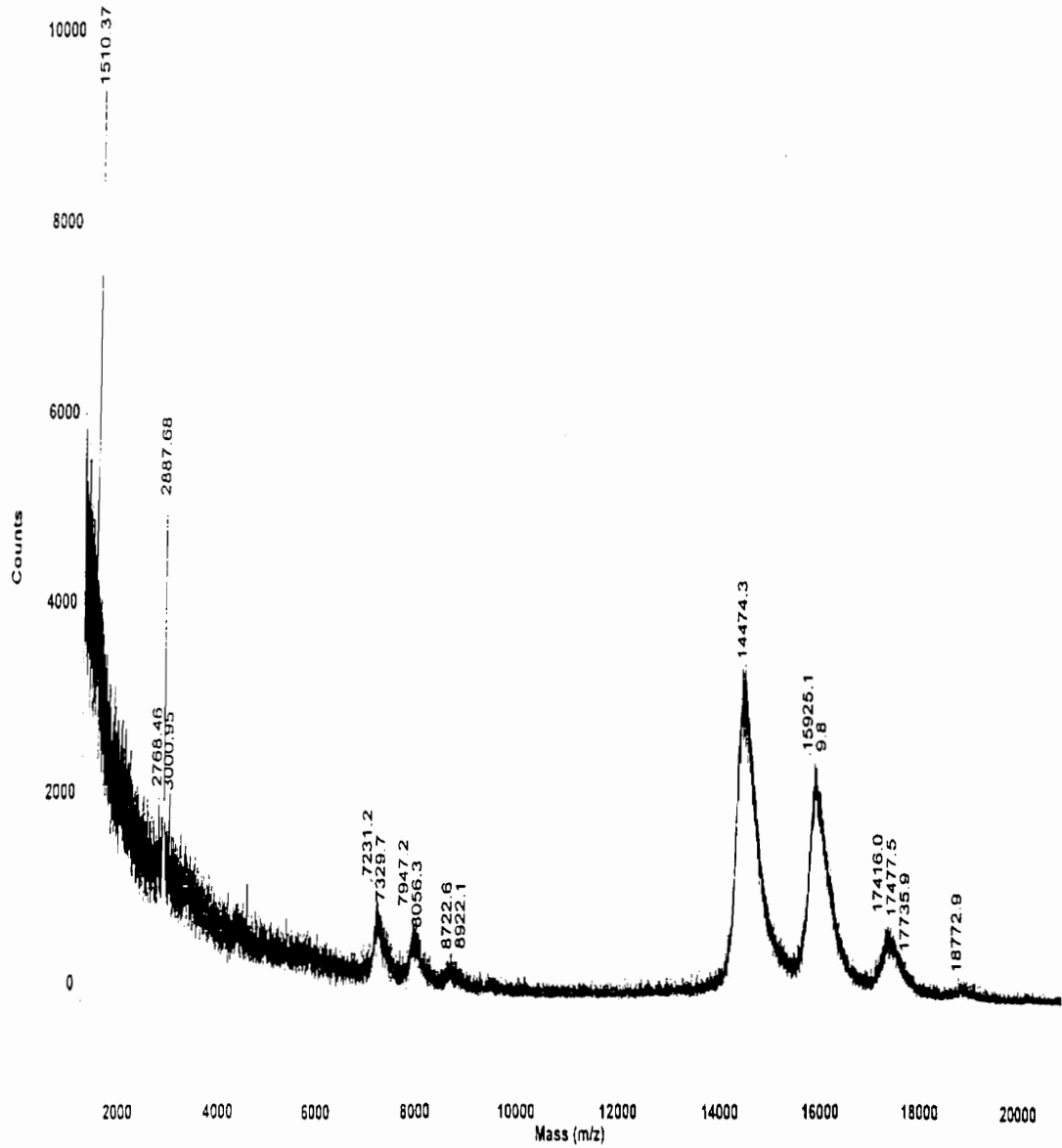**Figure 17.** MALDI-MS of (Bep)$_n$-HEL reaction mixture product. n = 0-3. The mass of the peptide plus DSG is 1395.5 + 98.1 = 1493.6, and HEL's mass is 14314, so the approximate expected masses are 14314, 15808, 17301, and 18795 amu. Given the fairly wide peaks, the measured masses are consistent with these theoretical values.
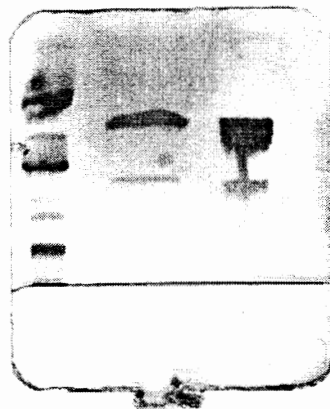
Figure 18. With PhastGel, migration is shown from bottom (negative) to top (positive). From left to right, bands are low m.w. markers, HEL (which dimerizes), and the $(Bep)_n$-HEL product, $n = 0$-3.

ELISAs

Nunc MaxiSorp™ plates were coated for 1 h with either 9-40 $F(ab')_2$ or with a Bep-BSA conjugate made analogously to the Bep-HEL conjugate described above or with BSA as control, then post-coated (blocked) with 1 g/L casein solution (in ELISA wash buffer, 150 mM NaCl, 10 mM Tris, 1 mM EDTA, 0.01-0.05% Tween 20) for 30 - 60 min, then serum samples were applied and incubated at room temperature for 1 h, then washed away, then the tracer antibody (goat anti-(mouse Fab) AP conjugate [Biodesign International]) was added and incubated for 1 h, then extensively washed away with deionized water, and finally substrate (Blue Phos, KPL) was added and the absorbance read at 630 nm after 30 min. The specificity of response was measured by sandwich ELISAs as described previously in Chapter 3 and elsewhere (69) with Fab fragments of 9-40, 4-4-20, BV04-01, or BDC1.

Results

The specificity of the anti-idiotype antibody response was established in pilot studies with female BALB/c mice immunized with (9-40)Fab'-HEL conjugate as part of another study (Chapter 3 and (69)). This was done by using Fab fragments of four different antibodies as ELISA plate coating antigens: 9-40, 4-4-20, BV04-01, and BDC1. 4-4-20 is a high-affinity anti-fluorescein antibody that is idiotypically crossreactive with 9-40 and is clonotypically related to 9-40 (47, 49). BDC1 is another anti-fluorescein antibody, developed in our laboratory, which is not idiotypically crossreactive with 4-4-20 or 9-40. BV04-01 is an anti-ssdT antibody that has extensive homology with 9-40 in the light chain but has only about 60% homology in the heavy chain (28). These results are seen in Figure 19 for the primary response and in Figure 20 for the secondary response. Oddly, the response for BV04-01 Fab was higher than the response for 4-4-20 Fab in the primary immunization (although not in the secondary). These measurements were repeatable (data not shown).

Having established the specificity of the (9-40)Fab'-HEL anti-idiotype response, the next question was how well an anti-idiotope peptide mimic can crossreact with the parent idiotype, i.e., the focus of this study. Figure 21 and Figure 22 show the average primary response for all mice after 2 weeks. By this time there was an anti-idiotype response (Figure 21) but no anti-idiotope response (Figure 22). As a negative control for the ELISA, an anti-BSA response was also measured and found to be negligible (Figure 23). However, by 44 days postimmunization, there was an anti-idiotope response (Figure 24), with again no anti-BSA response (Figure 25). The anti-idiotype response was still strong (Figure 26). These data indicate that the kinetics of the anti-idiotope response is

Anti-(9-40) response for 1st cohort after 1st immunization
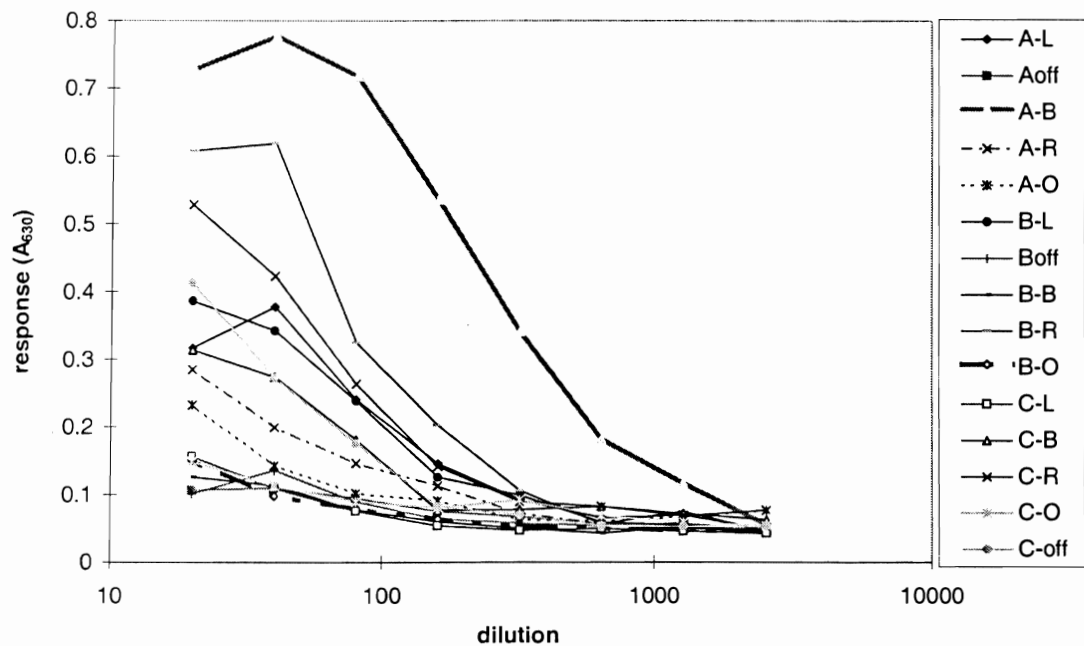
Panel A

Figure 19. These data are the titration curves for the primary immunization of the fifteen B10.A mice used in the pilot study to determine how specific the anti-idiotype response was. The individual mice are in the key to the right with the letter designating in which cage they were stored and the -0, -L, -R, -B, and -OFF suffixes designating how their ears were cut. See text for assay details. Panel A is for the anti-(9-40 Fab) response, Panel B is for the anti-(4-4-20 Fab) response, Panel C is for the anti-(BV04-01 Fab) response, and Panel D is for the anti-(BDC1 Fab) response. The other panels are shown on the succeeding pages.

Anti-(4-4-20) response for 1st cohort after 1st immunization
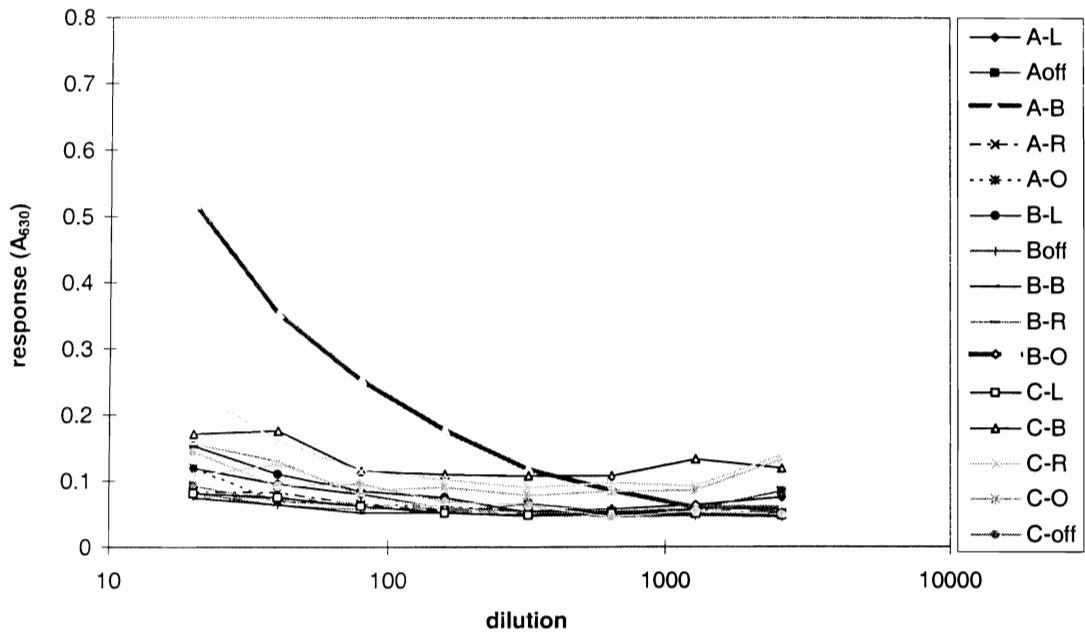
Panel B

Anti-(BV04-01) response for 1st cohort after 1st immunization
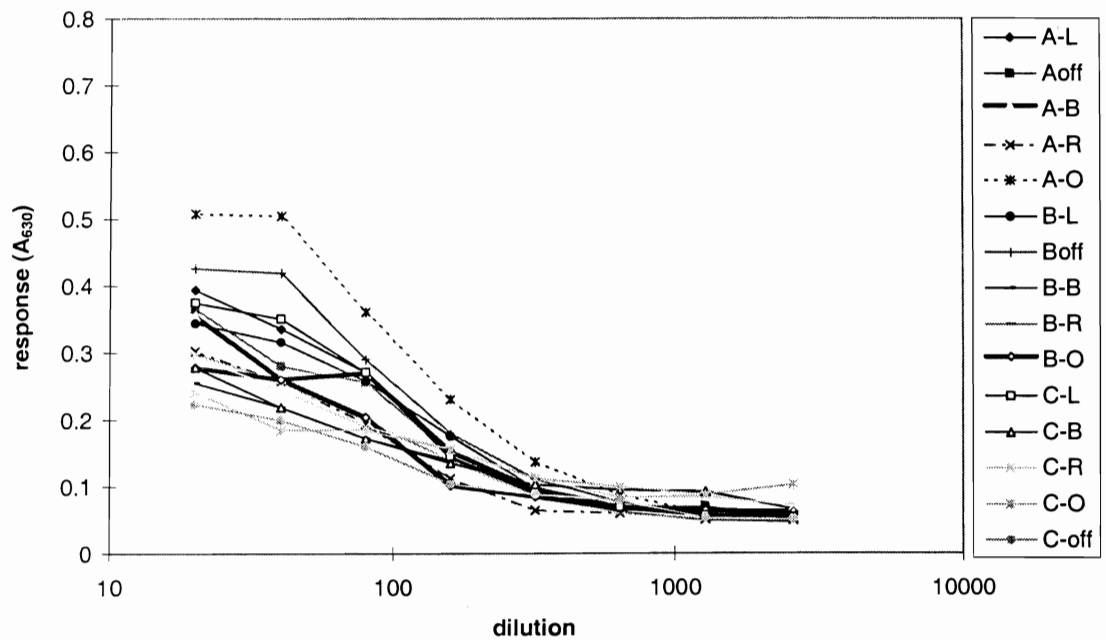
Panel C

Figure 19, continued.

Anti-BDC1 response for 1st cohort after 1st immunization
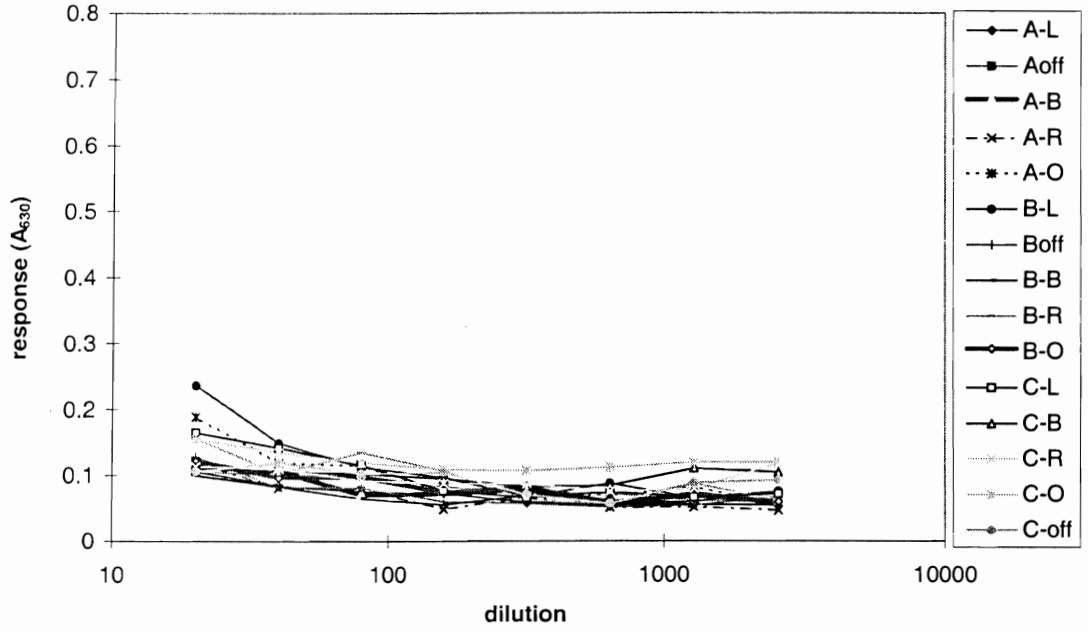
Panel D

Figure 19, continued.

Anti-(9-40) response for 1st cohort after 2nd immunization
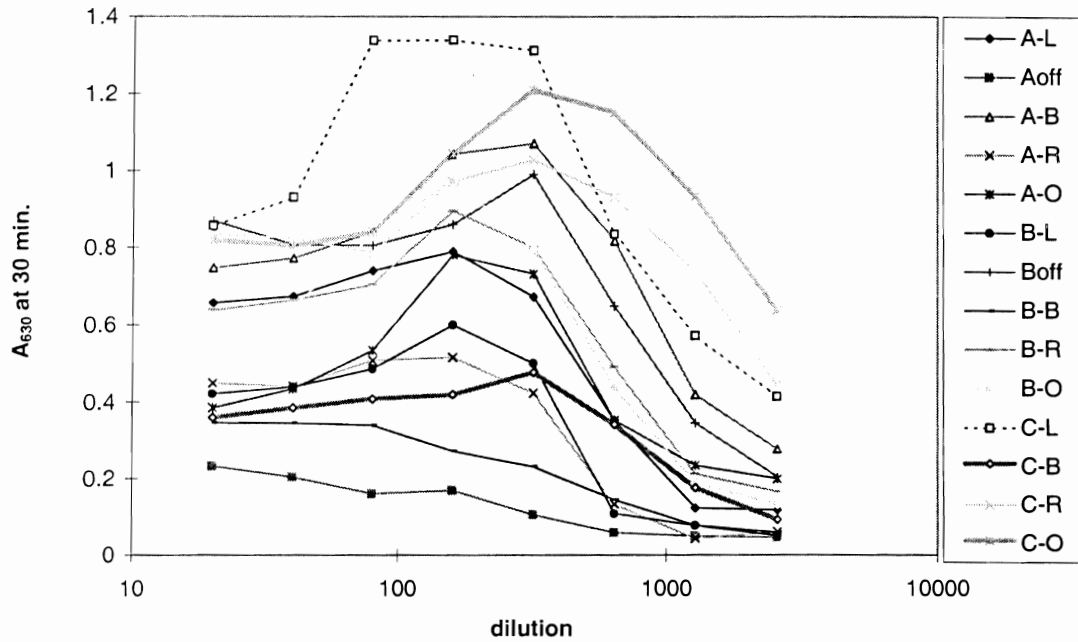
Panel A

Anti-(4-4-20) response for 1st cohort after 2nd immunization
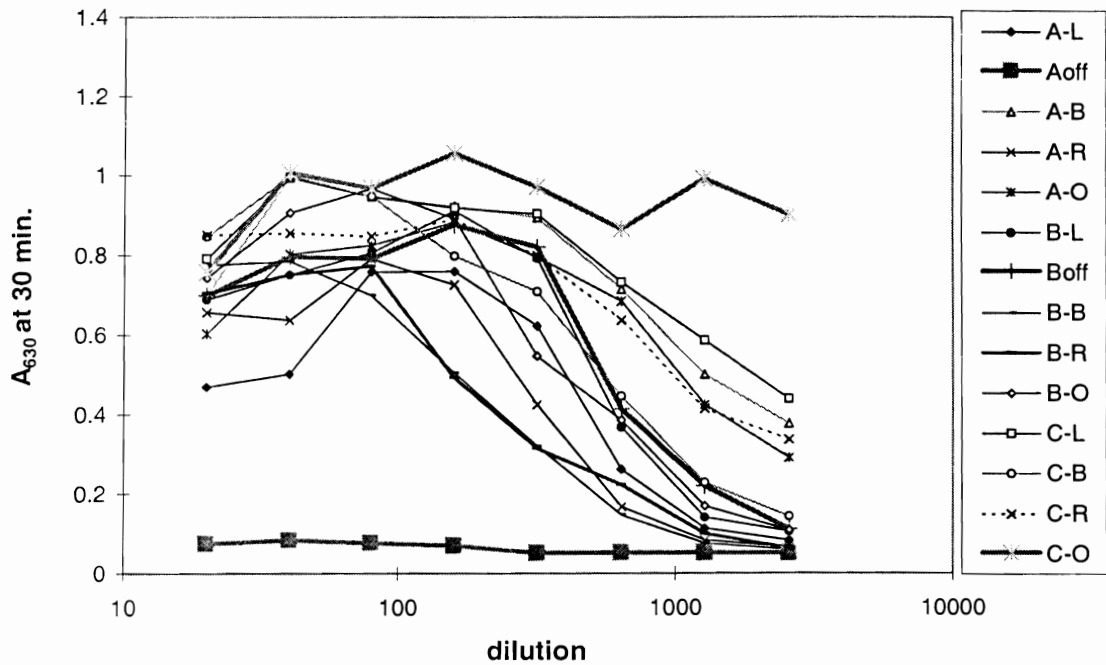
Panel B

Figure 20. These data are as in Figure 19 Panels A-D except that the samples were for the secondary response. Note the larger ordinate scale than for the primary response.

Anti-(BV04-01) response for 1st cohort after 2nd immunization
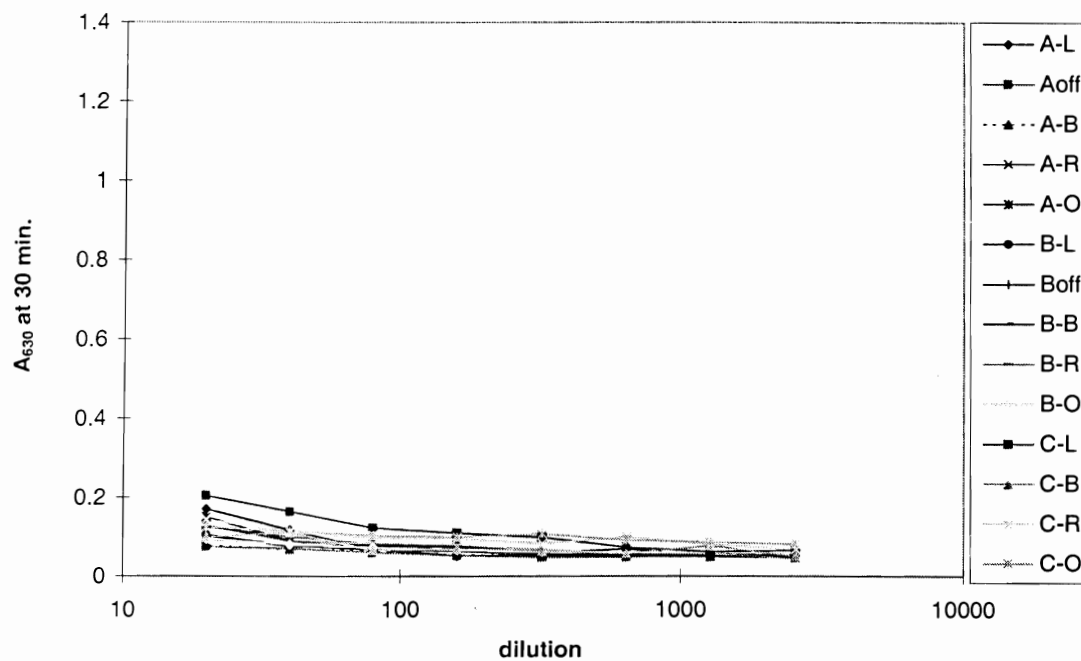
Panel C

Anti-BDC1 response for 1st cohort after 2nd immunization
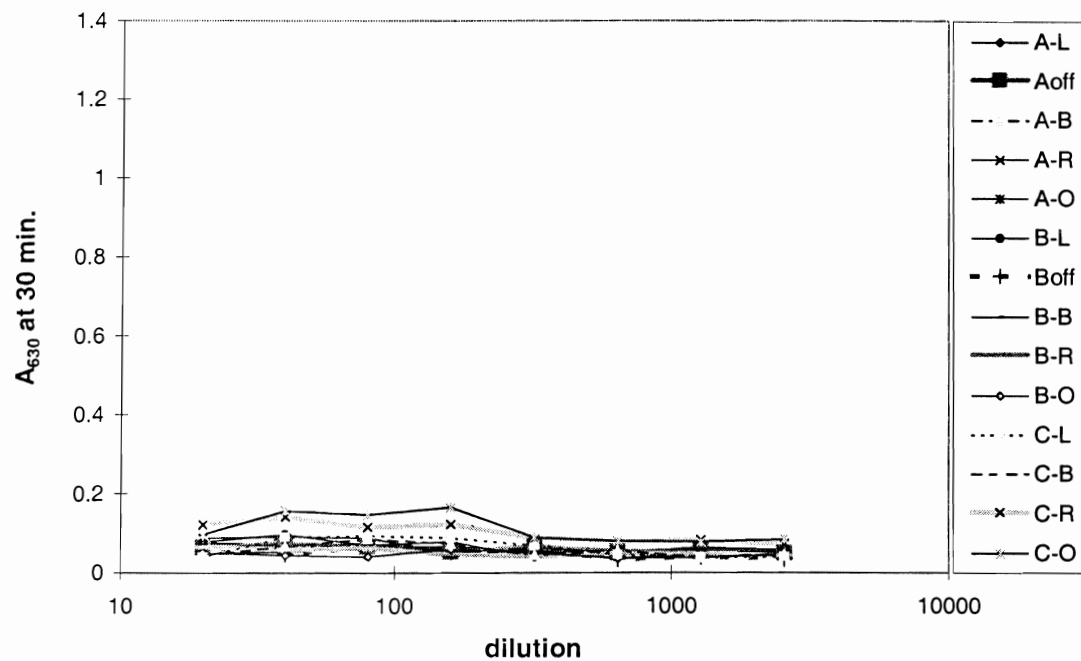
Panel D

Figure 20, continued.

Anti-((9-40)F(ab')$_2$) titers 2 weeks after primary immunization
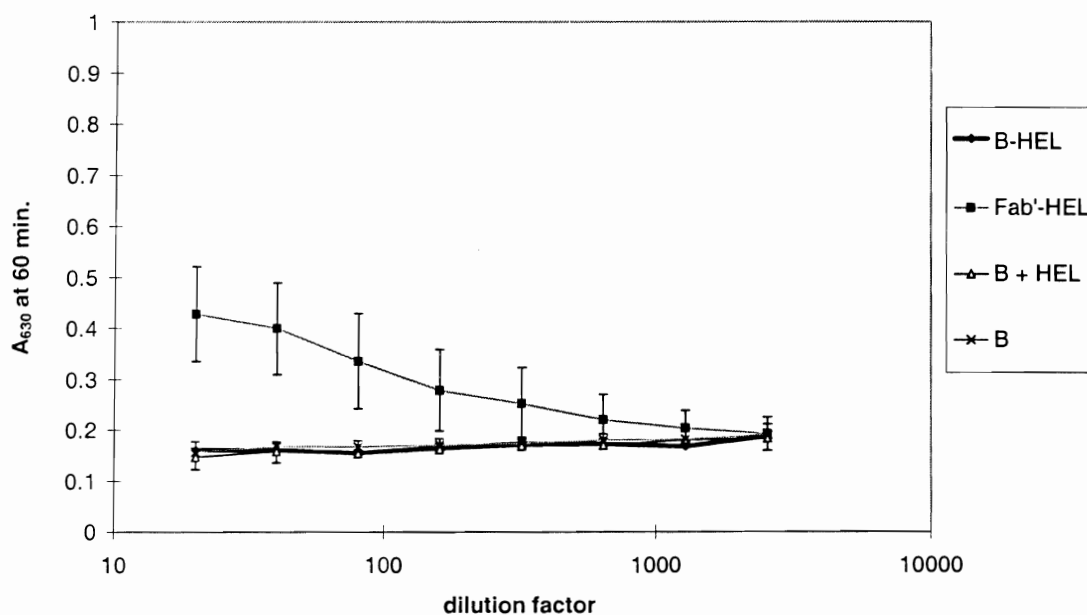
Figure 21. As the title indicates, these data are for the anti-idiotype response 2 weeks after primary immunization. The error bars represent the interanimal variability as given by the sample standard deviations for the four different cohorts. The slight increase in response for all the cohorts with increasing dilution is apparently a systematic error of this particular assay instance. Clearly, only the mice immunized with the idiotype conjugate gave an anti-idiotype response.

Anti-(Bep-BSA) titers 2 weeks after primary immunization
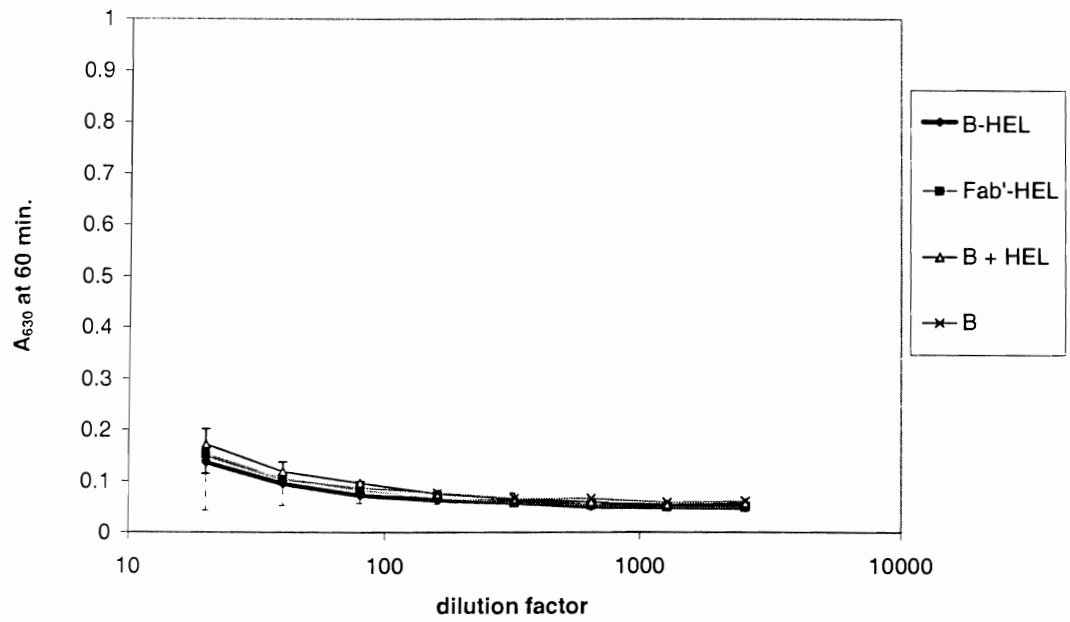
Figure 22. These data show the anti-idiotope response for the primary response of the four cohorts, similar to the data in Figure 21.

Anti-BSA titers 2 weeks after primary immunization
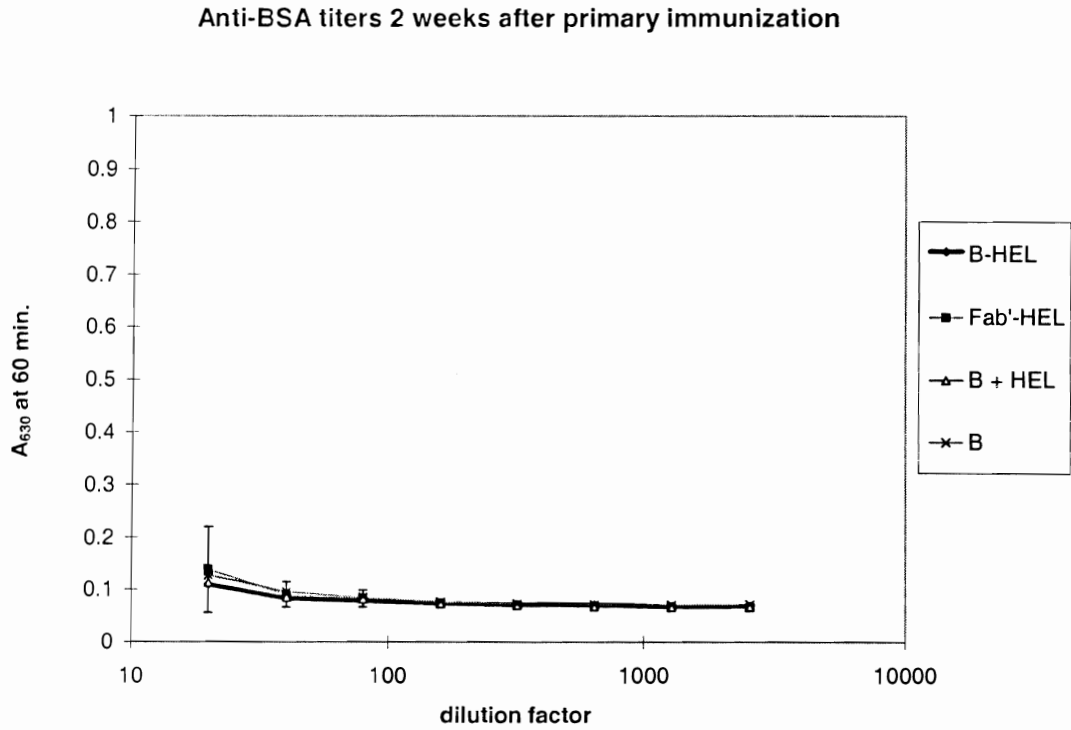
Figure 23. Since BSA was used as a protein to which the peptide was conjugated in Figure 22 in order to increase its adsorption to the polystyrene plate used for the assay, it seemed reasonable to measure the anti-BSA response as well for a negative control on the assay itself. The anti-BSA response is expected and observed to be negative.

Anti-(Bep-BSA) titers 44 days after primary immunization
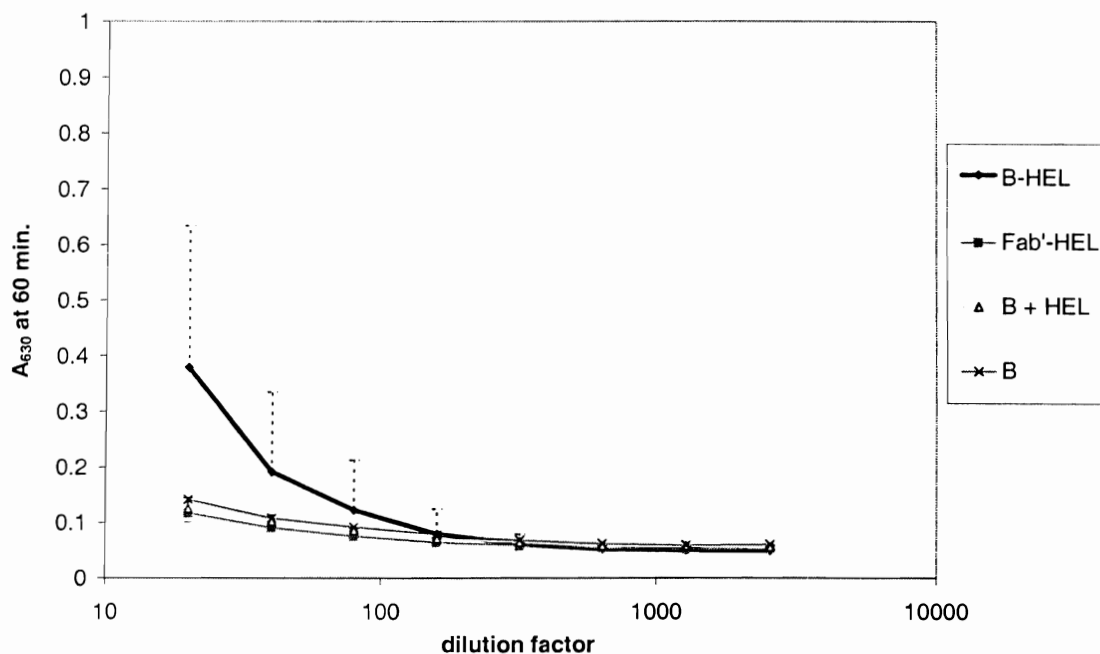
Figure 24. These data are similar to Figure 22 but for the carry-over of the primary immunization prior to the secondary. As in Figure 21 the error bars represent the sample standard deviation for the individual mice; the variability is primarily an interanimal variability rather than an intra-assay variability. Only the upper or lower error bars are shown for clarity. By this time period an anti-idiotope response is seen.

Anti-BSA titers 44 days after primary immunization
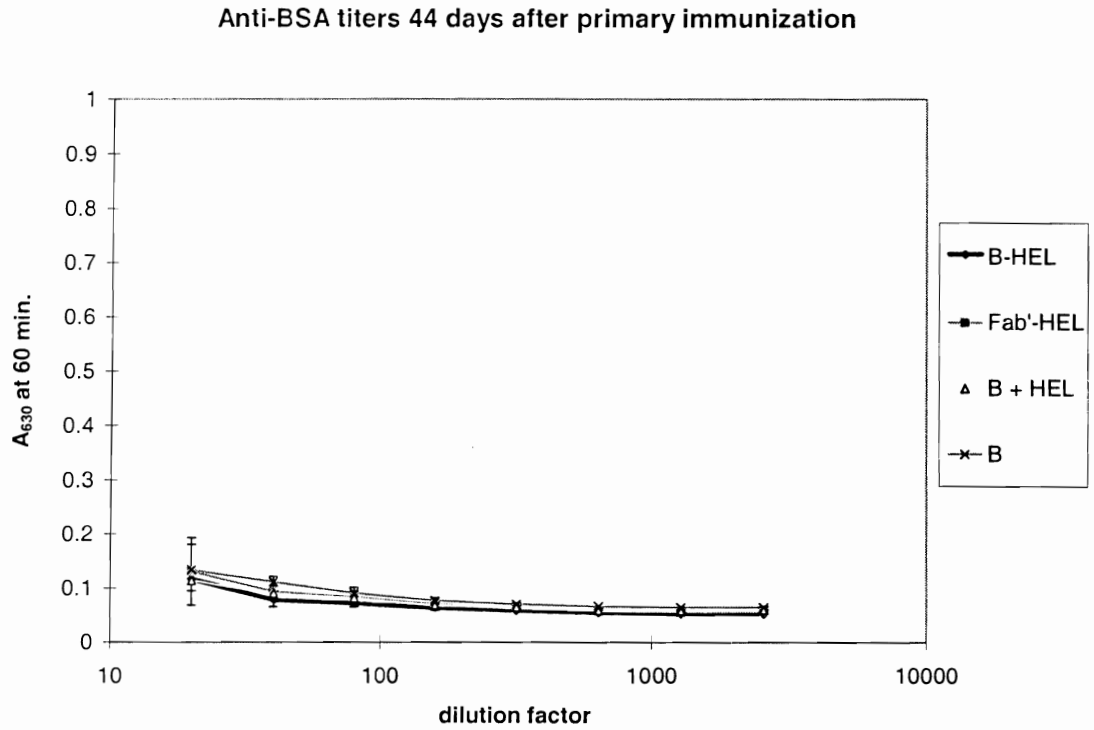
Figure 25. These data are analogous to Figure 23 except for the secondary response. No increase in BSA titers is seen.

Anti-((9-40)F(ab')₂) titers 44 days after primary immunization
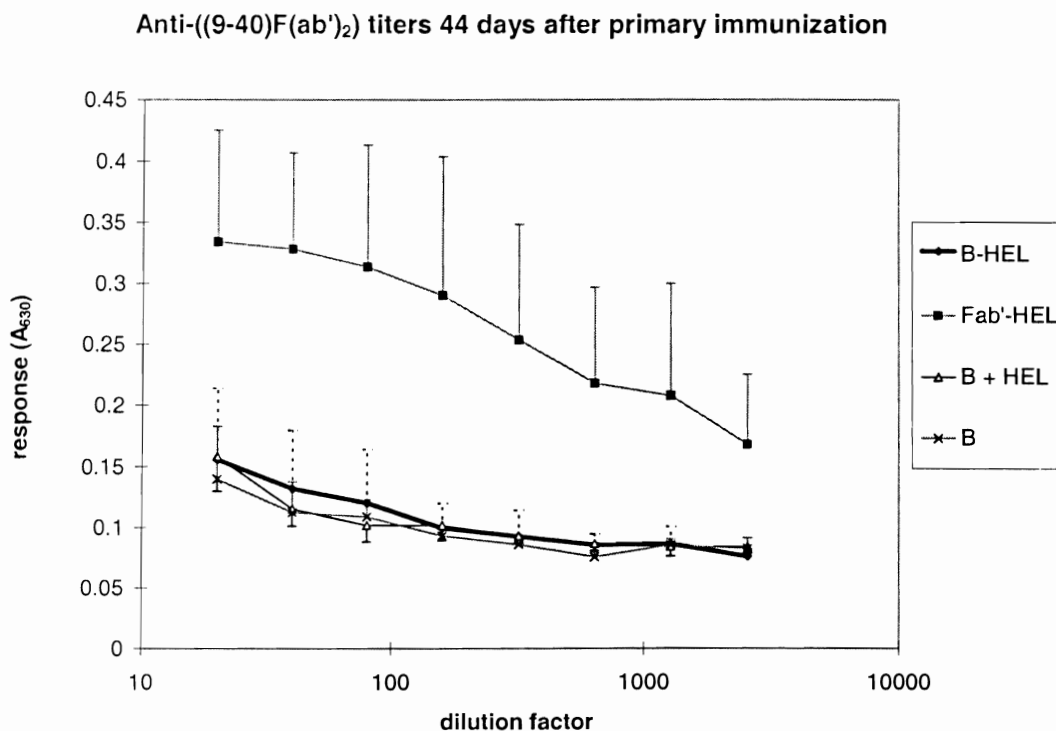
Figure 26. These data are for the anti-idiotype primary response carry-over prior to the secondary immunization. Only the upper or lower error bars are shown for clarity. The dotted line error bars are for the (Bep)-HEL cohort.

slower than the kinetics of the anti-idiotype response.

The secondary response is shown in Figure 27-Figure 28. Whereas there was no crossreactivity in the primary response after 2 weeks, there was some crossreactivity in the secondary response by this time. The data are summarized in Figure 27 for each mouse. It should be noted in Figure 27 that the assays used necessarily differed in detail (coating antigens, color development times) so that the scales are only valid in a relative sense. Although there is very poor correlation between the anti-idiotope and anti-idiotype responses for the mice immunized with Bep-HEL (y = 0.0853x + 0.1328; R^2 = 0.0101), this cohort did have 3 out of 10 crossreacting mice, using as a criterion for crossreactivity an anti-idiotype response of at least 0.2 (the approximate lower limit of

Summary of data for 2 weeks after secondary immunization
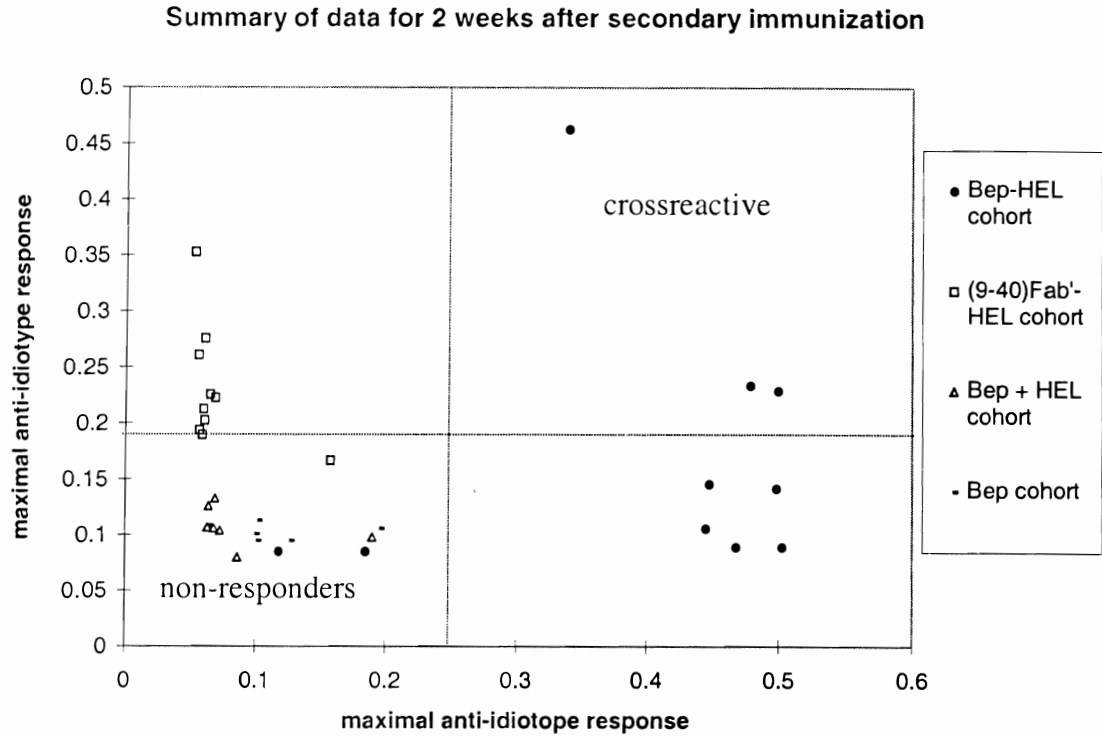
Figure 27. This graph summarizes the secondary response crossreactivity seen for the individual mice in all cohorts.

the anti-idiotype response among mice immunized with (9-40)Fab'-HEL). One mouse from this group actually had a better anti-idiotype response than did any of the mice immunized with the intact idiotype. It is also worth noting that the anti-idiotope response for this mouse was the third worst of all the mice immunized with the idiotope mimic, surpassed only by two mice that ranked in with the negative controls. Conversely, the only mouse that gave some anti-idiotope response among the mice immunized with the intact idiotype also had the worst anti-idiotype response of all those mice. However, this did not remain the case; prior to the tertiary immunization, another bleeding was taken (due to time constraints, at 39 days for the control cohorts and at 48 days for the experimental cohorts). The crossreactivity between the immunogens had dropped signif-
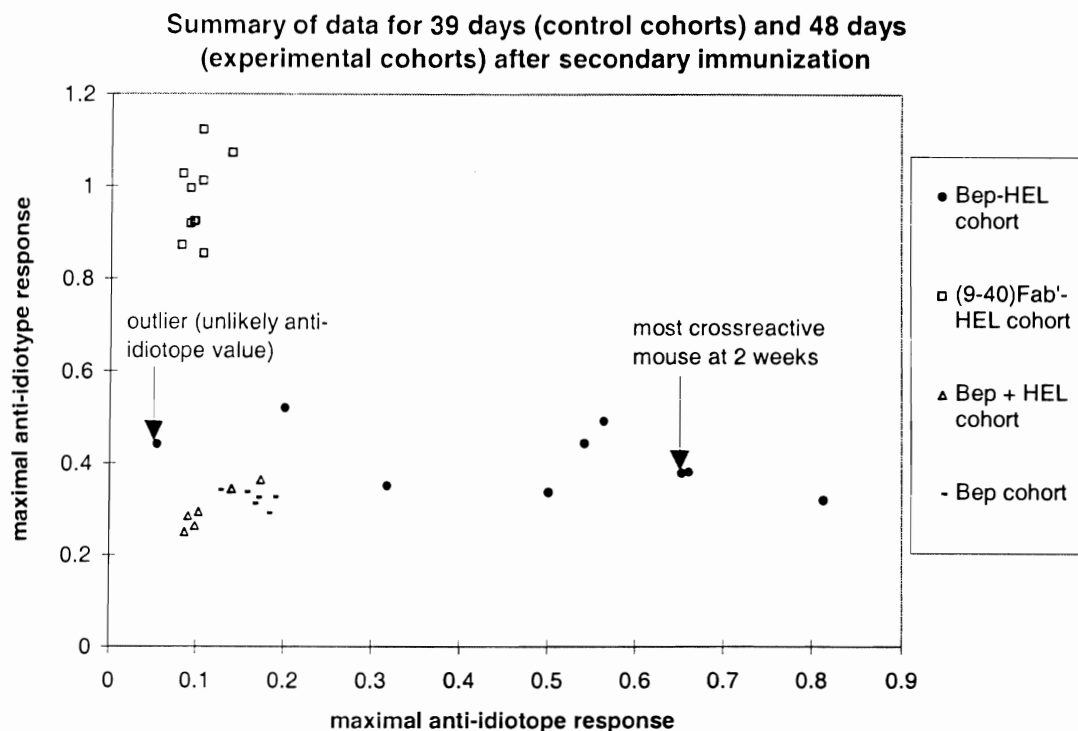
Figure 28. These data show the crossreactivity for the secondary immunization carry-over. Note that the most crossreactive mouse in Figure 27 is no longer so.

icantly, and the previously most crossreactive mouse with a low anti-idiotope response now had the third-highest anti-idiotope response. These data are presented in Figure 28.

The tertiary response is shown in Figure 29. Two mice from the (Bep)-HEL cohort showed excellent crossreactivity and especially high anti-idiotype titers at this point. Even stranger, the highest anti-idiotype response of the (9-40)Fab'-HEL cohort was lower than the lowest response of the (Bep)-HEL cohort. The control mice appeared to give significant responses even at high dilutions in the ELISAs. These could be real since earlier work (Chapter 4) has shown that peptides by themselves can give high titers after repeated immunization even at low doses, but it seems more likely that the background was too high, since one might expect an anti-idiotope response with the

Summary of data for 39 days (control cohorts) and 48 days (experimental cohorts) after secondary immunization
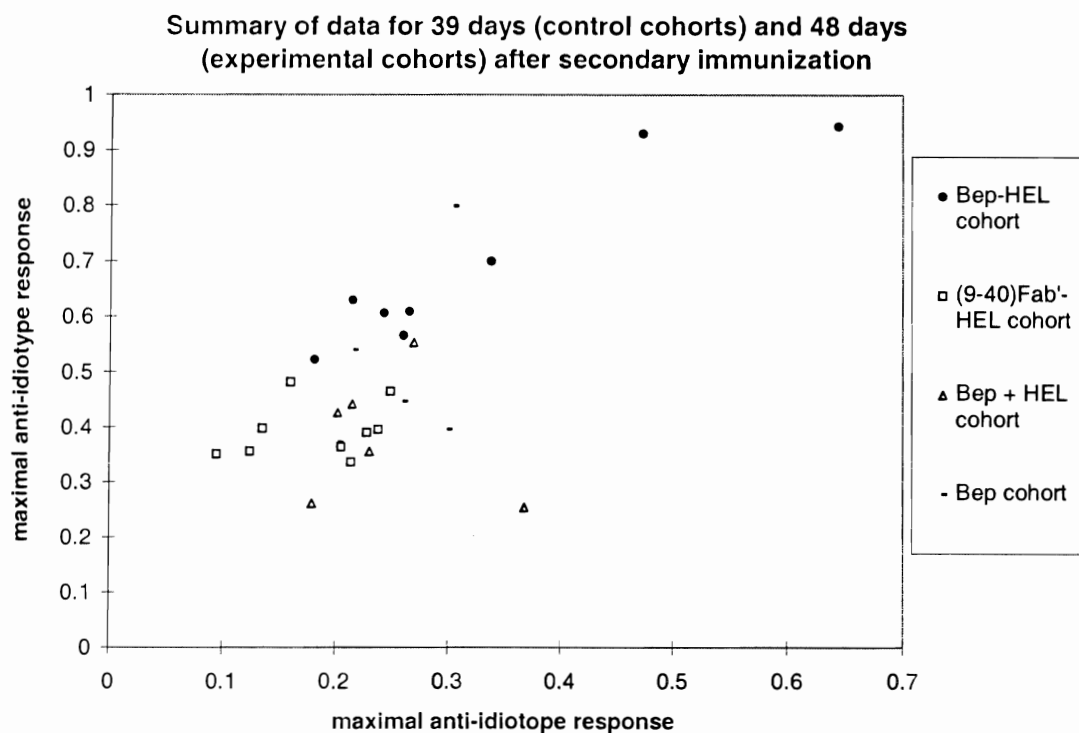
Figure 29. These data are for the tertiary immunization. The high response of the negative controls and the low anti-idiotype response of the idiotype cohorts was suspicious and motivated re-examination of the anti-idiotype responses.

idiotope peptide but would not expect that the response would surpass that of the idiotype immunogen itself, as seen in the figure.

Because of the especially low anti-idiotype titers of the Fab'-HEL cohort and also the high titers of the negative controls, the anti-idiotype data were re-measured (Figure 30). These data give results that are more consistent with what one might expect based on the results of the previous immunizations. The Fab'-HEL cohort gave the strongest anti-idiotype response. Interestingly, one of the mice in the Bep negative control cohort did show a strong anti-idiotype response, but the validity of this is questionable since it was this mouse that had the lowest anti-idiotype response in Figure 29. Otherwise it is

Summary of data for 16 days after tertiary immunization
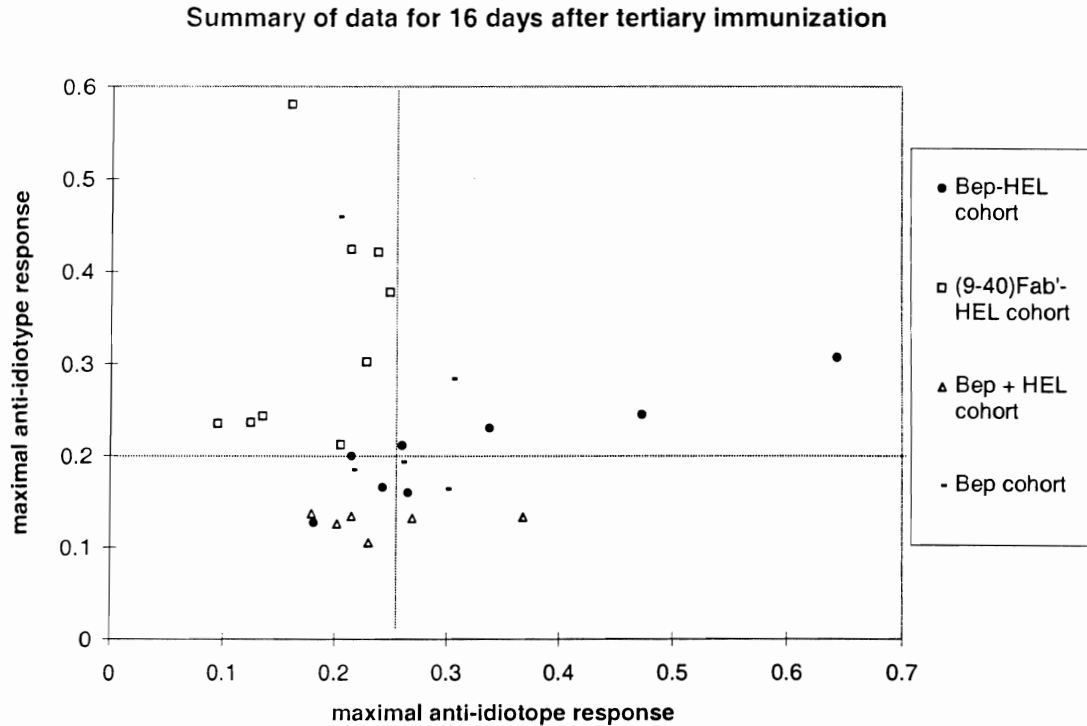
Figure 30. These data use the same abscissa as in Figure 29 but a re-measured ordinate. Note that the second highest response, from a negative control mouse that exhibited the lowest anti-idiotype response of its cohort in Figure 29, is possibly an outlier, but it did not show a single well with a high absorbance but rather a nicely sloping titer. More importantly, it can be seen that the crossreactivity of the peptide immunogen cohort is fairly high (5/8 mice), using again as a criterion an anti-idiotype response of 0.2.

worth noting that all of the Bep negative control mice had higher anti-idiotype titers than did all of the (Bep + HEL) cohorts. It is especially worth noting that the crossreactivity has increased between the second and third immunizations for the (Bep)-HEL cohort: 3/10 crossreactive mice for the secondary response compared with 5/8 for the tertiary.

Conclusions

The specificity of the anti-idiotype response was demonstrated in a pilot study with B10.A mice immunized with a (9-40)Fab'-SMCC-HEL conjugate. Those mice

responded well to the immunizing idiotype and to a clonotypically related antibody known to be idiotypically crossreactive, but not to another anti-fluorescein antibody (BDC1) nor to an anti-ss(dT) antibody that shares the same framework regions as does 9-40. It is significant that no anti-framework response was seen, since after all, those epitopes could also be considered part of an immunologically foreign molecule after coupling to HEL. This leads to speculation that the anti-framework reactive clones had been deleted or rendered anergic in the development of the mice' immune systems.

A peptide mimic based on the third hypervariable region of the heavy chain of monoclonal anti-fluorescein antibody 9-40 and incorporating a triglycyl spacer was coupled to chicken hen egg lysozyme and used to generate an anti-peptide response. This peptide represents an idiotope of primary importance. Another vaccine based on the entire idiotype was also coupled to HEL and also generated an anti-idiotype response. Control immunogens consisting of the peptide mimic by itself or of the peptide mimic mixed with HEL failed to give a primary or a secondary response, although possibly gave a tertiary response. (Recall from Chapter 4 that peptides by themselves after repeated immunizations were sometimes effective at generating high titer antibody responses.) The kinetics of the anti-idiotype vaccine were faster than for the anti-idiotope vaccine, since there was an anti-idiotype response after 2 weeks but no response for the anti-idiotope preparation. By 44 days, however, there was also an anti-idiotope response, and the anti-idiotype response was even stronger. The secondary response showed mild crossreactivity for the idiotope vaccine but only very little crossreactivity for the idiotype vaccine. This was also the case in the tertiary response – the idiotope vaccine resulted in a crossreactive response in some mice whereas the idiotype vaccine did not.

It seems reasonable that the anti-idiotope response should have greater cross-reactivity than the anti-idiotype response, since there are multiple idiotopes in an idiotype against which a response could be directed and which would perhaps not likely be the accessible portions of the CDR-H3. Likewise, some of the anti-Bep antibodies are probably also directed against the linker or against portions of the peptide mimic that are not accessible in the intact idiotype. (Certainly, both vaccines doubtless elicit antibodies against HEL.) A more important question is why the crossreactivity for the idiotope peptide mimic is not initially greater than it is. Probably this is because only a few residues of the CDR-H3 of an antibody are exposed to bulk solvent, the rest being either juxtaposed to the rest of the heavy chain or forming part of the antigen binding cavity. It may also be the case that the anti-idiotype antibodies generated from the Fab'-HEL immunogen are likely predominantly rather flat in their antigen binding sites, as is common in cases of antibodies against proteins, whereas the anti-idiotope antibodies generated from the Bep-HEL are likely to bind the peptide in deep pockets (104).

The present results are also consistent with earlier studies in which anti-(idiotope peptide mimic) antisera were generated against the CDR-H3 (22) or CDR-H2 (23). Those authors also reported that while one could use idiotope peptide mimics to generate anti-idiotype antisera, the converse did not occur. The present studies are a more direct comparison of the anti-idiotype response with the anti-idiotope response, since the same carrier protein was used for both immunogens.

Are anti-idiotope peptide mimic vaccines a promising approach to targeting pathological B lymphocytes? They do offer the significant advantage of being able to be prepared based only on the information obtainable from a biopsy followed by PCR and

sequencing, and they do have some ability to crossreact with the intact idiotype and probably also cause apoptosis in such B cells. Nevertheless, although the present studies do not specifically address lymphocyte targeting, it is clear from them that if one wants to target a specific idiotype, the best choice is to use the idiotype itself in some fashion to make it immunogenic. Such idiotype vaccines would generally be a fusion protein, an scFv, or a plasmid encoding such a fusion protein or scFv. Since DNA vaccines obviate the need for purified idiotype protein for immunogen preparation, and still allow for an intact idiotype to be targeted, they are a very promising alternative. Another alternative would be antisense, since the B cell's specificity could be exploited at the protein or the RNA level.

So what does the future hold for idiotope mimics? One very interesting question is whether or not a longer loop, such as the CDR-L1 or -H2 loop, would give a stronger response. The H3 loop was chosen primarily because it offers the most specificity, being the product of V-D-J gene rearrangements and not exhibiting any canonical structures. However, such a strong specificity requirement may be overkill, as anti-CD20 antibodies have shown utility in lymphoma therapy (75) and are not at all idiotype selective. In 9-40 the CDR-H3 is rather short, so perhaps another antibody would have been a better choice from the standpoint of testing the CDR-H3 loop. It would be interesting to use a panel of antibodies with different CDR-H3 loops.

Using such a panel could be advantageous for another reason: individualized therapy, as with all cancer therapy, is susceptible to failure. As noted in a footnote earlier, lymphocyte cancers are monoclonal at least from the standpoint of serologically defined surface antigens, but there can be numerous mutations giving rise to cancerous

phenotypes. Cancer therapies often result in an initial killing with survivors, likely mutants with only subtle differences from the clones susceptible to killing, being resistant. The broader issue of why tumors become resistant to drugs is still incompletely understood. As long as the cancer cells are monoclonal from the standpoint of expressed surface antigen - in the present case, the idiotype - then one would expect that a vaccine designed to target this antigen would still be effective even if other mutations are present that do not affect the idiotype expression. Indeed, this seems to be the case with the DNA idiotype vaccines intended to prevent relapse. If, on the other hand, small somatic mutations in the CDRs occur in the cancerous clones, then a panel of idiotope mimics could perhaps still be effective, since it is unlikely that one or a few mutations in one or two idiotopes would completely wipe out crossreactivity with all the idiotopes in the panel.

Another consideration is the fact that the crossreactivity increases with increasing immunizations. This leads me to wonder if co-immunization of both an idiotope vaccine and an idiotype vaccine could potentially lead to a synergistic effect, and that question should be pursued further. Another question is at how long such increases in crossreactivity continue with increasing immunizations: would the idiotope vaccine ever exhibit as strong or as consistent an anti-idiotype response as does the idiotype vaccine? (Another question would be whether there would be an increase in crossreactivity to seemingly irrelevant antigens.)

Another interesting area for further study is in the different kinetics of the cross-reactive clones. The crossreactivity seen at 14 days (Figure 27) has disappeared by 48 days (Figure 28). This is undoutedly due to the subsistence of the crossreactive clones

and the clearance of crossreactive antibody, but the overall anti-idiotope response at 48 days is still quite high. Is there a lack of continual stimulation of the crossreactive clones? Another study (18) investigating crossreactivity between an idiotope mimic and an internal image idiotype mimic of yet another antigen also found this same pattern of temporal crossreactivity – there was an initial idiotope, idiotype crossreactivity that subsided into a more specific anti-idiotope response.

Finally, the basis for the crossreactivity must lie in the antigenicity of the peptide rather than in any immunogenicity of the carrier protein. As shown more fully in the next chapter, CDR loops are quite mobile. What fraction of the 9-40 idiotype population has its CDR-H3 loop sufficiently exposed that it can be bound by anti-idiotope antibodies? That is for now an open ended question that one day may be solved by molecular modeling.

CHAPTER 6

MOLECULAR MODELING OF ANTIBODY

BV04-01'S VARIABLE FRAGMENT

Abstract

Purpose

We were interested in comparing different computational methodologies for antibody variable region structure prediction.

Methods

Four starting models of the variable region of monoclonal antibody BV04-01 were subjected to 1210 ps of equilibration plus simulated annealing (SA). This was followed by isothermal molecular dynamics (MD) at 300 K for 2 ns for generalized Born (GB) implicit solvent or for 1 ns for particle mesh Ewald (PME) with explicit solvent and periodic boundary conditions. Because the PME methodology was more time consuming than was GB, the PME simulations used the results of the GB SA for the four structures prior to hydration and actual PME computation, except that one of these structures was also hydrated prior to undergoing SA. Charge neutralization was not done for any of the structures.

Results

The GB methodology resulted in a general distortion or possible twisting of the two chains around the antigen binding site, but with the heavy chain slightly more distorted than the light chain. It also showed a decrease in the accessibility to the antigen binding pocket of the CDR-L1 and -H1 loops, which were pushed away by the CDR-L3 and -H3 loops. The four different starting structures did not converge to the same solution structure in the 2 ns isothermal simulation. In contrast to GB, the PME methodology did not cause severe distortions from the crystal structure, with the exception of the CDR-H3 loop, which was already removed from the crystal structure by the GB SA prior to hydration.

Conclusions

The additional computational expense of PME relative to GB for the purpose of solution structure prediction seems justified, but the question remains as to whether the deviations from the crystal structure of the CDR-H3 loop represent significantly populated solution substates or are merely a kinetic artifact of the SA.

Introduction

Recent years have seen incredible refinements of various techniques in science, resulting in a convergence that has greatly increased our understanding of numerous aspects of science, including structural biochemistry. Computational technology has improved by orders of magnitude in the last two decades, and molecular dynamics now plays a significant role in elucidating biochemical mechanisms and even in refining X-ray crystal structures (105). X-ray crystallography has played such an important role in structural biochemistry over the last several decades in elucidating basic biochemical

phenomena that it has achieved a sort of "gold standard" status, probably because high-resolution NMR solution structures of biomolecules had a later start historically than did X-ray crystallography, and because many biomolecules are simply too large to solve by NMR. In fact, the validity of NMR as a technique for protein structure determination was established by X-ray crystallography as a standard, rather than vice versa (103, p. 243-244), when the structure of the small protein tendamistat was solved by both techniques and was found to be in excellent agreement between the two.

Determining the structure of a biomolecule is not a trivial undertaking. Consequently, computational approaches have also been explored, and with the dramatic increase in computer power in the last several years this is a very promising field of study. The ab initio prediction of tertiary structure from primary structure is still far from being a robust science, but homology modeling has proven quite useful in cases for which significant homology does exist between proteins of known structure and the protein of interest of unknown structure. In fact, the primary criterion for the success of a homology model structure is the amount of homology that exists between the reference proteins and the homology model. In the case of the variable regions of antibodies, the framework regions are basically all the same, and the homology from one antibody to another is excellent. Because of this fact and because of their importance, a few homology prediction programs have been developed to obtain useful models with atomic detail especially for antibodies (e.g., AbM and its successor WAM (106)). In any case, most if not all homology modeling involves several steps, ending in a final minimization of the predicted structure.

Homology model structures are usually based on crystal structures rather than solution structures simply because there are more of the former in the Protein Data Bank (PDB). Nevertheless, X-ray crystal structures (and also neutron diffraction crystal structures) are just that – crystal structures, and it is generally the solution structure of a biomolecule that is of interest. As mentioned above, NMR can provide solution structural models for small proteins but cannot for large ones. However, the dramatic increases in computer power and molecular modeling in the last several years open up the possibility of converting a crystal structure into a solution structure. Because in principle such a model could be had within an arbitrary level of error by simply increasing the rigor of the computations (duration of calculation, number of solvent molecules, etc.; even with QM calculations with full CI) and no one would object to using such structures, and because such calculations of arbitrary exactness would generally be unfeasible, the germane question is, "What is the minimum requisite level of computation needed to establish a plausibly realistic solution model?" To this end we used molecular dynamics (MD) simulations to predict the structure of the variable region of one antibody (BV04-01, for which the crystal structures of both the liganded and unliganded forms of the Fab fragment are known (28)), given the structure of the variable region of a moderately homologous antibody (4-4-20, for which several high resolution structures have been determined in different solvents (52)) using both an explicit solvent approach and a faster but more approximate implicit solvent approach.

Because MD is by its very nature a time-dependent modeling approach, the question always will remain, What would happen if one went longer? Was the simulation long enough? The general strategy we decided to follow was to use a number of

starting structures each with BV04-01's sequence, and subject them all to the same set of molecular dynamics protocols. If the different structures converge to the same final solution structure, then that would lend credibility to the model.

Theory of electrostatic treatments

The function, or effect, of a dielectric is to shield charges separated by some distance from each other. The dielectric of a polar medium such as water is much higher than for a nonpolar medium such as the interior of a protein ($\varepsilon = 78$ for water at room temperature versus an estimated 4-10 for protein interiors (107)), although the value that should be chosen for the interior of a protein is ill-defined, as occasionally there are ionic interactions in protein interiors. Consequently one approach to dealing with this problem is to replace the bulk dielectric constant with a function. The simplest function sometimes chosen, and what is typically meant by the phrase "distance-dependent dielectric," is an inverse linear relationship, but that choice is not very accurate. Generalized Born (GB) is a way of providing a distance-dependent dielectric function that is more accurate than a simple inverse linear dependence. An outline derivation follows (108, 109). The free energy of solvation can be thought of as the free energy required to form a cavity in a solvent plus solute-solvent interaction terms, generally van der Waals and polarization:

$$G_{\text{solvation}} = G_{\text{cavity}} + G_{\text{vdW}} + G_{\text{polarization}} \qquad (1)$$

The cavity and van der Waals terms can be approximated by a linear function of the solvent accessible surface area of the solute, $\Sigma \gamma_i A_i$, where γ is an empirical constant

related to the surface tension and A_i is the solvent accessible surface area. The polarization term is given by a summation of the Born equation and Coulomb's law (algebraically written in a form similar to the Born equation):

$$\Delta G_{polarization} = \sum_{i}^{N} \frac{q_i^2}{2a_i}\left(\frac{1}{\varepsilon_w}-1\right) + \frac{1}{2}\sum_{i}^{N}\sum_{j\neq i}^{N}\frac{q_i q_j}{r_{ij}}\left(\frac{1}{\varepsilon_w}-1\right)$$

(2)

This gives the free energy of solvation as

$$\Delta G_{solvation} = \sum \gamma_i A_i - (1/2)(1-\frac{1}{\varepsilon_w})\sum_{i,j} q_i q_j / f_{GB}$$

(3)

where the function f_{GB} becomes an effective Born radius in the self terms but becomes an effective interaction distance in pairwise terms. The most common form chosen is

$$f_{GB}(r_{ij}) = [r_{ij}^2 + R_i R_j \exp(-r_{ij}^2 / 4R_i R_j)]^{1/2}$$

(4)

Whereas GB is like a glorified vacuum calculation, particle mesh Ewald (PME) employs full solvation and is an accurate treatment of electrostatics using periodic boundary conditions (110-112). Briefly, the electrostatic potential $\varphi(\mathbf{r})$ at point $\mathbf{r}$ is given by Poisson's equation:

$$\nabla \cdot \nabla \varphi(\mathbf{r})d\mathbf{r} = -4\pi\rho(\mathbf{r})$$

(5)

where $\rho(r)$ is a smooth charge density. For periodic boundary conditions the electrostatic potential at a point r not coincident with any atomic position r_i ($i = 1,2,...,N$) is given by summing the direct Coulomb potential over all atoms and all their images:

$$\varphi(\mathbf{r}) = \sum_{\mathbf{n}} \sum_{i=1}^{N} \frac{q_i}{|\mathbf{r}_i + \mathbf{n}L - \mathbf{r}|}$$

(6)

This general lattice sum is conditionally convergent. Ewald's approach was to imagine that each charge in the crystal is surrounded by a pair of continuous charge densities: a counterion density and a co-ion density. Then $\phi(\mathbf{r}) = \phi_1(\mathbf{r}) + \phi_2(\mathbf{r})$. This is equivalent to multiplying the function by a rapidly converging function F and, to maintain equality, adding a term equal to the function multiplied by (1-F). Ewald's insight was that the second term can also be made rapidly converging by a Fourier transform, giving a direct sum, a reciprocal sum, and a self term:

$$\phi_{Ew}(\mathbf{r}_i) = \sum_{\substack{\mathbf{n} \\ \text{when } \mathbf{n}=0}} \sum_{\substack{j \neq i \\ j}} q_j \frac{erfc(\beta|\mathbf{r}_j - \mathbf{r}_i + \mathbf{n}|)}{|\mathbf{r}_j - \mathbf{r}_i + \mathbf{n}|} + \frac{1}{\pi L} \sum_{m \neq 0} \frac{\exp[-\pi^2 m^2 / \beta^2 L^2]}{m^2} S(\mathbf{m}) \exp[2\pi i \frac{\mathbf{m} \cdot \mathbf{r}_i}{L}] - q_i \frac{2\beta}{\sqrt{\pi}}$$

(7)

Essentially, Ewald summation is a periodic boundary approach that yields a neutralizing field of counter charge. Particle mesh Ewald is a fast Ewald sum algorithm, scaling as N log N (110).

Methodology

Choice of initial coordinates

BV04-01 is an anti-ssdT murine autoantibody (28). It has two entries in the PDB for its Fab fragments: 1NBV and 1CBV, which correspond to the unliganded and the liganded states respectively. (The ligand is dT_3.) 4-4-20 is a high-affinity anti-fluorescein antibody which also has two sets of coordinates for its Fab fragment in the PDB: 4FAB and 1FLR, both of which are for the liganded state. The 4FAB structure was solved to 2.70 Å (113) but has been further refined and has served as the basis for MD simulation studies (107), whereas the 1FLR structure was solved to 1.85 Å (114). However, both of these structures suffer from errors. The 4FAB has GLN L33 instead of ASN L33, and the 1FLR structure is even more problematic despite its higher resolution, since it completely omits residues H77 and H78, and also has LYS L24 instead of ARG L24. Fortunately our laboratory has produced other high-resolution structure determinations of 4-4-20 (52), although the data have not been deposited yet into the PDB. The coordinate data used herein is from the file 44p_258.pdb, for the triclinic (P1) structure in PEG solved to 1.78 Å.

BV04-01 differs from 4-4-20 in the third hypervariable region of the heavy chain in having a comletely different sequence along with three additional amino acids. Hence it was necessary to insert these amino acids into the CDR-H3. This was done using the *InsightII* program (Accelrys, Inc.) using the 4-4-20 Fab structure. Hydrogens were added with *InsightII* at pH 7.4 with the termini charged. The total charge on the molecule was +4. The structure was allowed to relax in the gas phase either with or without the only shared residue (Gly H104) in the CDR-H3 being held fixed. (The minimization was

performed with the *Discover* program; Accelrys, Inc.) This resulted in two starting structures. We also decided to use the structure of liganded BV04-01 minus the ligand as another starting structure. Finally, we used the unliganded BV04-01 structure as an internal control. These structures are denoted herein respectively as A_struc, B_struc, CBV, and NBV. They each have 112 residues in the light chain and 121 residues in the heavy chain, with 3,566 atoms total.

Rationale for charges

An important issue that needs to be addressed is the validity of not using counterions in the simulations. The present results suggest that perhaps better agreement between the GB simulations and the more accurate but more time-consuming PME simulations could be obtained by a better treatment of the electrostatics, and that may include counterions. However, a priori that was unknown, since there was some debate in the literature when this study was begun about what is the best option for modeling: (a) no ions, (b) net-neutralizing (balance charge), (c) enough + and - ions to balance each -/+ charge in protein, or (d) excess salt (Thomas E. Cheatham, III, personal correspondence). For continuum calculations without explicit solvent, we felt that it may be better to not include explicit salt. Had explicit counterions been added, their van der Waals radii would need to have been sufficiently large to represent a hydrated ion lest they bind directly and too tightly to charged residues (since there is no explicit water present). For the simulations in explicit solvent, there are many sources of error. Is ion presence or placement one of them? A much bigger source of error is lack of proper treatment of the electrostatics (e.g., cutoffs instead of PME). Some research has shown that net-neutralizing is bad and that one needs to include excess salt (115), but Cheatham and

others have shown that in general what is more important is proper equilibration (Nephi Thompson and Thomas E. Cheatham, III, personal communication). It may have been better for the explicit solvent simulations to include some counterions, but since it likely does not have a major effect (TEC, personal correspondence) and since no counterions were added for the general Born calculations, no explicit counterions were included for the PME calculations either.

Implicit solvent simulations

The program AMBER 6 (116, 117) was used for all the MD in this study. Trajectories were analyzed primarily with the ptraj program, which is part of AMBER. For the generalized Born calculations the conditions were pairwise generalized Born (igb = 1 in AMBER), with the residues that are shared by both 4-4-20 and BV04-01 being restrained with a force constant of 2.0 kcal/molÅ. Temperature coupling was by the Berendsen method with $\tau_p = 0.2$. SHAKE was used with constraining bonds involving hydrogen. The time step for integrating Newton's equations of motion was 2 fs. For other details, see Appendix C.

The simulated annealing was performed as follows: The molecules were quickly increased from 0 K to 1000 K in 10 ps, then held at 1000 K for 600 ps, cooled to 400 K over the next 300 ps, then cooled to 300 K over another 300 ps. After this period of simulated annealing the molecules were ran at 300 K for 2 ns with the restraints removed for all residues except the C termini of the two chains. The reason for this is that in a preliminary run the two chains rotated with respect to each other in a physically unrealistic way, since in a real antibody the Fv fragment is attached to the first constant region and therefore the two chains would not be free to rotate with respect to each other.

However, because the H chain C terminus is not shared between the two antibodies (Ala H121 in BV04-01 vs. Ser H 118 in 4-4-20, absolute numbering), it had been allowed to move freely during the SA so that when the constraint was applied it was trapped at the location at the end of the SA. (This is a fairly minor point but is the reason why the H chain C terminus of the crystal and solution structures do not coincide.)

Solvated simulations

The next level of rigor was with explicit solvent. The molecules were hydrated with 8,163 TIP3 waters in a truncated octahedron shell and then relaxed (28,052 atoms total). As with the implicit solvent above, no counterions were included. The solvent was then relaxed with a minimization to prevent SHAKE failure and then equilibrated. The solvated simulations were performed under periodic boundary conditions with the same temperature scaling as were the GB calculations described above except that the initial ramping of the temperature from 0 to 1000 K was omitted due to its irrelevance after performing solvent equilibration. Particle mesh Ewald (PME) was used for treating the electrostatics. However, after performing simulated annealing on the solvated A_struc structure (denoted as A_solv), we decided that it would be preferable to use the structures resulting from the end of the simulated annealing under GB conditions, so these were hydrated with the same number of waters as had been used for A_solv, and then they were subjected to further isothermal MD. All the atoms were relaxed by minimization prior to the isothermal MD. These systems are denoted as A_solv.GB, B_solv.GB, C_solv.GB, and N_solv.GB. As before, the C termini of both chains were restrained; however, the restraint was to the position after minimization (during which no restraints were applied).

Homology modeling

An interesting question is how well this extensive and computationally expensive MD methodology compares with static homology modeling. Due to their importance and the fact that antibodies all show high homology because of their framework regions, considerable effort has gone into optimizing antibody homology modeling programs. The most recent and probably the best of these is Web Antibody Modelling (WAM) (106), the successor to AbM. The sequence for the BV04-01 variable region was submitted to the online WAM program with the request to exclude BV04-01's own crystal structures from the modeling attempt.

Results and discussion

The root-mean-square deviations (RMSD) of the four initial structures versus the unliganded BV04-01 crystal structure (Fv region only, of course) for GB calculations are shown in Figure 31. The most obvious thing to notice from this plot is the sudden increase in RMSD seen when the simulated annealing ends and the restraints on the residues shared between BV04-01 and 4-4-20 were removed, except for the C termini as noted above. In fact, it is the unliganded control structure that shows the greatest initial jump when the constraints were relaxed. Clearly the molecules were held in a higher energy state by these restraints, which would suggest that the excipients used for crystallization play an important role in the structure obtained. This is reasonable; if there are differences between the crystal and solution structures, then the excipients used for crystallization would favor the crystal structure over the solution structure. Previous research with different solvent systems for the crystallization of the 4-4-20 Fab fragment also shows that the nature of the solvent can affect the structure obtained (52).

GB: rms deviation vs. unliganded crystal structure (i.e. nbv.inpcrd)
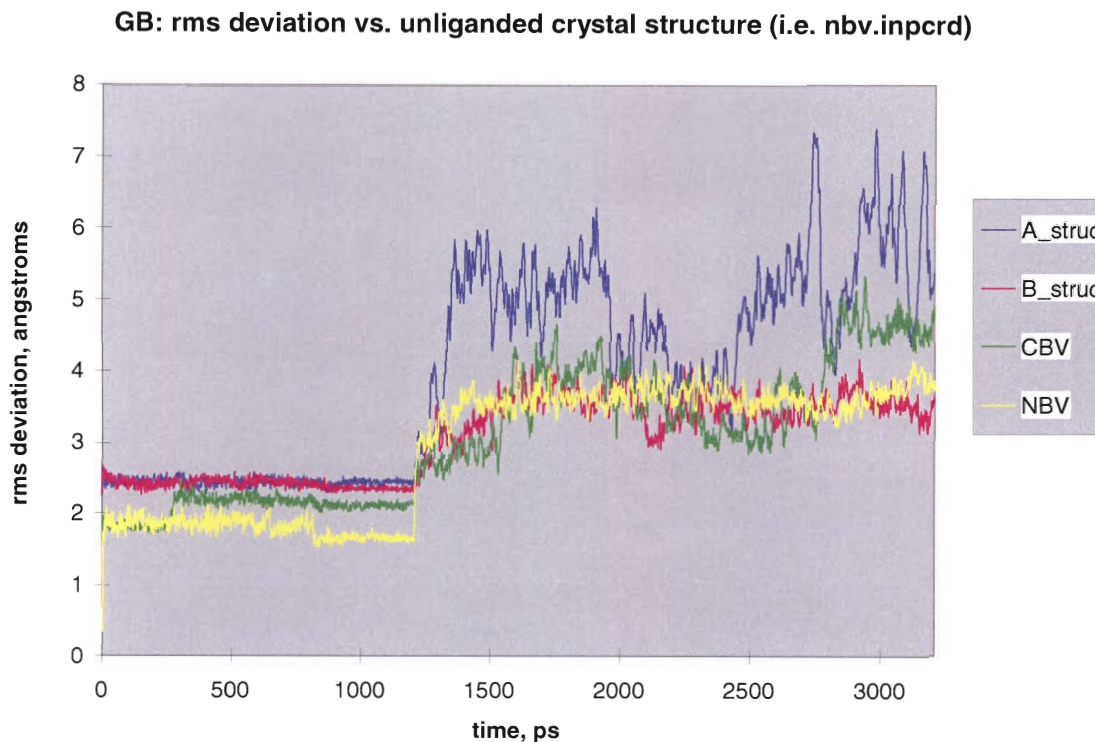
Figure 31. All-atom minimum rms deviations for each of the four starting structures in comparison to the unliganded crystal structure's Fv. (Although they are completely invisible with the thousands of data points shown, because of run failures there are a handful of data missing from these runs that perhaps should be mentioned simply for the sakes of honesty and completeness. The restart files were fine and so the runs could continue with those few points being omitted.)

Several questions are suggested by Figure 31: (1) What are the primary changes seen between the 1NBV crystal structure and the latter part of the simulated annealing, when the RMSD has stabilized? (2) What is the cause of the abrupt and persistent increase in RMSD for the CBV structure at about 275 ps? (3) Why does the A_struc structure, which has the same framework coordinates as does the B_struc structure (i.e., 4-4-20's framework coordinates), have such a higher RMSD than does B_struc? One would expect that the simulated annealing should remove the initial differences between them. (4) What is the cause of the apparent departure from equilibrium at about 2500 ps

that seems to have been achieved by about 2200 ps for A_struc? (5) For each of these structures, what are the main structural features that are responsible for the changes? (6) Are there biases due to the modeling that account for these deformations (e.g., forcefield or GB solvation model)?

Changes seen between 1NBV crystal structure and

the NBV control run under GB

The RMSD for the control run (NBV) immediately jumps from 0.35699 Å (the crystal structure, minimized prior to SA) to a fairly constant value (~1.8 Å) during the high temperature portion of the simulated annealing, and then at about 830 ps (corresponding to a temperature of 560 K) the RMSD drops to ~1.6 Å and remains there for the rest of the simulated annealing. Not surprisingly, the magnitude of the fluctuations is less at the lower temperatures than at 1000 K. Consequently it makes sense to use the region from 830 ps to 1210 ps as a basis for computing an average structure for comparison against the crystal structure, to see what are the immediate changes that result from partial removal of the restraints of the crystal structure. The interval from 850 ps to 1200 ps (a slightly more conservative choice) was used to generate an average structure. This structure differs primarily in the CDR-H3 from the crystal structure since that is the region with the greatest number of contiguous non-shared residues (between 4-4-20 and BV04-01).

Figure 32 shows the CDR-H3 loop for the crystal structure (tube representation) and the time averaged structure (line representation of backbone). The first four residues (DQTG) of the CDR-H3 loop do not differ much from the crystal structure, but the next five (TAWFA) are shifted away from the light chain. Trp H107 is shown in yellow for
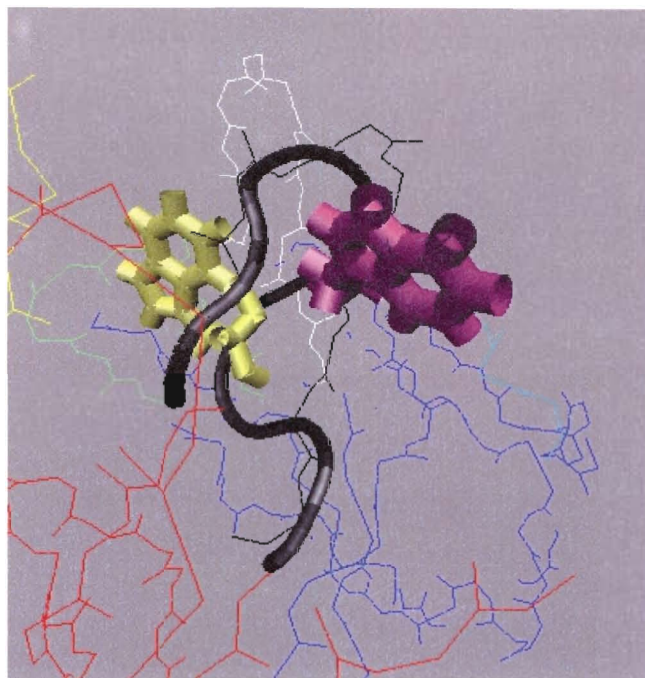
Figure 32. The yellow Trp H107 is for the crystal structure whereas the purple one is for the time averaged structure during the latter portion of the restrained SA. The other time averaged structure residues are represented by a line representation of the backbone atoms. The heavy black tube represents the crystal structure CDR-H3 loop backbone atoms. This figure, and others like it, were produced with VMD 1.7.2 (Windows) (117).

the starting structure and in purple for the time averaged structure. Surprisingly, this hydrophobic residue is actually more exposed to solvent than it is in the crystal structure. The same is true for the next residue, Phe H108 (not explicitly shown). The reason is probably entropic or kinetic: both Trp H107 and Phe H108 are bulky residues, and having been pushed out of their mostly constrained pocket by the sudden increase in temperature from 0 to 1000 K, may have a difficult time finding their way back in, given the greater degrees of rotational freedom available at the exterior of the molecule compared to buried in a pocket.

At the end of the simulated annealing period there is a sudden increase in the RMSD for all four of the starting structures, but especially for the control run NBV. This

is due to the sudden removal of constraints (except for the two C termini). The time-averaged solution structure of the control run from 1.5 to 3.2 ns (total time, including simulated annealing) is shown in Figure 33 (line representation of backbone) with a best fit rms superposition onto the crystal structure (tube representation). This solution structure model exhibits a general deformation throughout most of the H chain and to a slightly lesser extent the L chain. Both the CDR-L1 and the CDR-H1 get squeezed away from the antigen binding site by CDR-L3 and CDR-H3. Another significant change seen in the time-averaged solution structure relative to the crystal structure is in the vicinity of Ser H77, which flips out to the side in the solution model but is held close to the rest of the β-barrel immunoglobulin fold in the crystal structure.

Other changes seen in the GB simulations relative

to the crystal structure

The unliganded crystal structure is a natural choice for a reference structure, but so is the time-averaged solution structure of the control run after it has reached an equilibrium value. From Figure 31 it could appear that three of the four structures converge to a common solution structure (under the GB approximation), with the exception of A_struc. However, the RMSD relative to this model for the four runs are shown in Figure 34, and from this figure it is clear that only the RMSD for the control run is low; the others have roughly the same amount of distortion (RMSD) with respect to the control solution structure (designated as NBV_av_1.5-3.2ns) as with respect to the crystal structure. Hence, the four structures did not converge in 2 ns of MD, or at least did not converge very well. The greater RMSD seen with A_struc as compared to B_struc is probably a result of random fluctuations, since the only difference between
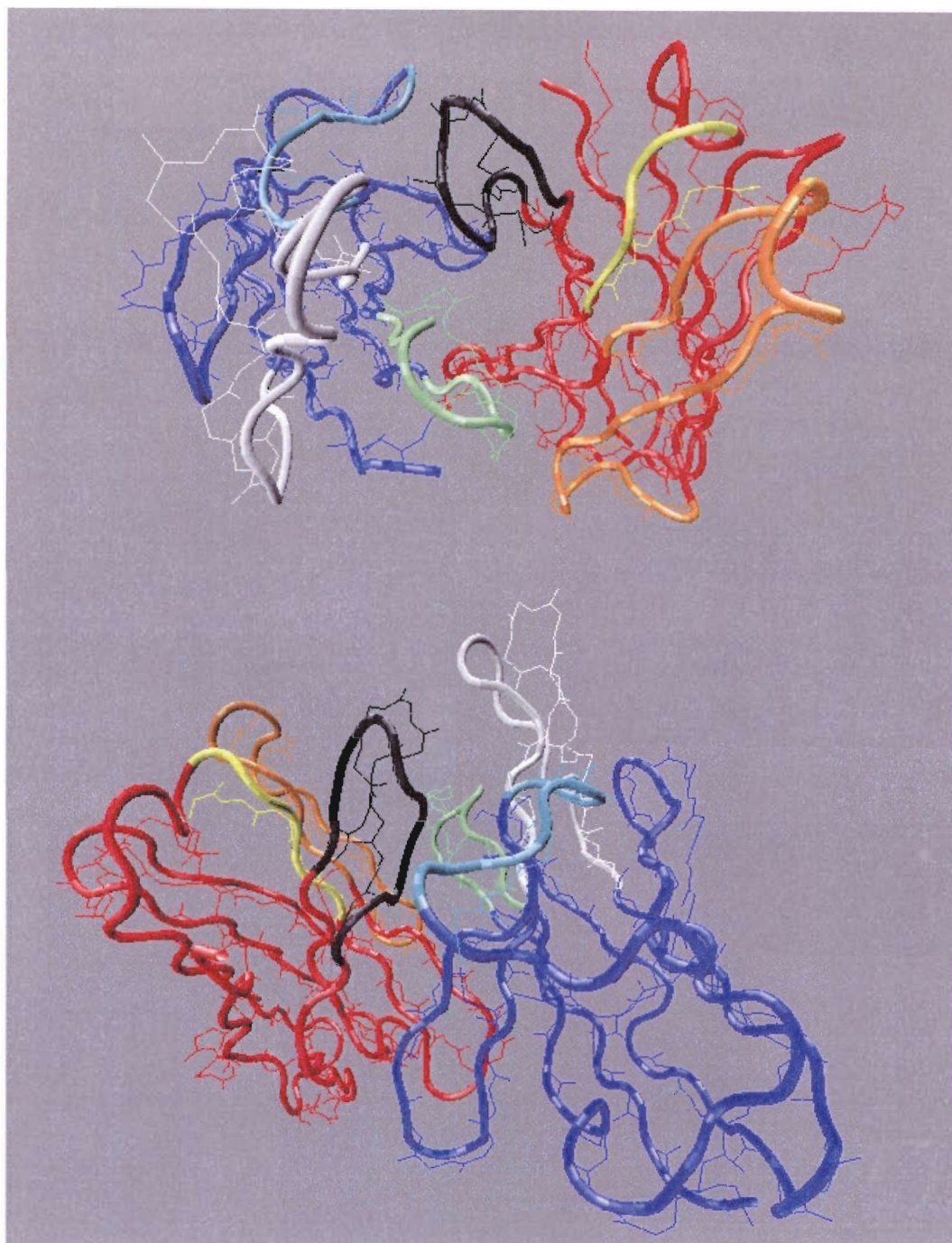
Figure 33. Superimposed backbone Fv structures. The top view is looking down into the Fv's antigen binding site and the bottom view is looking from the side. The heavy, tubular representation is for the backbone of the crystal structure and the line representation is for the time averaged GB structure between 1.5 and 3.2 ns total simulation time. Blue represents the light chain non-CDR regions. Red represents the heavy chain non-CDR regions. White is the CDR-L1, cyan is the CDR-L2, lime green is the CDR-L3, yellow is the CDR-H1, orange is the CDR-H2, and black is the CDR-H3.

GB: RMSD vs. NBV solution structure (NBV_av1.5-3.2ns)
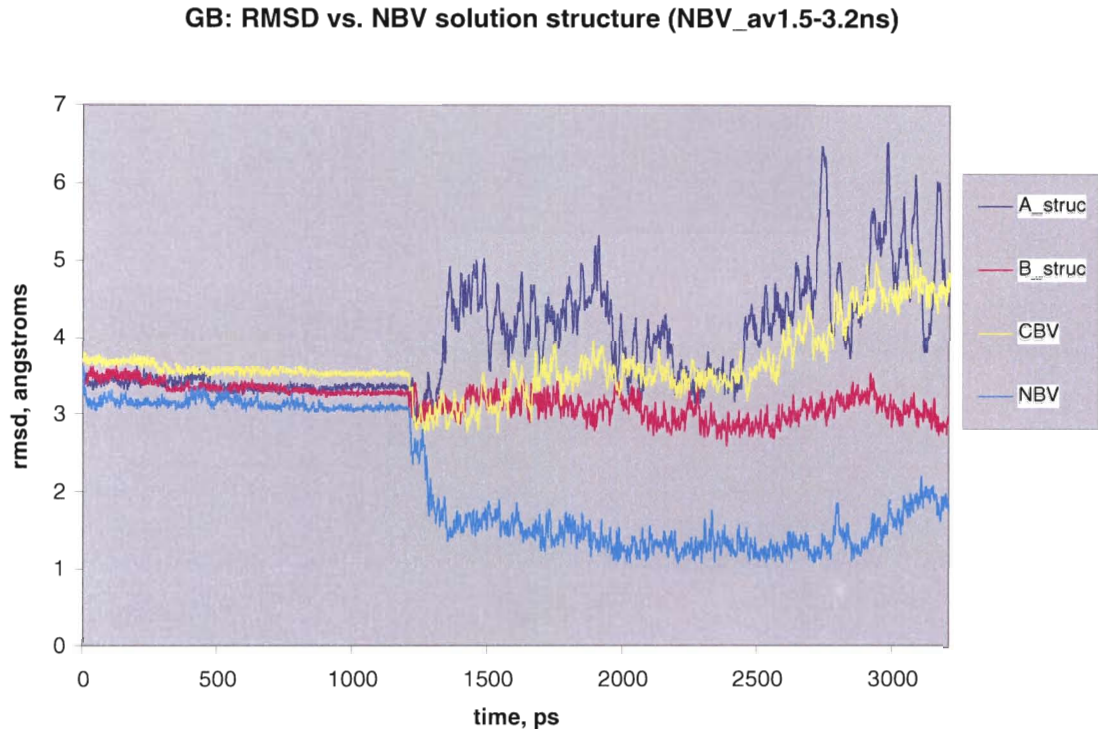
Figure 34. All-atom minimum rms deviations for the starting structures compared to the time averaged solution structure from the NBV trajectory from 1.5 to 3.2 ns total time.

A_struc and B_struc is the initial position of residue Gly H104, and after the period of simulated annealing that difference should be completely erased, and since the RMSD for A_struc drops and then rises again for a brief period (~1900 to 2400 ps). These facts would also suggest that a much greater sampling period may be necessary to achieve convergence of the four starting structures, perhaps by an order of magnitude or more.

Particle mesh Ewald simulations

A_struc was hydrated and then simulated with explicit solvent both during the SA and during the isothermal portion; the structure for this run is designated as A_solv. Due to the time involved in simulating with explicit water rather than with GB, we decided that it would be a reasonable strategy to dispense with the explicit solvent during the SA,

in which most of the residues are restrained anyway. Hence, another set of four runs was done in which the starting structures for full solvation were based on the GB structures at the end of the SA portion of the GB runs. These structures/runs are designated as A_solv.GB, B_solv.GB, C_solv.GB, and N_solv.GB. They were subjected to a brief all-atom mimimization to prevent SHAKE failure due to too high initial energies.

Unlike the GB simulations, the RMSD vs. time relative to the unliganded crystal structure does not vary much (Figure 35); in fact, all the runs are essentially the same. The control run does have a slightly lower RMSD than do the other runs, but the difference is small and of marginal significance. Equilibrium seems to be reached fairly quickly for all four starting structures, within about 200 ps or less. The time averaged

PME: RMSD against nbv (all atoms)
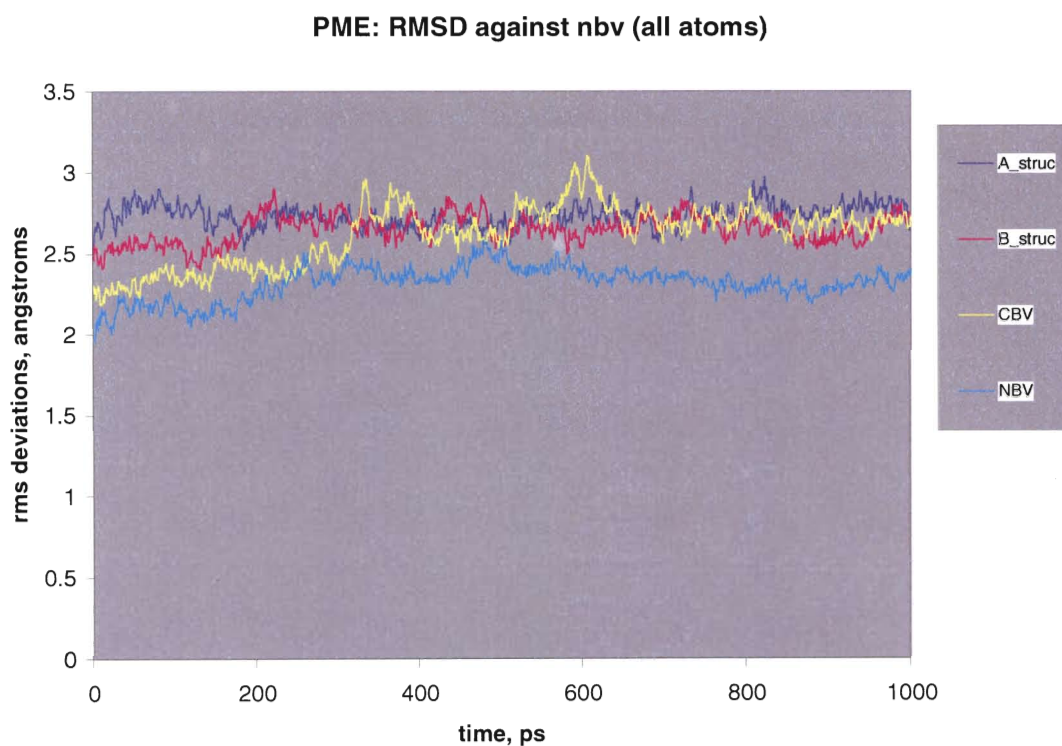
Figure 35. All-atom minimum rms deviations for the starting structures compared to the unliganded crystal structure for the post-SA isothermal trajectories with PME conditions.

(over the entire isothermal MD period) solution structure for the control run is shown in Figure 36 superimposed on the unliganded crystal structure. The most signficant differences that do exist are in the CDR-H3, which could be a kinetic carryover from the sudden ejection of the bulky Trp H107 and Phe H108 from the binding pocket, or it could reflect a true solution state. Figure 37 shows the RMSD of the four trajectories relative to the PME time-averaged solution structure. Only the control run used to generate the solution structure shows a very low RMSD (as would be expected), but the other runs also show an RMSD within that typically seen for different isoforms (52) or upon ligand binding of BV04-01 (28).
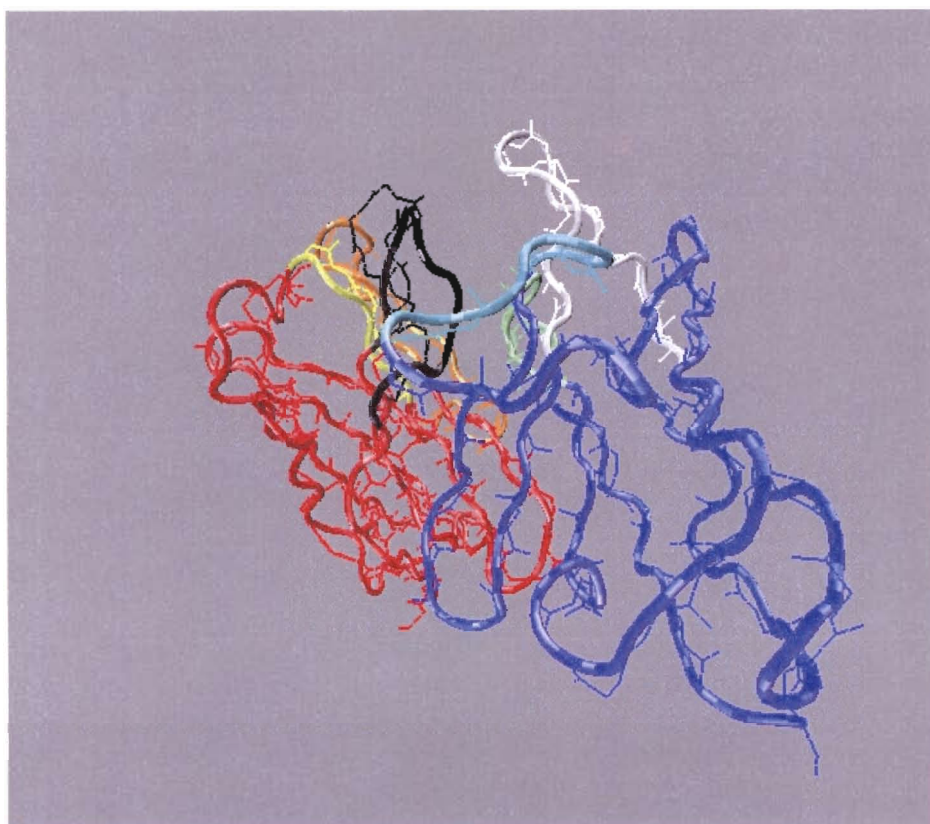
Figure 36. Superimposed Fv backbone structures. This figure is analogous to Figure 33 (bottom portion) except that the time averaged structure was for the entire PME simulation (post-SA). Note the considerably better agreement between the two structures (except in the CDR-H3 loop, which is probably a carry-over from the SA).

PME: rmsd against time-averaged PME control run
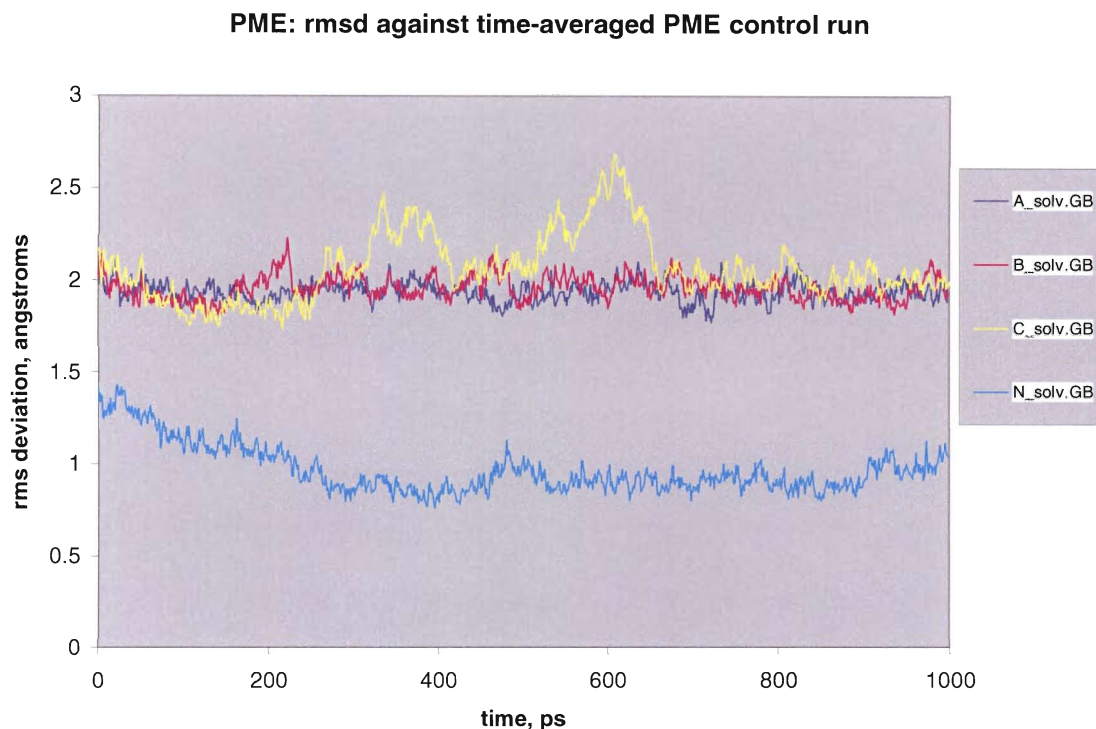
Figure 37. All-atom minimum rms deviations for the starting structures compared to the time averaged solution structure from the NBV trajectory. This graph is analogous to Figure 34 except that the curves are post-SA only and pertain to the PME simulations.

Comparison to homology model

The RMSD for the C-α atoms of the WAM BV04-01 Fv structure against the unliganded 1NBV control structure was 8.0113 Å and for the carbonyl atoms was 7.9279 Å (by VMD). This is a worse value than is usually the case with WAM, which can make homology models within the rms deviations typically seen for X-ray refinement of crystal structures, ~2-3 Å (105). It is significantly greater than most of the distortions seen from GB simulations (Figure 31). The WAM model was made using the following antibodies as a basis: L chain: 1mre, H chain: 1sbs; Canonicals: L1-L3 loops: 1mre, H1 loop: 1dlf, and H2 loop: 1dlf.

Conclusions

The main questions that can be addressed by isothermal MD simulations on a biological macromolecule are (1) Does the molecule move much relative to its canonical (e.g., crystal) structure? and (2) If it does move, then how and where? The present results indicate that the generalized Born implicit solvent model disagrees substantially in the solution structure predictions relative to the case with explicit solvent, which has close agreement to the crystal structure. The GB distortions appear throughout the entire H chain as well as in the CDR-L1 loop of the light chain, and to a slightly lesser extent throughout the majority of the light chain as well. Severe discrepancies between solution and crystal structures are rare, and given the good agreement between the PME simulations and the crystal structure, as well as the fact that all four PME solution structures agree with each other, at first glance it seems likely that the PME structures may accurately represent the solution structure and that the distortions seen in the GB runs are artifacts of the GB methodology. In particular, the distortion seen with GB is probably due to too severe approximation inherent in the GB model, as well as the fact that the total charge on the molecule was +4. Had implicit counterions been included, then perhaps less distortion relative to the case of full solvation might have been seen. Also, generalized Born is not a periodic boundary simulation condition, unlike PME. This probably contributes to the distortion by allowing charged surface-exposed side chains to seek to minimize their repulsions, resulting in a twist of the molecule.

The bane of all MD studies is the question of how long is long enough. The present study incorporates an objective means of answering that: four slightly different initial configurations were used to generate trajectories that at equilibrium and averaged

over a sufficiently long interval should be indistinguishable. While the difference is small for the PME.GB runs, it is significant for the GB runs, about the same as the distortion seen in going from the unliganded crystal structure to the control run solution structure NBV_av_1.5-3.2ns. Most disturbing is the fact that the GB structures did not converge in 2 ns, so the apparent semi-convergence of the PME structures in 1 ns is possibly fortuitous. The simulation time needed to adequately sample the accessible configuration space, and hence to achieve equilibrium, ought to be independent of whether the solute is exploring its configurational space in explicit or implicit solvent. However, it is known that GB simulations sample conformations faster than do PME calculations due to the lack of viscous solvent resistance. This is an advantage from the standpoint of exploring conformational space but is a disadvantage if one is primarily interested in accurate dynamics. Similar problems with GB in which a known solution structure (of thioredoxin) is known by NMR to be in close agreement with its crystal structure but is distorted by GB have been noted (119).

The initial question posed was, "What is the minimum requisite level of computation needed to establish a plausibly realistic solution model?" From the present results it would seem that full solvation under periodic boundary conditions using particle mesh Ewald treatment of electrostatics would be the preferred methodology; generalized Born was too severe an approximation − at least without implicit counterions. But the ideal way to answer this question would be to carry out a number of simulations with different levels of rigor and then to compare them to a known solution structure. For that a different protein choice may be optimal, particularly one that is known to exhibit differences between the solution and crystal structures. However, recent advances in

NMR structure determination with isotopic enrichment have pushed the size limit for determining structure to about 50 kDa (120), so that it may actually be possible to solve the solution structure of the Fab fragment of BV04-01.

A caveat to the entire hypothesis of being able to compute solution structures given crystal structures is the time scales involved: weeks to months for crystallization, picoseconds to nanoseconds for MD. It is entirely possible that the solution structures that were determined in this paper are metastable. This is especially suggested by the increase in solvent exposure of Trp H107 and Phe H108 resulting from the simulated annealing. However, the potential for metastability is and probably always will be a caveat to most MD studies (e.g., the persistence of B-RNA in (121)); it is not likely that this caveat can be overcome in the near future. Simulated annealing can in principle overcome the problem of metastability, but without constraints or restraints would instead result in a general protein folding problem, which is not feasible to solve by this method. Since the solutions could be metastable, it would be very interesting to see if they are supported by NMR.

In the case of antibodies, a very recent paper has appeared that does indicate differences between solution structures of llama heavy chain variable (VHH) domains (122). (Camelids produce antibodies that lack light chains.) In that paper the solution structure of a 117 residue VHH was solved by NMR. (For comparison, the Fv's used herein are 233 residues.) The authors compared the solution structure with the previously determined crystal structure and found a high similarity to the framework but significant conformational differences in the CDRs, and concluded that the antigen recognition site is a more mobile part. The present results would support the conclusion that the antigen

recognition site is more mobile, but some differences were also observed with the framework regions. An even more recent paper describes the solution structure of a llama heavy chain antibody and finds that the loop regions, especially the H3 loop, are more mobile (123).

How does all this affect antigenicity? As mentioned in Chapter 2's modeling, the conformation of a peptide is crucial to its antigenicity; the shape the immune system sees will determine which B cells are capable of binding the antigen. If the CDR-H3 loop does in fact exhibit a significant portion of its time exposed, then it is probably more accessible for binding by anti-idiotope antibodies. Hence, a knowledge of the solution structure would be useful for predicting the antigenic qualities of various epitopes.

CHAPTER 7

CONCLUSIONS AND FUTURE WORK

Whereas in previous chapters conclusions pertinent to that chapter were presented in their context, in this chapter my goal is to draw together the work as a whole and to suggest areas of future endeavor. Chapter 2 introduced me to molecular modeling, protein derivatization, fluorescence spectroscopy, cell culture, animal handling, chromatography, electrophoresis, dynamic light scattering, and various other laboratory techniques, as well as experimental design and data analysis. While this was personally a time of scientific growth, the end result was that BV04-01 was a difficult protein with which to work – the yield or the analysis of the idiotype, carrier protein conjugate was unsatisfactory, and we decided to abandon BV04-01 in favor of an IgG1 mAb, 9-40, for which the requisite chemistry and analysis went much smoother.

T cell epitope mimicry

Chapter 3 dealt with the use of chicken hen egg lysozyme (HEL) as a carrier protein, compared to its immunodominant T cell epitope in a given mouse strain (B10.A). That research showed that the T cell epitope completely failed to replace its parent carrier protein and suggested the work in Chapter 4, a dose response study using the same T cell epitope. That study examined the T cell epitope by itself (with fluorescein attached as the B cell epitope against which antibodies were raised), the T cell epitope incorporated into

a "tetrameric" multiple antigen peptide (MAP) construct, and as part of the carrier protein. A control MAP was also made but with the T cell epitope sequence replaced by glycine residues. Further analysis showed that the control MAP was in fact mostly tetrameric with a minor dimeric component, whereas the experimental MAP was mostly dimeric with a minor tetrameric component. Hence, one rather pragmatic conclusion is to not trust a vendor's analysis and labeling of a MAP without first preparing and analyzing a short test peptide sequence with the resin in question. More immunologically important was the result that incorporation of a T cell epitope into a branched oligomer such as a MAP greatly increased its potency, at least 300 fold, making it indistinguishable from the carrier protein over the concentration range examined. This confirms and extends in a quantitative fashion numerous other MAP papers.

It also is the most promising area of future wet lab experiments arising out of my research. For example, some questions that these results suggest are:

(1) What is it about oligomerization that causes the T cell epitope's potency to increase? Is it a matter of more efficient antigen uptake? If so, predominantly by which cells, and how is efficiency increased? Or is it a matter of more effective antigen processing and presentation? Again, if that is the case, why? The use of fluorescent dyes as model B cell epitopes, coupled to a T cell epitope of interest, as in my present studies but with purity of branched products, would be a good model system for further study in this area.

(2) From a pharmaceutical perspective, would another oligomer or polymer be a better choice than a MAP? One could easily envisage a polymeric backbone to which are attached T and B cell epitopes as pendant groups. Again, the choice of a dye such as

fluorescein as a B cell epitope would probably be an excellent one for furthering these studies. The present T cell epitope, for B10.A mice, could continue to be used to extend these studies more directly, or another T cell epitope could be used. One such epitope would be the immunodominant epitope of HEL in BALB/c mice (H-2^d), since that strain recognizes only one epitope from HEL, p107-120 (45). (In fact, that strain would have been a better choice for the present studies except for the fact that its epitope has both Cys and Lys. Lys could complicate comparison to HEL derivatized via its Lys side chains, and Cys could potentially cause solubility and analysis difficulties with MAPs. Those are probably not insurmountable complications, but given the unexpected difficulties with BV04-01 we felt that it would be better to use the B10.A strain and epitope.)

(3) As discussed in Chapter 1, peptide vaccines are more promising for certain conditions than for others – in particular, for autologous antigens, such as for cancer vaccines, and for pathogens that have repeating peptide units and that are difficult to culture, such as malaria parasites. For some illnesses, a Th1 response is efficaceous, whereas for others a Th2 response is needed (104). Can one influence the type of immunity by the type of polymeric carrier? Besides providing a quantitative magnification of the humoral response, is there a qualitative change with epitope oligomerization that also occurs, which one could exploit to provide the most appropriate type of immunity for a given malady?

(4) The secondary response was really no better than the primary response at 2 weeks for most of the cohorts. Why was this? The secondary response did increase further and at 56 days the response was still quite high. There is no guarantee that the

four immunogens examined exhibit the same kinetics, nor that the kinetics is independent of the dose. These questions warrant further study.

B cell epitope mimicry

Chapter 5 examined the response obtained from immunizing with an idiotope peptide mimic based on the third complementarity determining region of the heavy chain, the CDR-H3, with the response obtained from immunizing with the parent idiotype, conjugated to the same carrier protein as that to which the idiotope peptide mimic was conjugated (HEL). The results showed that (1) an idiotope vaccine did result in crossreactive antisera in some animals, (2) the converse was not true (or barely so) – an idiotype vaccine did not elicit antisera that recognized the idiotope peptide mimic, (3) the number of crossreactive mice increases with increasing immunizations, and (4) the anti-idiotype response from the idiotype vaccine is more consistent and overall stronger than the anti-idiotype response from the idiotope vaccine, so that if one wants to target pathological B cells expressing a given idiotype, an anti-idiotype vaccine is a better bet than is an anti-idiotope vaccine. This would suggest that future work for idiotype targeting proceed along the lines of DNA vaccination, antisense therapy, and genetically engineered idiotype expressing proteins (single chain variable fragment (scFv), phage display, and the like).

Of course, one could also pursue both anti-idiotype and anti-idiotope immunotherapies in order to achieve exquisite specificity and perhaps synergy. That has not been examined. It would also be worthwhile to examine other CDR loops besides the H3 loop for crossreactivity, in particular the L1 and H2 loops, which are also rather large and exposed. Would crossreactivity be increased by using a cocktail of CDR antigens in

the vaccine? If so, that would fit in well with some of the potential polymeric constructs mentioned above in the T cell epitope mimicry conclusions and future work.

On a more basic science level, one question suggested by the present results is, "Why does the crossreactivity increase with increasing immunizations?" Increasing crossreactivity is not the same as increasing affinity (i.e., affinity maturation), yet it seems likely that these events are somehow related. Is the increase in crossreactivity merely an accident of the immune system trying out different antibodies? That seems to be the most reasonable explanation at present.

The question of the accessibility of the CDR-H3 to cognate antibodies is an interesting issue. In what fraction of 9-40 molecules is the CDR-H3 loop exposed? Chapter 6 includes simulations for BV04-01 that suggest that the CDR-H3 in solution can be exposed rather than buried as a wall of the antigen binding pocket. Is this real, and if so, is this what is needed for crossreactivity? It would be interesting but probably difficult to identify the fraction of the population of Id that is exposed in its CDR-H3. Molecular modeling can probably be useful in this regard by calculating the free energy difference between the exposed and the buried states.

Computational studies in idiotypy

Chapter 6 continues the theme of idiotope and idiotype studies by molecular modeling, in a sense coming full circle back to the beginning of this project. Although idiotope mimicry by peptide vaccines may not be the immunotherapy of choice, modeling antibody variable regions is still a very promising academic endeavor with the potential to be applied to peptide-MHC and TCR-peptide-MHC complexes (124, 125) and other areas. Some questions suggested by the present results are:

(1) Is locally enhanced sampling (LES) a superior way of predicting CDR loops than SA? LES is a mean field methodology in which additional computational effort is expended towards a region of interest – often loop regions of globular proteins – thereby allowing increased sampling of this region relative to the sampling that would be found in typical room temperature nanosecond timescale simulations (116, 126, 127). It essentially allows one to get multiple trajectories from a single simulation by replacing the regions of interest with multiple copies which are free to move apart and explore different regions of conformational space. It also lowers the barriers to conformational transitions, resulting in more frequent conformational changes. This should avoid the issue of the potential artifact of CDR-H3 loop motion due to the SA.

(2) Would MD with different counterions and protonation states give greater consistency between the generalized Born (GB) results and the particle mesh Ewald (PME) results? This opens up an entire set of simulations in which pH and ionic strength can be varied and compared to measured values of antibody affinity.

(3) Can one take the time-averaged solution structures obtained herein and re-create the crystal structure of unliganded BV04-01 with explicit modeling of the crystallization excipients? Likewise, can one reproduce by simulation the differences seen in the Fab fragments due to different crystallization milieus for 4-4-20 (52)?

(4) How much is Ag binding site flexibility diminished upon Ag binding? This is a fascinating question that has been touched upon in earlier computational work involving 4-4-20 (107, 128). A comparison of various antibody-antigen complexes shows that some utilize induced fit and others utilize more lock-and-key (128). What are the structural parameters that determine this, and how are they manifested in the

dynamics of the Fv? Is this why 4-4-20 crystallizes easier with antigen? Such studies, combined with NMR, could also support or refute a neo-instructional theory suggested by observations that an scFv of anti-fluorescein antibody 9-40 has different affinities for fluorescein depending on whether, how recently, and how long it has been exposed to antigen (Prof. David M. Kranz, University of Illinois at Urbana-Champaign, Prof. James N. Herron, personal communication).

(5) Can one experimentally verify or refute the MD solution structures (either the BV04-01 structures presented herein or another set of structures, e.g., a 9-40 scFv) with NMR?

(6) Can one use free energy calculations with the appropriate antigen for 4-4-20 in different solvent systems, for the WAM model of 9-40, or for BV04-01 crystal or time averaged solution structures to provide an excellent measure of the validity of the modeling? Likewise, could one correlate alpha carbon RMSD to Δ G, as per reference (129)? Can one achieve the two goals mentioned in (129) – high resolution structural refinement and accurate ranking of model predictions?

APPENDIX A

SOME MISCELLANEOUS SYNTHESES AND OBSERVATIONS
FROM WET LAB WORK WITH BV04-01 AS THE FOCUS

Kinetics of antibody oxidation with NaIO$_4$

Monoclonal antibody 9-40 was used in this kinetics study of carbohydrate

oxidation instead of BV04-01 in order to save on the available BV04-01. Although these

antibodies are from different classes (IgG1 vs. IgG2b respectively), they probably would

not exhibit very different kinetics of NaIO$_4$ oxidation. The data are fitted to a pseudo-

first order function and plotted in Figure 44. The pseudo-first order rate constant is $k =$

0.05347 h^{-1} (95% CL [univar]: 0.022 to 0.085 h^{-1}), according to the statistical summary

from Scientist v. 2.0 (MicroMath, Inc., now defunct). Unlike another report (130)

studying the kinetics of periodate oxidation but using polyclonal rabbit antibodies, the

present results with monoclonal murine antibody 9-40 do not seem to require postulation

of two classes of sites; a single class of sites appears satisfactory.

Instability of hydrazone linkage to oxidized antibody

Fluorescent dyes containing hydrazide or maleimide functional groups were used

in diagnostic reactions to probe the unsuccessful IgG^{ox}-MPBH + SPDP-HEL reaction

mentioned in Chapter 2. For the hydrazide dyes, two were used: Lucifer yellow

(Molecular Probes, Eugene, OR) and FL-MPBH. For the latter, SAMSA-FL (Molecular
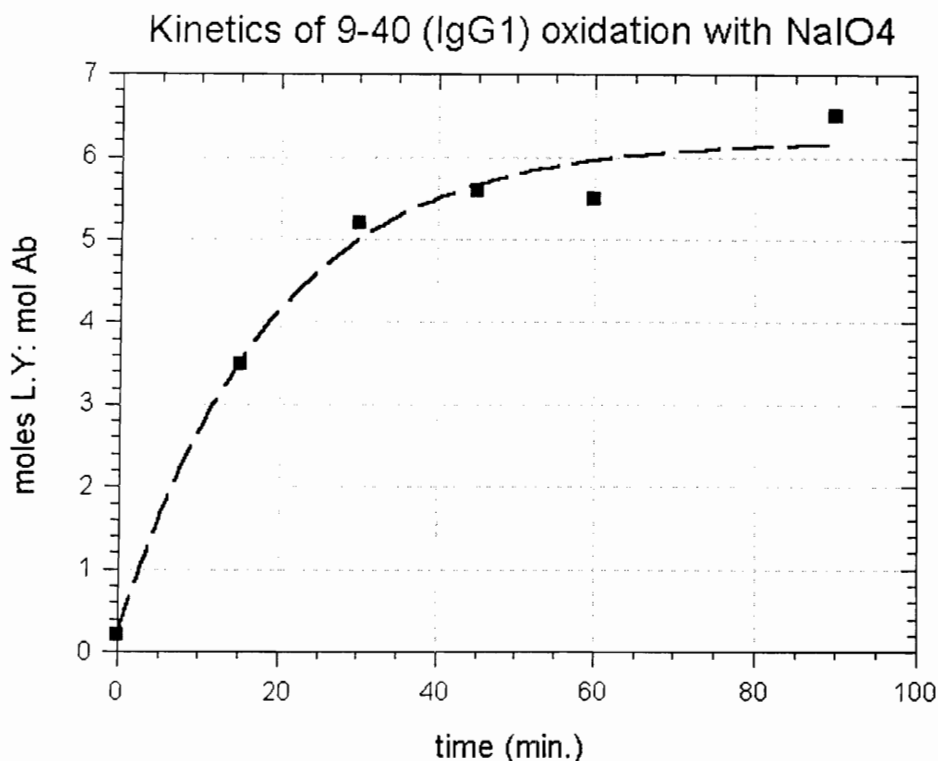
Kinetics of 9-40 (IgG1) oxidation with NaIO4

Figure 38. The antibody 9-40 (6.68 mL of 4.20 mg/mL) was oxidized at room temperature in the dark (according to a protocol from Pierce, although oxidations in the light seem to have proceeded quite satisfactorily) with a 1000-fold excess (42.1 mg) of $NaIO_4$. At 0, 15, 30, 45, 60, and 90 min an aliquot (1.34 mL) was removed and put into an Eppendorf tube containing 20 µL of glycerol and vortexed to quench further oxidation. These samples were then passed through a Superdex 75 size exclusion column (Amersham Pharmacia) and eluted with 0.1 M NH_4Ac, pH 5.5, then concentrated. Then to each reaction was added 200 µL of Lucifer yellow (LY on ordinate) stock solution (1.3 mg of Lucifer yellow in 1.0 mL of water, ~13-fold excess of Lucifer yellow). The next day this was passed through a PD-10 size exclusion column (Amersham Pharmacia) and the degree of labeling analyzed by UV/VIS spectroscopy.

Probes) was reacted with base according to the manufacturer's instructions. The resulting FL-SH was then reacted with MPBH, giving a hydrazide derivative of fluorescein (MPBH-FL) (Figure 39), which was reacted (in pH 5.5 0.1 M NH_4Ac) with IgG^{ox}, prepared as described above. (This also demonstrates the expected reactivity of the resulting aldehydes.) The fact that the MPBH reacted as it did with the activated SAMSA fluorescein strongly implies that the MPBH was fine, at least with regards to its
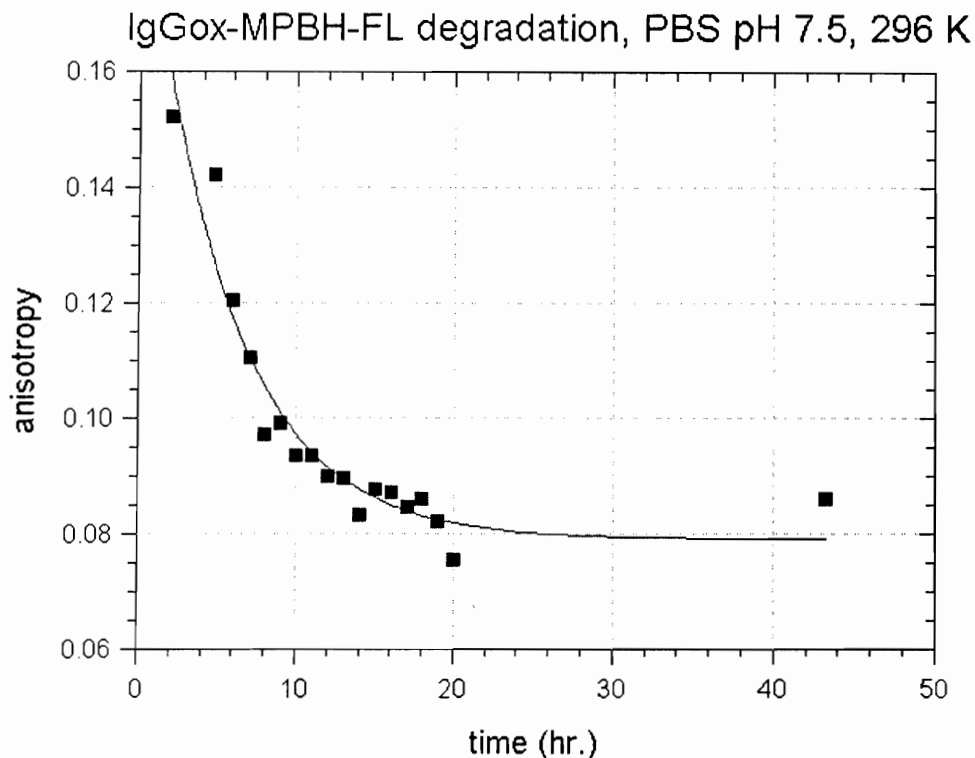
Figure 39. Reacting MPBH-FL with the oxidized IgG (designated IgG^{ox}) gave a fluorescent product, as expected, but it was unstable. (Almost certainly the degradation reaction is hydrolysis.) After removing the free MPBH-FL from the IgG^{ox} by size exclusion chromatography (SEC), the fluorescence polarization of the dye was measured as a function of time using a macro written in the ISS software (ISS, Inc., Champaign, IL) and found to decay according to a first-order equation with rate constant $k = 0.19\,h^{-1}$.

maleimide group, and the fact of the reactivity with IgG^{ox} shows it was fine with regards to its hydrazide group. The satisfactory synthesis of HS-HEL was shown by its conjugation to fluorescein maleimide. That would leave in question only the reactivity of IgG^{ox}-MPBH with HS-HEL – precisely the desired reaction.

Lucifer yellow was also reacted with IgG^{ox} and the kinetics were followed (Figure 40). It seems that with Lucifer yellow the nitrogen α to the carbonyl closer to the dye stabilizes the hydrazone bond (Figure 41).

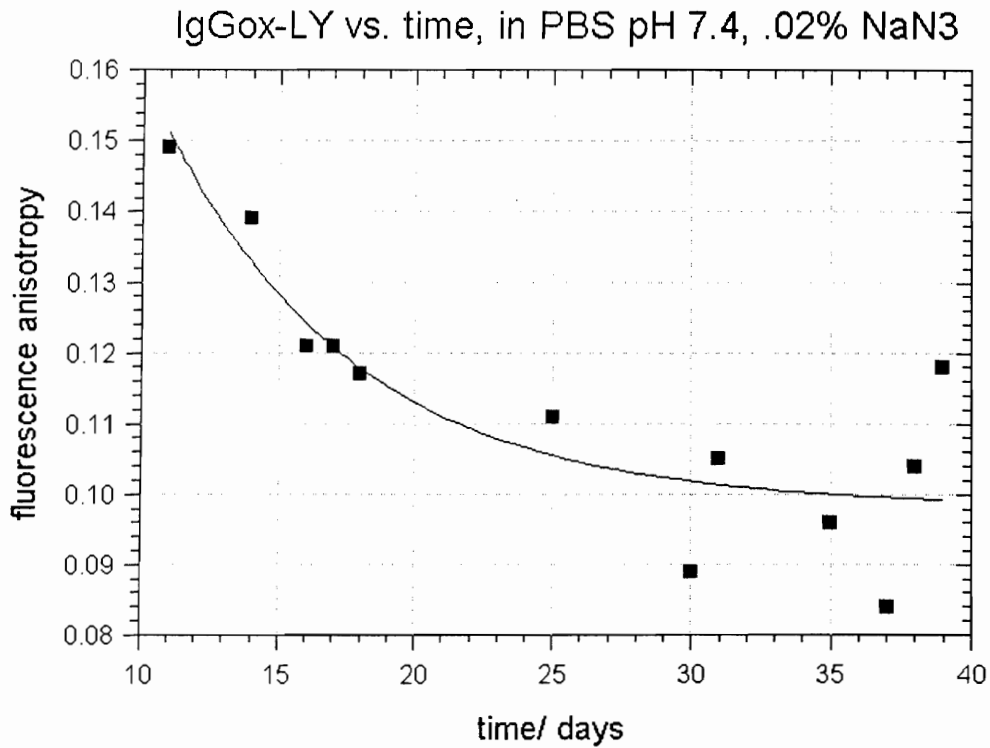**Figure 40.** Degradation of (9-40)IgG^{ox}-(Lucifer yellow). Lucifer yellow (Molecular Probes), another fluorescent dye possessing a hydrazide group, was more stable (but unfortunately the rate constant determined for that system had a poorly defined t_0, so that the parameter values were too uncertain to be worth reporting). Note the longer time scale from Figure 39. Here, the data were collected manually (not by macro).
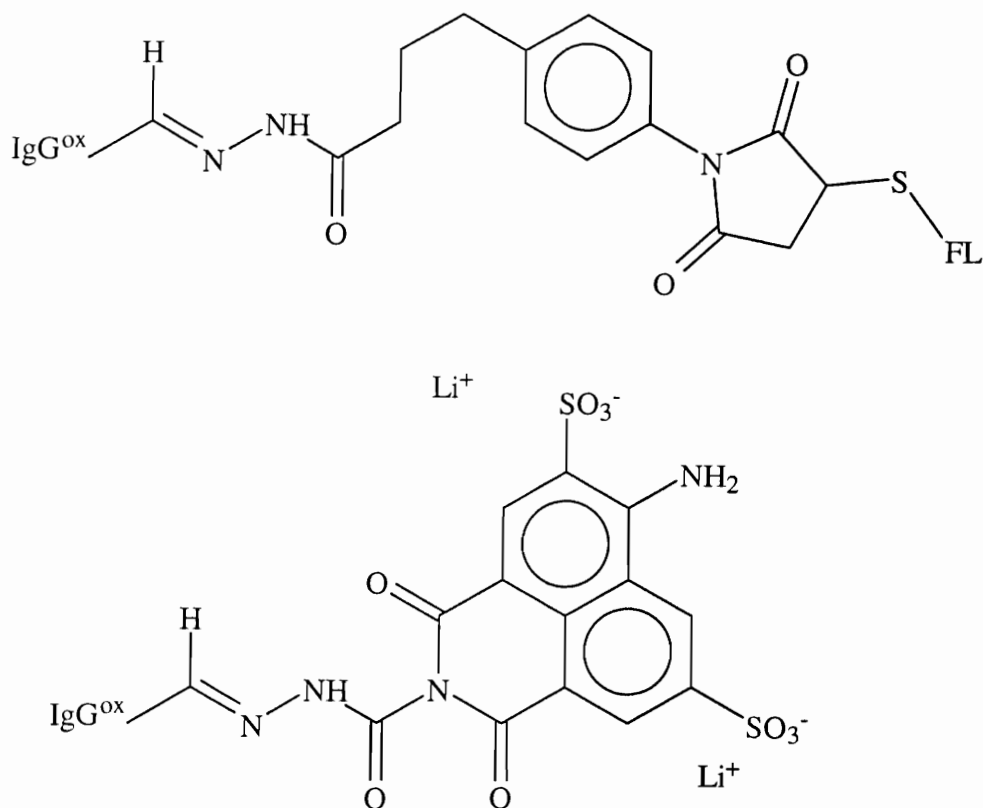
Figure 41. The hydrazone linkage formed by MPBH-FL (top) is less stable (easier to hydrolyze) than that formed by Lucifer yellow (bottom).

Synthesis and characterization of the homobifunctional

crosslinker 1,5-bis-(*p*-nitrophenylformyl)pentane

p-Nitrophenylate (pNP) is a convenient leaving group because its bright yellow color allows easy visual assessment of reaction progress. Because no suitably spaced commercially available amine reactive homobifunctional crosslinker containing this group was found, 1,5-bis-(*p*-nitrophenylformyl)pentane was prepared by derivatizing 1,5-pentanediol with *p*-nitrophenylchloroformate. A 2.05:1 molar excess of the latter (8.6362 g), dissolved in 26 mL of toluene, was added to the former (1.9751 g; nominally 96% pure, the balance being mostly water), to which was then added 24 mL of anhydrous

THF. The resulting crystals were washed with hexane and dried, then stored sealed in a freezer. A small quantity of the material was dissolved in THF, spotted onto a silica TLC strip, and eluted with hexane: chloroform: ethyl acetate (2:1:1) as a single spot. Proton NMR (Figure 42) was used to confirm the structure of the 1,5-bis-(p-nitrophenylformyl)-pentane product (Figure 43).

Fluorescein as a leaving group

Various diagnostic experiments using fluorescent dyes together suggested that fluorescein attached by an amide linkage to Lys side chains (via reaction of fluorescein NHS ester to HEL) was unstable to nucleophiles such as 2-mercaptoethanol (2-ME) or hydrazine (Hz). FL-HEL was made using 5-FAM (i.e., fluorescein NHS ester – Molecular Probes, Eugene, OR) and later treated with 2-mercaptoethanol and heat or with hydrazine at room temperature or just left alone (Figure 44). The conditions used can make a big difference with regards to the stability of the FL linkage.

SAMPLE PENTYL -(ONP)2
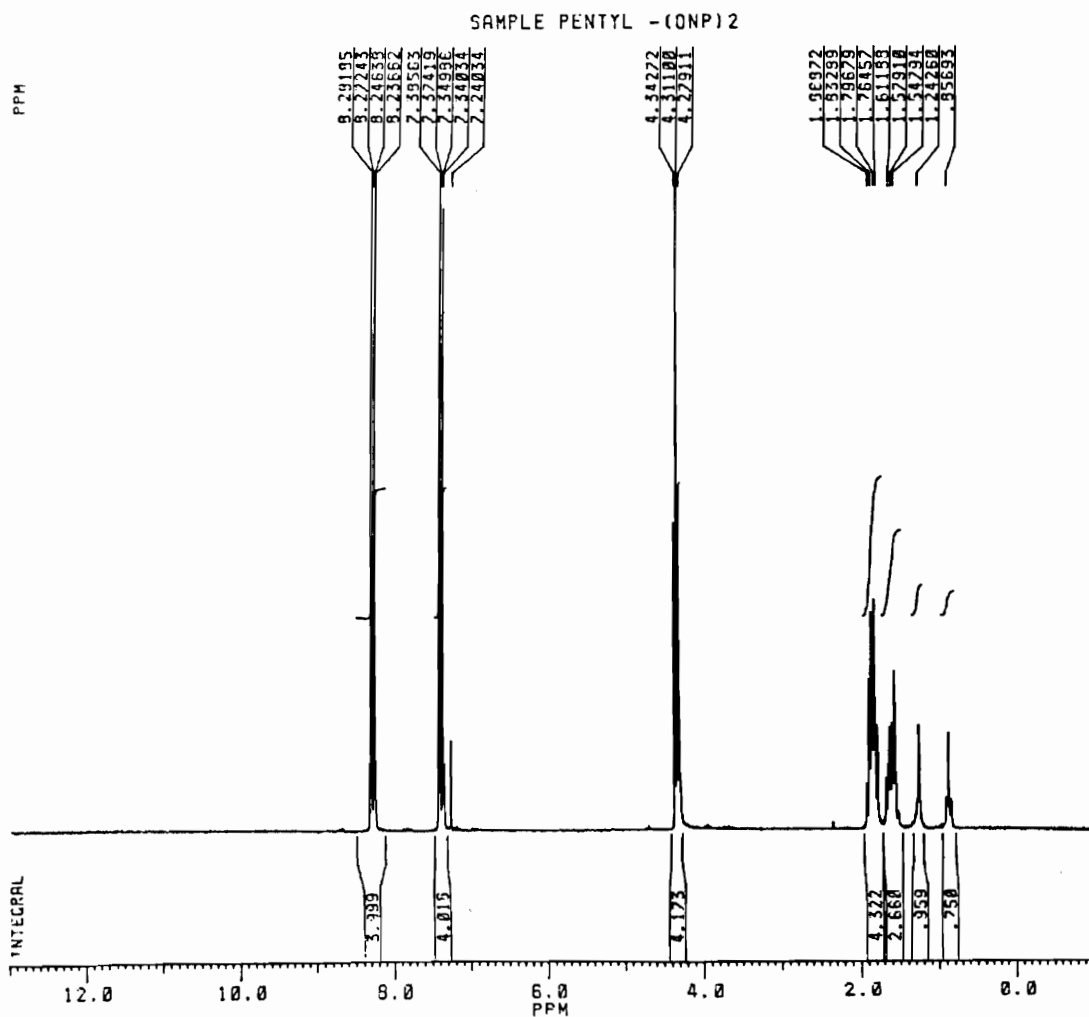
Panel A

Figure 42. ^{1}H NMR verification of 1,5-bis-(*p*-nitrophenylformyl)pentane synthesis. Panel A is the full spectrum taken (with the sample dissolved in deuterated chloroform). Panels B and C are expanded views and follow on succeeding pages.
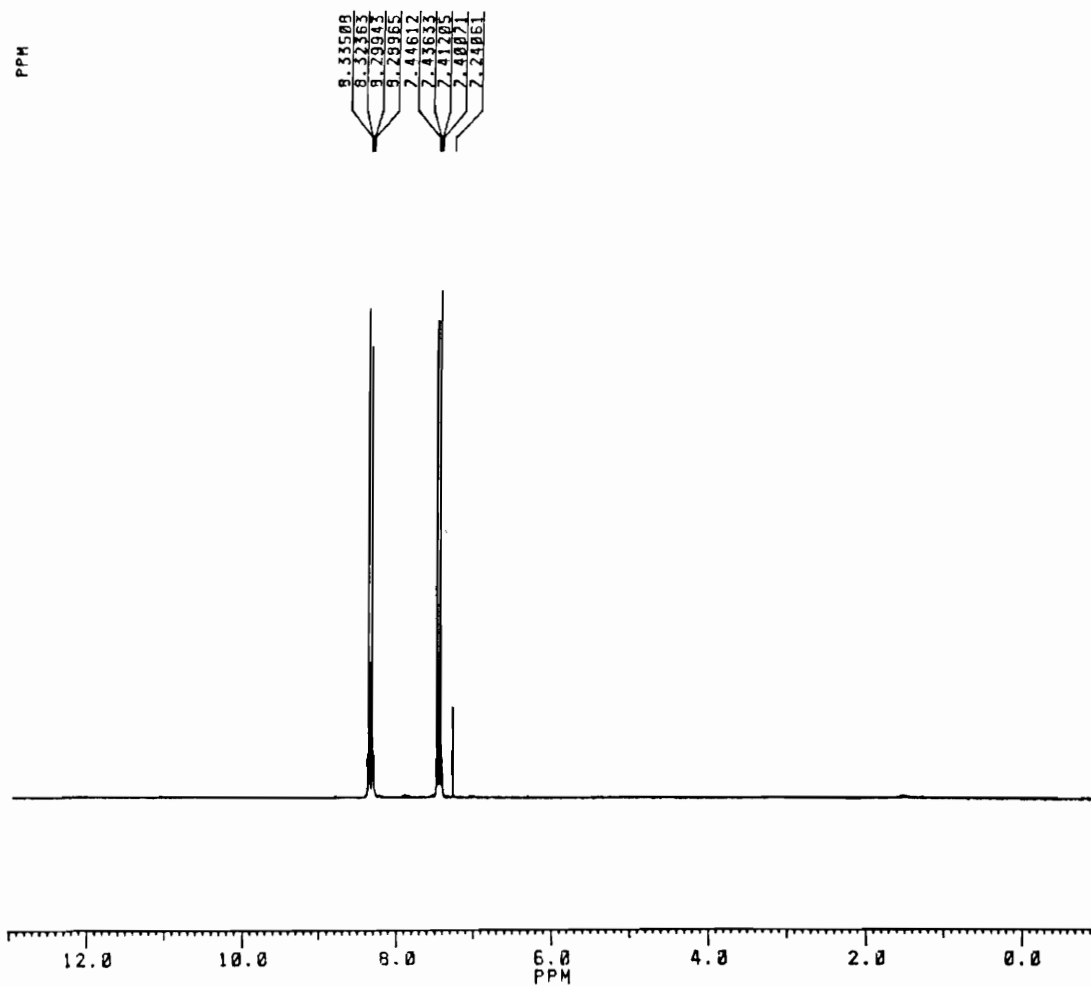
Panel B

Figure 42, continued. Aromatic region of the spectrum of 1,5-bis-(*p*-nitrophenyl-formyl)pentane.

SAMPLE PENTYL -(DNP)2
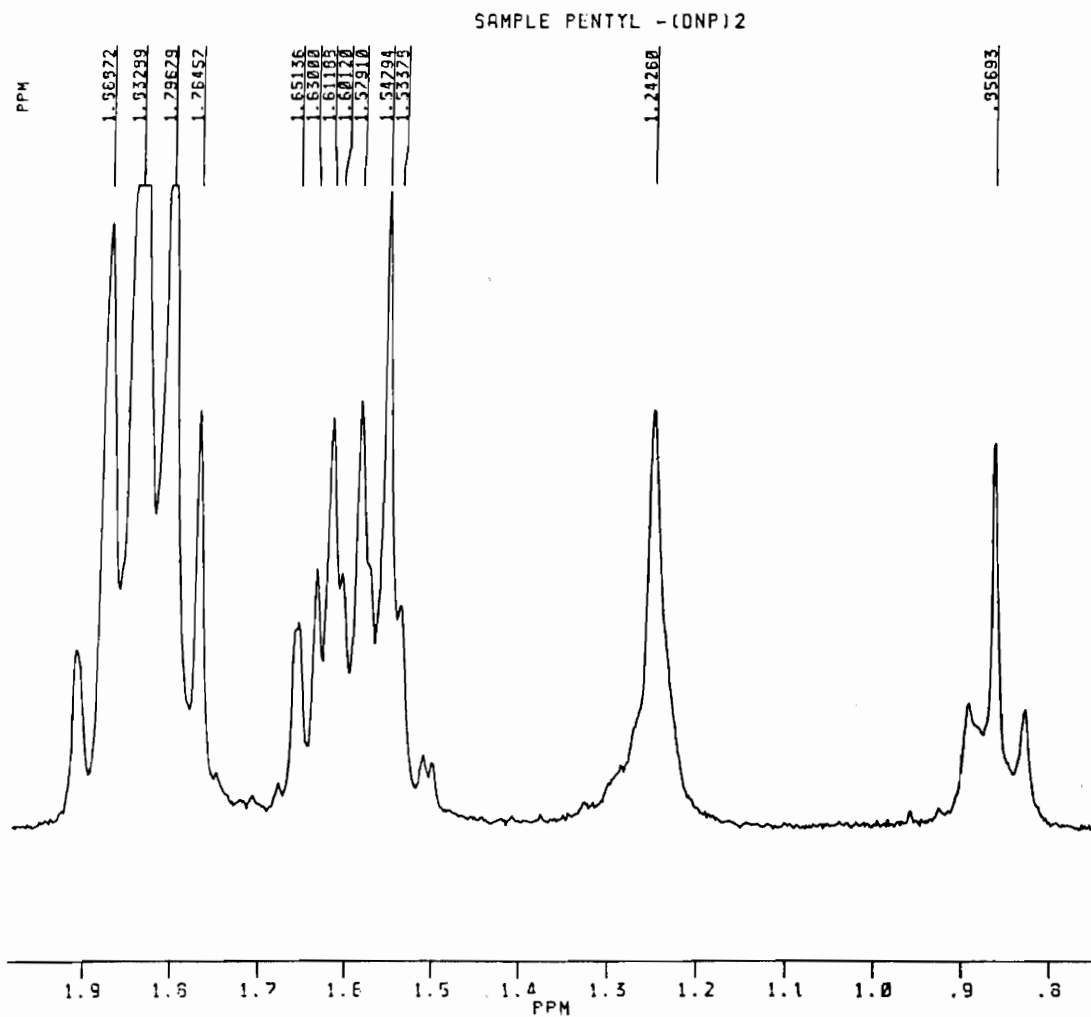
Panel C

Figure 42, continued. Aliphatic region of the spectrum of 1,5-bis-(*p*-nitrophenyl-formyl)pentane.
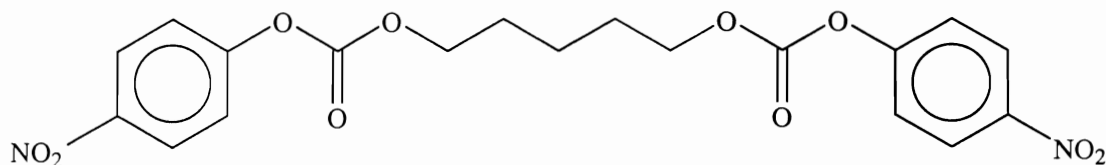
1,5-bis-(*p* -nitrophenylformyl)pentane
(or simply pentyl-(pNP)₂)

Figure 43. Structure of a homobifunctional crosslinker prepared in this work.
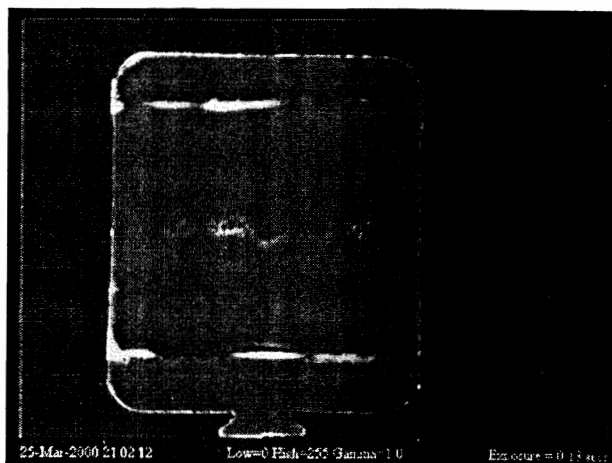
Figure 44. PhastGel IEF 5-8 prior to staining. Lane 1 is untreated HEL-FL; lanes 2, 3 were treated with 2-ME and heated ~15 min at 90-92 °C, lanes 4, 5 were as lane 1 except diluted 1:2, and lane 6 was treated at room temperature with Hz. Note that HEL, which has a very high pI (~10), still has a sufficiently high pI after derivatization with dye to put it entirely at the negative electrode (the bottom of the gel), whereas free fluorescein is acidic and migrates at the top of the gel. The samples were applied in the middle of the gel (visible as an artifact).

APPENDIX B

EXTINCTION COEFFICIENTS OF SOME SPECIES USED

Based on the counted Trp (W), Tyr (Y), and Phe (F) content of the antibodies and their Fabs, ε are as follows:

Protein	W	Y	F	M.W.	ε, M^{-1} cm^{-1}	ε, $(g/L)^{-1}$ cm^{-1}
BV04-01	26	50	44	150,000	225,268	1.5018
BV04-01 Fab	9	18	15	47,588	78,915	1.6583
9-40	28	52	52	150,000	240,884	1.6059
9-40 Fab	9	22	14	47,600	84,398	1.7731
9-40 Fab-HEL, 1:1 conjugate	15	25	17	62,300	122,849	1.9719
4-4-20	28	58	42	150,000	247,434	1.6496
4-4-20 Fab	10	22	14	47,600	89,998	1.8907
HEL	6	3	3	14,314	38,100	2.2

APPENDIX C

AMBER INPUT FILES USED FOR GB AND

PME SIMULATIONS

Here is a sample input file (for NBV), used with simulated annealing:

JSC's GB S.A. file, for use after GB minimization on entire molecule

&cntrl

timlim = 9999999,   nmropt = 1,

ntpr = 500,   ntwx = 500,   ntwe = 500,

ntwr = 500,

ntb = 0,   igb = 1,

ntr = 1,   tautp = 0.2,

nstlim = 25000,   dt = 0.002,   ntc = 2,   ntf = 2,

ntt = 1,   tempi = 0.0,

&end

&wt type = 'TEMP0',   istep1 = 0,   istep2 = 5000,

        value1 = 0.,   value2 = 1000., &end

&wt type = 'TEMP0',   istep1 = 5001,   istep2 = 25000,

        value1 = 1000., value2 = 1000., &end

&wt type='END' &end

&rst

iat = 0,

&end

AP-N L1 to LEU L38

2.0

RES 1 38

END

TRP L40 to LYS+ L50

2.0

RES 40 50

END

LEU L52 to PRO L100

2.0

RES 52 100

END

THR L102 to GLY L104

2

RES 102 104

END

GLY L106 to GLU- L110

2

RES 106 110

END

LY+C L112

2

RES 112

END

GL-N H1 to VAL H2

2

RES 113 114

END

GLU- H6 to PRO H14

2

RES 118 126

END

LYS+ H19 to CYS H22

2

RES 131 134

END

ALA H24 to PHE H27

2

RES 136 139

END

PHE H29

2

RES 141

END

MET H34 to GLN H39

2

RES 146 151

END

PRO H41

2

RES 153

END

LYS+ H43 to ALA H49

2

RES 155 161

END

ILE H51 to ARG+ H52

2

RES 163 164

END

LYS+ H54

2

RES 166

END

ASN H57 to TYR H58

2

RES 169 170

END

THR H60 to TYR H62

2

RES 172 174

END

ASP- H64 to LYS+ H67

2

RES 176 179

END

ARG+ H69 to SER H77

2

RES 181 189

END

TYR H82 to LEU H88

2

RES 194 200

END

GLU- H91 to ASP- H92

2

RES 203 204

END

TYR H96 to CYS H98

2

RES 208 210

END

TYR H110 to THR H115

2

RES 222 227

END

VAL H117 to SER H120

2

RES 229 232

END

END

Here is a sample input file (for NBV) used with simulated annealing:

JSC's GB isothermal run, 3010 - 3210 ps:

&cntrl

 nmropt = 1,

 ntpr = 500,   ntwr = 500,   ntwx = 500,   ntwe = 500,

 ntb = 0,   igb   = 1,

 ntr = 1,   tautp = 0.2,

 nstlim = 100000,   dt = 0.002,   ntc = 2,   ntf = 2,

 ntt = 1,   tempi = 0.0,

```
&end

&wt type = 'TEMP0',    istep1 = 1,          istep2 = 100000,

        value1 = 300.,  value2 = 300.,  &end

&wt type='END' &end

&rst

 iat = 0,

&end

LY+C L112

5

RES 112

END

AL+C H121

5

RES 233

END

END
```

REFERENCES

1.   Brown F, et al.: *Vaccine Design*, John Wiley & Sons Ltd., West Sussex, England, 1993.

2.   Hood LE, et al.: *Immunology*, The Benjamin/Cummings Publishing Company, Inc., 1984.

3.   Roitt I: *Immunology*, Blackwell Science, London, 1997.

4.   Stites DP, Terr AI, Parslow TG: *Basic & Clinical Immunology*, Appleton & Lange, Norwalk, CT, USA, 1994.

5.   Anonymous: JAX Catalog 2000, The Jackson Laboratory, 2000, pp 483.

6.   Chothia C, et al.: Conformations of immunoglobulin hypervariable regions. *Nature.* **342**:877-883 (1989).

7.   Wu TT, Johnson G, Kabat EA: Length Distribution of CDRH3 in Antibodies. *PROTEINS: Structure, Function, and Genetics.* **16**:1-7 (1993).

8.   Silverstein AM, Rose NR: There is only one immune system! The view from immunopathology. *Seminars in Immunology.* **12**:173-178 (2000).

9.   Howes M: Self, intentionality, and immunological explanation. *Seminars in Immunology.* **12**:249-256 (2000).

10.   Tam JP: Synthetic peptide vaccine design: Synthesis and properties of a high-density multiple antigenic peptide system. *Proceedings of the National Academy of Sciences of the United States of America.* **85**:5409-5413 (1988).

11.   Tam JP: Recent advances in multiple antigen peptides. *Journal of Immunological Methods.* **196**:17-32 (1996).

12.   Mayforth RD: *Designing Antibodies*, Academic Press, San Diego, CA, USA, 1993.

13.   Smith LJ, et al.: Production of Heterologous Antibodies Specific for Murine B-cell leukemia (BCL1) Immunoglobulin by Immunization with Synthetic Peptides

Homologous to Heavy Chain Hypervariable Regions. *Cancer Research.* **45**:6119-23 (1985).

14.   Hamblin TJ, et al.: Preliminary experience in treating lymphocytic leukaemia with antibody to immunoglobulin idiotypes on the cell surfaces. *British Journal of Cancer.* **42**:495-502 (1980).

15.   Miller RA, et al.: Treatment of B-cell lymphoma with monoclonal anti-idiotype antibody. *New England Journal of Medicine.* **306**:517-522 (1982).

16.   Krolick KA, et al.: A murine model for chronic lymphocytic leukemia: use of the surface immunoglobulin idiotype for the detection and treatment of tumor. *Immunological Reviews.* **48**:81-106 (1979).

17.   Lanier LL, et al.: Antigen-induced murine B cell lymphomas. III. Passive antiidiotype serum therapy and its combined effect with chemotherapy. *J. Natl. Cancer Inst.* **63**:1417-1422 (1979).

18.   Rajadhyaksha M, Yang Y, Thanavala Y: Immunological evaluation of three generations of anti-idiotype vaccine: study of B and T cell response following priming with anti-idiotype, anti-idiotype peptide and its MAP structure. *Vaccine.* **13**:1421-1426 (1995).

19.   Araga S, Blalock JE: Use of complementary peptides and their antibodies in B-cell-mediated autoimmune disease: prevention of experimental autoimmune myasthenia gravis with a peptide vaccine. *Immunomethods.* **5**:130-5 (1994).

20.   Seiden MV, et al.: Hypervariable region peptides variably induce specific anti-idiotypic antibodies: an approach to determining antigenic dominance. *The Journal of Immunology.* **136**:582-587 (1986).

21.   Kanda P, et al.: Dependence of the murine antibody response to an anti-CD4 CDR2 V_H peptide on immunogen formulation. *Molecular Immunology.* **32**:1319-1328 (1996).

22.   Attanasio R, et al.: Anti-idiotypic antibodies of a predefined specificity generated against CDR3V_H synthetic peptides define a private anti-CD4 idiotype. *Molecular Immunology.* **27**:513-522 (1990).

23.   Attanasio R, et al.: Anti-peptide reagent identifies a primary-structure-dependent, cross-reactive idiotype expressed on heavy and light chains from a murine monoclonal anti-CD4. *Molecular Immunology.* **30**:9-17 (1993).

24.   Chen PP, et al.: Delineation of a cross-reactive idiotype on human autoantibodies with antibody against a synthetic peptide. *Journal of Experimental Medicine.* **159**:1502-1511 (1984).

25. Hakim I, Levy S, Levy R: A nine-amino acid peptide from IL-1beta augments antitumor immune responses induced by protein and DNA vaccines. *The Journal of Immunology.* **157**:5503-11 (1996).

26. Spellerberg MB, et al.: DNA Vaccines Against Lymphoma: Promotion of Anti-Idiotypic Antibody Responses Induced by Single Chain Fv Genes by Fusion to Tetanus Toxin Fragment C. *The Journal of Immunology.* **159**:1885-92 (1997).

27. Stevenson FK, et al.: Idiotypic DNA Vaccines Against B-Cell Lymphoma. *Immunological Reviews.* **145**:211-228 (1995).

28. Herron JN, et al.: An Autoantibody to Single-Stranded DNA: Comparison of the Three-Dimensional Structures of the Unliganded Fab and a Deoxynucleotide-Fab Complex. *PROTEINS: Structure, Function, and Genetics.* **11**:159-175 (1991).

29. Kabat EA, et al.: Sequences of Proteins of Immunological Interest, U. S. Department of Health and Human Services, Public Health Service, National Institutes of Health, 1991.

30. Fremont DH, et al.: Structures of an MHC Class II Molecule with Covalently Bound Single Peptides. *Science.* **272**:1001-1004 (1996).

31. O'Shannessy DJ, Quarles RH: Specific Conjugation Reactions of the Oligosaccharide Moieties of Immunoglobulins. *Journal of Applied Biochemistry.* **7**:347-355 (1985).

32. Fowers KD, et al.: Preparation of Fab' from murine IgG2a for thiol reactive conjugation. *Journal of Drug Targeting.* **9**:281-294 (2001).

33. Abbas AK, Lichtman AH, Pober JS: *Cellular and Molecular Immunology*, W.B. Saunders Company, Philadelphia, Pennsylvania, USA, 1997.

34. Nardin EH, et al.: The Use of Multiple Antigen Peptides in the Analysis and Induction of Protective Immune Responses against Infectious Diseases. *Advances in Immunology.* **60**:105-149 (1995).

35. Pintó RM, et al.: Enhancement of the immumonogenicity of a synthetic peptide bearing a VP3 epitope of hepatitis A virus. *FEBS Letters.* **438**:106-110 (1998).

36. Gregoriadis G, et al.: Liposome-entrapped T-cell peptide provides help for a co-entrapped B-cell peptide to overcome genetic restriction in mice and induce immunological memory. *Immunology.* **80**:535-540 (1993).

37. Garcon NMJ, Six HR: UNIVERSAL VACCINE CARRIER: Liposomes That Provide T-Dependent Help to Weak Antigens. *The Journal of Immunology.* **146**:3697-3702 (1991).

38. Fortin A, Lagacé, Thérien H-M: Trafficking of Surface-linked and Encapsulated Liposomal Antigens in Macrophages: an Immunocytochemical Study. *The Journal of Histochemistry & Cytochemistry.* **49**:1407-1420 (2001).

39. Leclerc C, et al.: A synthetic vaccine constructed by copolymerization of B and T cell determinants. *European Journal of Immunology.* **17**:269-273 (1987).

40. Schott ME, et al.: Comparison of Linear and Branched Peptide Forms (MAPs) in the Induction of T Helper Responses to Point-Mutated ras Immunogens. *Cellular Immunology.* **174**:199-209 (1996).

41. Wilkinson KA, et al.: Synthesis and in Vitro T-Cell Immunogenicity of Conjugates with Dual Specificity: Attachment of Epitope Peptides of 16 and 38 kDa Proteins from *Mycobacterium tuberculosis* to Branched Polypeptide. *Bioconjugate Chemistry.* **9**:539-547 (1998).

42. Evavold BD, Sloan-Lancaster J, Allen PM: Tickling the TCR: selective T-cell functions stimulated by altered peptide ligands. *Immunology Today.* **14**:602-609 (1993).

43. Lairmore MD, et al.: Human T-Lymphotrophic Virus Type 1 Peptides in Chimeric and Multivalent Constructs with Promiscuous T-Cell Epitopes Enhance Immunogenicity and Overcome Genetic Restriction. *Journal of Virology.* **69**:6077-6089 (1995).

44. Smith-Gill SJ, Sercarz EE (eds): The Immune Response to Structurally Defined Proteins: The Lysozyme Model. Schenectady, NY, Adenine Press, 1989.

45. Gammon G, et al.: T Cell Determinant Structure: Cores and Determinant Envelopes in Three Mouse Major Histocompatibility Complex Haplotypes. *Journal of Experimental Medicine.* **173**:609-617 (1991).

46. Bates RM, Ballard DW, Voss EW, Jr.: Comparative properties of monoclonal antibodies comprising a high-affinity anti-fluorescyl idiotype family. *Molecular Immunology.* **22**:871-877 (1985).

47. Bedzyk WD, et al.: Active Site Structure and Antigen Binding Properties of Idiotypically Cross-Reactive Anti-Fluorescein Monoclonal Antibodies. *The Journal of Biological Chemistry.* **265**:133-138 (1990).

48. Bedzyk WD, Reinitz DM, Voss EW, Jr.: Linkage of low and high affinity anti-fluorescein idiotype families. *Molecular Immunology.* **23**:1319-1328 (1986).

49. Bedzyk WD, et al.: Comparison of Variable Region Primary Structures within an Anti-fluorescein Idiotype Family. *The Journal of Biological Chemistry.* **264**:1565-1569 (1989).

50. Kranz DM, Voss EW, Jr.: Idiotypic analysis of monoclonal anti-fluorescyl antibodies: localization and characterization of idiotypic determinants. *Molecular Immunology.* **20**:1301-1312 (1983).

51. Kranz DM, Ballard DW, Voss EW, Jr.: Expression of defined idiotypes throughout the BALB/c anti-fluorescyl antibody response: affinity and idiotype analyses of heterogeneous antibodies. *Molecular Immunology.* **20**:1313-1322 (1983).

52. Herron JN, et al.: High Resolution Structures of the 4-4-20 Fab-Fluorescein Complex in Two Solvent Systems: Effects of Solvent on Structure and Antigen-Binding Affinity. *Biophysical Journal.* **67**:2167-2183 (1994).

53. Grey HM, Kunkel HG: H Chain subgroups of myeloma proteins and normal 7S globulin. *Journal of Experimental Medicine.* **120**:253-266 (1964).

54. Gibson AL, et al.: Differences in Crystal Properties and Ligand Affinities of an Antifluorescyl Fab (4-4-20) in Two Solvent Systems. *PROTEINS: Structure, Function, and Genetics.* **3**:155-160 (1988).

55. Harlow E, Lane D: *Antibodies: A Laboratory Manual*, Cold Spring Harbor Laboratory, 1988.

56. Hu KF, Lovgren-Bengtsson K, Morein B: Immunostimulating complexes (ISCOMs) for nasal vaccination. *Advances in Drug Delivery Reviews.* **23**:149-59 (2001).

57. Sjolander A, et al.: Immune responses to ISCOM formulations in animal and primate models. *Vaccine.* **19**:2661-5 (2001).

58. Langer R, Cleland JL, Hanes J: New advances in microsphere-based single-dose vaccines. *Advances in Drug Delivery Reviews.* **28**:97-119 (1997).

59. O'Hagan DT, MacKichan ML, Singh M: Recent developments in adjuvants for vaccines against infectious diseases. *Biomolecular Engineering.* **18**:69-85 (2001).

60. Lu Y-A, et al.: Chemically unambiguous peptide immunogen: preparation, orientation and antigenicity of purified peptide conjugated to the multiple antigen peptide system. *Molecular Immunology.* **28**:623-630 (1991).

61.   McLean GW, et al.: Generation of anti-peptide and anti-protein sera. Effect of peptide presentation on immunogenicity. *Journal of Immunological Methods.* **137**:149-157 (1991).

62.   Tam JP, et al.: Incorporation of T and B epitopes of the circumsporozoite protein in a chemically defined synthetic vaccine against malaria. *Journal of Experimental Medicine.* **171**:299-306 (1990).

63.   Munesinghe DY, et al.: Immunogenicity of multiple antigen peptides (MAP) containing T and B cell epitopes of the repeat region of the *P. falciparum* circumsporozoite protein. *European Journal of Immunology.* **21**:3015-3020 (1991).

64.   Chai SK, et al.: Immunogenic properties of multiple antigenic peptide systems containing defined T and B epitopes. *The Journal of Immunology.* **149**:2385-2390 (1992).

65.   Briand J-P, et al.: Application and limitations of the multiple antigen peptide (MAP) system in the production and evaluation of anti-peptide and anti-protein antibodies. *Journal of Immunological Methods.* **156**:255-265 (1992).

66.   Francis MJ, et al.: Immunological evaluation of the multiple antigen peptide (MAP) system using the major immunogenic site of foot-and-mouth disease virus. *Immunology.* **73**:249-254 (1991).

67.   Voss EW, Jr. (ed): Fluorescein Hapten: An Immunological Probe. Boca Raton, FL, CRC Press, Inc., 1984.

68.   Keah HH, Kecorius E, Hearn MTW: Direct synthesis and characterisation of multi-dendritic peptides for use as immunogens. *Journal of Peptide Research.* **51**:2-8 (1998).

69.   Cavenaugh JS, et al.: How well can a T cell epitope replace its parent carrier protein? Part I: An ANOVA study. *Pharmaceutical Research.* (submitted).

70.   Fishman MA, Perelson AS: Lymphocyte Memory and Affinity Selection. *Journal of Theoretical Biology.* **173**:241-262 (1995).

71.   Nardelli B, Tam JP: Cellular immune responses induced by *in vivo* priming with a lipid-conjugated multimeric antigen peptide. *Immunology.* **79**:355-361 (1993).

72.   Grillot D, et al.: Presentation of T-Cell Epitopes Assembled as Multiple-Antigen Peptides to Murine and Human T Lymphocytes. *Infection and Immunity.* **61**:3064-3067 (1993).

73. Huang W, Nardelli B, Tam JP: Lipophilic multiple antigen peptide system for peptide immunogen and synthetic vaccine. *Molecular Immunology.* **31**:1191-1199 (1994).

74. Oprea M, Perelson AS: Exploring the Mechanisms of Primary Antibody Responses to T Cell-Dependent Antigens. *Journal of Theoretical Biology.* **181**:215-236 (1996).

75. Levy R: Karnofsky Lecture: Immunotherapy of Lymphoma. *Journal of Clinical Oncology.* **17**:7-13 (1999).

76. Thielemans K, et al.: Strategies for production of monoclonal anti-idiotype antibodies against human B cell lymphomas. *Journal of Immunology.* **133**:495-501 (1984).

77. Kaminski MS, et al.: Importance of antibody isotype in monoclonal anti-idiotype therapy of a murine B cell lymphoma. A study of hybridoma class switch variants. *The Journal of Immunology.* **136**:1123-1130 (1986).

78. Cambell MJ, et al.: Idiotype vaccination against murine B cell lymphoma. Humoral and Cellular Responses Elicited by Tumor-Derived Immunoglobulin M and Its Molecular Subunits. *The Journal of Immunology.* **139**:2825-2833 (1987).

79. Kaminski MS, et al.: Idiotype vaccination against murine B cell lymphoma. Inhibition of tumor immunity by free idiotype protein. *The Journal of Immunology.* **138**:1289-1296 (1987).

80. Kwak LW, et al.: Induction of immune responses in patients with B-cell lymphoma against the surface-immunoglobulin idiotype expressed by their tumors. *New England Journal of Medicine.* **327**:1209-15 (1992).

81. Hsu FJ, et al.: Clinical Trials of Idiotype-Specific Vaccine in B-Cell Lymphomas. *Annals of the New York Academy of Sciences.* **690**:385-7 (1993).

82. Tao M-H, Levy R: Idiotype/granulocyte-macrophage colony-stimulating factor fusion protein as a vaccine for B-cell lymphoma. *Nature.* **362**:755-8 (1993).

83. Syrengelas AD, Chen TT, Levy R: DNA immunization induces protective immunity against B-cell lymphoma. *Nature Medicine.* **2**:1038-41 (1996).

84. Nelson EL, et al.: Tumor-Specific, Cytotoxic T-lymphocyte Response After Idiotype Vaccination for B-cell, Non-Hodgkin's Lymphoma. *Blood.* **88**:580-9 (1996).

85. Hsu FJ, et al.: Vaccination of patients with B-cell lymphoma using autologous antigen-pulsed dendritic cells. *Nature Medicine.* **2**:52-8 (1996).

86.   Hsu FJ, et al.: Tumor-Specific Idiotype Vaccines in the Treatment of Patients With B-Cell Lymphoma—Long-Term Results of a Clinical Trial. *Blood.* **89**:3129-3135 (1997).

87.   Caspar CB, Levy S, Levy R: Idiotype Vaccines for Non-Hodgkin's Lymphoma Induce Polyclonal Immune Responses That Cover Mutated Tumor Idiotypes: Comparison of Different Vaccine Formulations. *Blood.* **90**:3699-3706 (1997).

88.   Davis TA, et al.: Anti-Idiotype Antibodies Can Induce Long-Term Complete Remissions in Non-Hodgkin's Lymphoma Without Eradicating the Malignant Clone. *Blood.* **92**:1184-1190 (1998).

89.   Wong CP, Okada CY, Levy R: TCR Vaccines Against T Cell Lymphoma: QS-21 and IL-12 Adjuvants Induce a Protective CD8+ T Cell Response. *The Journal of Immunology.* **162**:2251-2258 (1999).

90.   McCormick AA, et al.: Rapid production of specific vaccines for lymphoma by expression of the tumor-derived single-chain Fv epitopes in tobacco plants. *Proceedings of the National Academy of Sciences of the United States of America.* **96**:703-708 (1999).

91.   Reichardt VL, et al.: Idiotype Vaccination Using Dendritic Cells After Autologous Peripheral Blood Stem Cell Transplantation for Multiple Myeloma—A Feasibility Study. *Blood.* **93**:2411-2419 (1999).

92.   Syrengelas AD, Levy R: DNA Vaccination Against the Idiotype of a Murine B Cell Lymphoma: Mechanism of Tumor Protection. *The Journal of Immunology.* **162**:4790-4795 (1999).

93.   Levy R: 1999 Keystone Symposium on B Lymphocyte Biology and Disease: B Cell Malignancy II Session. *Biochimica et Biophysica Acta.* **1424**:R43-R44 (1999).

94.   Timmerman JM, Levy R: Linkage of Foreign Carrier Protein to a Self-Tumor Antigen Enhances the Immunogenicity of a Pulsed Dendritic Cell Vaccine. *The Journal of Immunology.* **164**:4797-4803 (2000).

95.   Stevenson FK, Gordon J: Immunization with idiotypic immunoglobulin protects against development of B lymphocytic leukemia, but emerging tumor cells can evade antibody attack by modulation. *The Journal of Immunology.* **130**:970-973 (1983).

96.   Hawkins RE, et al.: A Genetic Approach to Idiotypic Vaccination. *Journal of Immunotherapy.* **14**:273-278 (1993).

97. Hawkins RE, et al.: Idiotypic Vaccination Against Human B-cell Lymphoma. Rescue of Variable Region Gene Sequences From Biopsy Material for Assembly as Single-Chain Fv Personal Vaccines. *Blood.* **83**:3279-88 (1994).

98. Stevenson FK, et al.: A Genetic Approach to Idiotypic Vaccination for B Cell Lymphoma. *Annals of the New York Academy of Sciences.* **772**:212-226 (1995).

99. Terness P, et al.: Idiotypic Vaccine for Treatment of Human B-Cell Lymphoma: Construction of IgG Variable Regions from Single Malignant B Cells. *Human · Immunology.* **56**:17-27 (1997).

100. McMillan S, et al.: Synthetic Idiotypes: The Third Hypervariable Region of Murine Anti-Dextran Antibodies. *Cell.* **35**:859-863 (1983).

101. Seiden MV, et al.: Chemical synthesis of idiotopes. *Journal of Experimental Medicine.* **159**:1338-1350 (1984).

102. Smales CM, Moore CH, Blackwell LF: Characterization of Lysozyme-Estrone Glucuronide Conjugates. The Effect of the Coupling Reagent on the Substitution Level and Sites of Acylation. *Bioconjugate Chemistry.* **10**:693-700 (1999).

103. Creighton TE: *Proteins: Structures and Molecular Properties*, W. H. Freeman and Company, 1993.

104. Janeway CA, et al.: *Immunobiology*, Garland Publishing, New York, 2001.

105. Brunger AT, Adams PD: Molecular Dynamics Applied to X-ray Structure Refinement. *Accounts of Chemical Research.* **35**:404-412 (2002).

106. Whitelegg NRJ, Rees AR: WAM: an improved algorithm for modelling antibodies on the WEB. *Protein Engineering.* **13**:819-824 (2000).

107. Lim K. Structural Studies of Antifluorescein Antibody and Molecular Simulations of Protein-Surface Interaction; doctoral dissertation University of Utah, 1992.

108. Still WC, et al.: Semianalytical Treatment of Solvation for Molecular Mechanics and Dynamics. *Journal of the American Chemical Society.* **112**:6127-6129 (1990).

109. Bashford D, Case DA: Generalized Born Models of Macromolecular Solvation Effects. *Annual Reviews of Physical Chemistry.* **51**:129-152 (2000).

110. Essmann U, Perera L, Berkowitz ML: A smooth particle mesh Ewald method. *Journal of Chemical Physics.* **103**:8577-8593 (1995).

111. Bogusz S, Cheatham TE, III, Brooks BR: Removal of pressure and free energy artifacts in charged periodic systems via net charge corrections to the Ewald potential. *Journal of Chemical Physics.* **108**:7070-7084 (1998).

112. Anonymous: *Discover User's Guide*, Biosym Technologies, Inc., San Diego, CA, 1997.

113. Herron JN, et al.: Three-dimensional structure of a fluorescein-Fab complex crystallized in 2-methyl-2,4-pentanediol. *Proteins.* **5**:271-280 (1989).

114. Whitlow M, et al.: 1.85-A structure of anti-fluorescein 4-4-20 Fab. *Protein Engineering.* **8**:749-761 (1995).

115. Ibragimova GT, Wade RC: Importance of Explicit Salt Ions for Protein Stability in Molecular Dynamics Simulation. *Biophysical Journal.* **74**:2906-2911 (1998).

116. Case DA, et al.: AMBER 6. San Francisco, University of California, San Francisco, 1999.

117. Pearlman DA, et al.: AMBER, a package of computer programs for applying molecular mechanics, normal mode analysis, molecular dynamics and free engergy calculations to simulate the structural and energetic properties of molecules. *Comp. Phys. Commun.* **91**:1-41 (1995).

118. Humphrey W, Dalke A, Schulten K: VMD - Visual Molecular Dynamics. *Journal of Molecular Graphics.* **14**:33-38 (1996).

119. Tsui V, Case DA: Theory and Applications of the Generalized Born Solvation Model in Macromolecular Simulations. *Biopolymers (Nucleic Acid Science).* **56**:275-291 (2001).

120. Prestegard JH, et al.: Nuclear Magnetic Resonance in the Era of Structural Genomics. *Biochemistry.* **40**:8677-8685 (2001).

121. Srinivasan J, et al.: Continuum Solvent Studies of the Stability of DNA, RNA, and Phosphoramidate-DNA Helices. *Journal of the American Chemical Society.* **120**:9401-9409 (1998).

122. Renisio J-G, et al.: Solution Structure and Backbone Dynamics of an Antigen-Free Heavy Chain Variable Domain (VHH) From *Llama. PROTEINS: Structure, Function, and Genetics.* **47**:546-555 (2002).

123. Vranken W, et al.: Solution Structure of a Llama Single-Domain Antibody with Hydrophobic Residues Typical of the VH/VL Interface. *Biochemistry.* **41**:8570-8579 (2002).

124. Tissot AC, et al.: Viral Escape at the Molecular Level Explained by Quantitative T-cell Receptor/Peptide/MHC Interactions and the Crystal Structure of a Peptide/MHC Comlex. *Journal of Molecular Biology.* **29**:873-885 (2000).

125. Toh H, et al.: Magnitude of structural changes of the T-cell receptor binding regions determine the strength of T-cell antagonism: molecular dynamics simulations of HLA-DR4 (DRB1*0405) complexed with analogue peptide. *Protein Engineering.* **13**:423-429 (2000).

126. Elber R, Karplus M: Enhanced Sampling in Molecular Dynamics: Use of the Time-Dependent Hartree Approximation for a Simulation of Carbon Monoxide Diffusion through Myoglobin. *Journal of the American Chemical Society.* **112**:9161-9175 (1990).

127. Roitberg A, Elber R: Modeling side chains in peptides and proteins: Application of the locally enhanced sampling and the simulated annealing methods to find minimum energy conformations. *Journal of Chemical Physics.* **95**:9277-9287 (1991).

128. Lim K, Herron JN: Molecular Dynamics of the Anti-Fluorescein 4-4-20 Antigen-Binding Fragment. 1 Computer Simulations. *Biochemistry.* **34**:6962-6974 (1995).

129. Chong LT, et al.: Molecular dynamics and free-energy calculations applied to affinity maturation in antibody 48G7. *Proceedings of the National Academy of Sciences of the United States of America.* **96**:14330-14335 (1999).

130. Hage DS, Wolfe CAC, Oates MR: Development of a Kinetic Model To Describe the Effective Rate of Antibody Oxidation by Periodate. *Bioconjugate Chemistry.* **8**:914-920 (1997).